



Conjunctive Surface Water and Groundwater Modeling for Sustainable use in the Colorado River Delta using MODFLOW, Mexico

A Dissertation Submitted to the Faculty of the
UNIVERSIDAD AUTÓNOMA DE BAJA CALIFORNIA

INSTITUTO DE INGENIERÍA

In Partial Fulfillment of the Requirements

For the Degree of

DOCTOR OF PHILOSOPHY

WITH A MAJOR IN HYDROLOGY

Student

Kedir Mohammed Bushira

Advisor

Dr. Jorge Ramírez Hernández

2018

**Conjunctive Surface Water and Groundwater
Modeling for Sustainable use in the Colorado
River Delta using MODFLOW, Mexico**

PART ONE

Groundwater Modeling for Sustainable use in the Colorado River Delta using MODFLOW, Mexico

Abstract

The Mexicali valley in Colorado River delta has been one of the most productive agricultural regions in the area. The valley also is rapidly becoming an important area for Baja California's expanding urban population. Quantification of groundwater flow dynamics and groundwater flow components represent a key component for a development of better water management strategies. This paper is aimed to simulate the groundwater flow dynamics and groundwater flow components of the Mexicali Valley aquifer for better water management strategies by applying a hydrological conceptual model into an integrated hydrological numerical model. The numerical model was developed using the MODFLOW-OWHM code under the ModelMuse Graphical User Interface, where the surface-groundwater interactions through unsaturated zone were simulated using the River Package (RIV) and Unsaturated-Zone Flow (UZFI) MODFLOW packages. A conceptual model was developed to simulate the groundwater flow and to estimate groundwater balance components from 2002 to 2010 stress periods. After reasonable calibration on the most uncertain parameters (Horizontal hydraulic conductivity and specific yield), the model produced a general view of the groundwater fluxes in the study area and generated insights into the groundwater balance components in the study period. A steady-state model was calibrated using 27 observation wells of average hydraulic heads and the transient simulation was calibrated using 45 observation wells. In the steady-state calibration, gross recharge, contributed 93.3%, lateral inflow 3.2% and stream leakage 3.4% of the total groundwater inflow. The groundwater outflow consisted of groundwater evapotranspiration 87.5%, surface leakage 3.1%, groundwater pumping 3.09% and lateral outflow 6.31%.

In the transient model simulation, the water budget components that contributed to the groundwater input were: gross recharge (34.35%) and lateral inflow (65.64%). The discharges that contributed to the groundwater output were: pumping (45.61%), groundwater evapotranspiration (8.9%), outflow through drain (12.66%), lateral outflow (21.58%), groundwater exfiltration (10.81 %), leakage from groundwater to streams (0.44 %), and storage change (Δs) of $-19.91 \times 10^6 \text{ m}^3$.

The calibrated transient model showed temporally and spatially variable patterns of groundwater fluxes. The groundwater evapotranspiration (ETg) ranged from -40.2

$\text{Mm}^3\text{year}^{-1}$ at the end of the transient modeling period to $-100.4 \text{ Mm}^3 \text{ year}^{-1}$ in the year 2004 with an average of $-78.32 \text{ Mm}^3 \text{ year}^{-1}$; the groundwater exfiltration (Exfgw) ranged from $93.5 \text{ Mm}^3 \text{ year}^{-1}$ in 2003 to $104.4 \text{ Mm}^3 \text{ year}^{-1}$ in the year 2008 with an average of $94.9 \text{ Mm}^3 \text{ year}^{-1}$; The calculated net recharge was ranged from $95.8 \text{ Mm}^3 \text{ year}^{-1}$ to $212.2 \text{ Mm}^3 \text{ year}^{-1}$.

Processes encountered in the calibrated parameterizations show groundwater flows axially from almost all directions of the model towards the Gulf of California at the south border of the model, match the course of the Colorado River and laterally towards the new river in the North-west, with a larger portion flowing out Southward than North-westward. The numerical modeling results showed that if the irrigation demands continue to increase, the current situation would lead to an acceleration of the groundwater depletion which might introduce ecological problems to the study area. Overall, the model provides a detailed MODFLOW analysis of changes in groundwater availability.

Keywords: Colorado River Delta, MODFLOW-OWHM; Conjunctive use; Modeling; Mexicali Valley; Mexico.

Acknowledgments

First of All, I want to say Alhamdulillah's. Thanks to God who gave me the power, patience, and knowledge to finish this study successfully with full health.

I would like to extend my warm and heartfelt appreciation to my supervisor, Dr Jorge Ramirez Hernandez, for introducing me to the world of modeling and for his relentless, invaluable and critical comments, advice and encouragement during the study and for all types of assistance and guidance during this work.

I offer my sincere appreciation for the scholarship opportunities provided by Agencia Mexicana de Cooperación Internacional para el Desarrollo de la Secretaria de Relaciones Exteriores del Gobierno Mexicano (SRE). I am also grateful to Arba Minch University, Ethiopia, for allowing me to participate in this Ph.D. program.

My thanks also go to the following individuals: Dr.Zhuping Sheng in providing help during half a year of the external research stay at the Texas A&M AgriLife Research Center at El Paso; Dr. Eliana Rodríguez-Burgueño, for providing me raw data that assisted me during this study; Dr. Concepción Carreón for providing professional support during the study period by evaluating the course research activities. Mehretab Yohannes Weldemichael former students of ITC, Netherlands , who gave me some comments on ModelMuse GUI and helping me when I faced problem in running the model and Dr. Wolfgang Schmid, one of the main author of 'The Farm Process' for MODFLOW from CSIRO, Australia, in giving some technical support by clarifying issues about Farm process.

At last but not least, I would like to express my heartfelt love and gratitude to my family: my kids and my sisters for their moral encouragement when I stay away from home.

Table of Content

PART ONE

Abstract	iv
Acknowledgments	vi
Table of Figures	x
List of Tables.....	xiii
Preface	1
1: Introduction	2
1.1. Background of the study	2
1.2. Problem Definition.....	5
1.3. Research objectives	5
1.3.1. Main objectives	5
1.3.2. Specific objectives.....	5
1.3.3. Research hypothesis and assumptions.....	5
1.3.4. The novelty of the study.....	6
1.4. Study Area.....	6
1.4.1. Water Use in the Irrigation District 014.....	8
2. Literature Review	12
2.1. Introduction	12
2.1.1 Various components of surface water and groundwater	13
2.2 Detailed literature Review.....	14
2.3. Evaluation of surface water-groundwater interaction using Numerical Models.....	17
2.4. Flow Model	18
2.4.1 MODFLOW	19
2.4.2. Setting up a finite difference numerical model	22
2.4.3. The initial conditions, boundary conditions and model input parameters.....	24
2.5. Uncertainty in the Conceptual Model	24
2.6. Common Modeling Errors	25
3. Research Methods and Materials	26
3.1. Methodology flow chart	26
3.2. Data collection and model input preparation	27
3.2.1. Precipitation	28
3.2.2. Potential evapotranspiration.....	28
3.2.3. Infiltration rate.....	29
3.3. Conceptual Hydrological Model	30

3.3.1. The Areal extent of the Model Domain.....	30
3.3.2. Geo-hydrological conditions at the model borders	30
3.4. Geology and hydrogeology	33
3.4.1. Model Layer 1	35
3.4.2. Model Layer 2.....	35
3.4.3. Surface water features	35
3.5. Parent model grid design.....	37
3.6. Software selection	38
3.7. Numerical model.....	38
3.8. Hydraulic properties.....	40
3.9. Head observations (HOB).....	41
3.10. Water budget	41
3.11. Model calibration	43
3.11.1. Steady-state model calibration	43
3.12. Error assessment.....	44
4. Results and Discussions	45
4.1. Metrological and Hydrological analysis result.....	45
4.1.1. Metrological data analysis.....	45
4.1.2. Infiltration rate.....	45
4.2. Steady-state model calibration	46
4.2.1. Calibrated head and error assessment	46
4.2.2. Hydraulic conductivities	49
4.2.3. Water budget of the steady-state simulation	50
4.2.4. Groundwater fluxes spatially.....	51
4.3. Transient state model Calibration	51
4.3.1. Initial Condition	51
4.3.2. Calibration Results	52
4.3.3. Hydraulic Conductivity	54
4.3.4. Regional water Budget	57
4.3.5. Groundwater fluxes spatially.....	62
5. Conclusion and Recommendations	63
5.1. Conclusions	63
5.2. Recommendations	66
6: References	68
Abstract	74
1. Introduction.....	75

1.1.	Review on MF-FMP.....	77
1.1.1.	Governing Equations.....	77
1.1.2.	Land Use and Root Zone Processes	80
1.1.3.	Water Demand and Supply.....	91
2.	Purpose and Scope	96
2.1.	Approach.....	98
2.2.	Description of the Study Area.....	99
2.2.1.	Water-Balance Subregions (WBS).....	100
3.	Irrigation Unit 16 FARM Process Model Development	101
3.1.	Temporal and spatial Discretization.....	101
3.2.	Distribution of Landscape Attributes	102
3.3.	Initial Condition and structural model setting	106
3.4.	Flow Boundary.....	108
3.5.	Surface Water Inflows and Outflows	108
3.6.	Groundwater Pumpage	109
3.7.	Crop Data	110
3.8.	Potential Evapotranspiration	112
4.	Results and Discussion.....	113
4.1.	Model calibration	113
4.2.	Water Budget	115
4.3.	Conclusions and Recommendations.....	119
5.	References	121
	Annex 1: Data used for developing river package (RIV) in the model.....	124
	Annex 2: Data used for developing drain package (DRN) in the model.....	128
	Annex 3: Distribution of simulated head (m.asl) at the year 2003-2004	130
	Annex 4: Distribution of simulated head (m.asl) at the year 2004-2005	131
	Annex 5: Distribution of simulated head (m.asl) at the year 2005-2006	132
	Annex 6: Distribution of simulated head (m.asl) at the year 2006-2007	133
	Annex 7: Distribution of simulated head (m.asl) at the year 2007-2008	134
	Annex 8: Calculated agricultural Related Recharge for each irrigation units in irrigation district 014.....	135
	Annex 9. Farm Budget for Farm 2 for a specific stress period and time step in m ³ /year.....	136
	Annex10. Farm Budget for Farm 4 for a specific stress period and time step in m ³ /year.....	136

Table of Figures

PART ONE

Figure 1. Colorado River Flow at U.S. – Mexico border from 1878 to 2009. Red dotted line indicates 1944 U.S. – Mexico treaty obligation, IBWC (2011).	4
Figure 2. Location of the study area in the Mexicali Valley; US–Mexico border along with pumping wells, metrological stations, observation wells and cross section. Initial Groundwater level contour lines in the study area showing the groundwater flow direction following the path of Colorado River.....	8
Figure 3. Distribution of Main water sources for Irrigation district 014.....	9
Figure 4. Colorado River flows received at NIB and SIB during the period 1935-2006 by Mexico’s Irrigation District 014-Rio Colorado (calculated from CONAGUA 2007a), reprinted from Carrillo-Guerrero, Y.K., 2009.	10
Figure 5. Total annual groundwater extraction for MODFLOW model development	11
Figure 6. Distribution of large production wells within the study area.....	12
Figure 7. Various components of surface water and groundwater (Berner and Berner, 1987)	14
Figure 8. Groundwater flow paths vary greatly in length, depth, and travel time from points of recharge to points of discharge in the groundwater system.	15
Figure 9. Gaining and losing streams situations which receive water from the Groundwater system and Losing streams lose water to groundwater system	16
Figure 10. Typical Examples of disconnected streams and Bank storage.....	17
Figure 11. A discretized hypothetical aquifer system (Harbaugh et al. 2000)	19
Figure 12: Schematic diagram of Flowchart for methodologies applied and the processes followed during the study	27
Figure 13: (a) Boundary conditions for the model Colorado River Delta (MCRD), (b) Hydrologic Features for MODFLOW simulation.	32
Figure 14 Representation of rivers, and drains in the model.....	36
Figure 15: Model domain showing a grid and active cell boundary	37
Figure 16: Precipitation (P), infiltration rate (Inf), and potential evapotranspiration (PET) for 8-year periods (hydrologic years 2002 to 2010) for the study area	46

Figure 17: Relationship between simulated and observed head in the study area for steady-state condition.....	47
Figure 18: Residuals vs. Observed head of steady-state simulation	47
Figure 19: Calibrated head distribution (a) first layer (b) second layer of the steady-state model simulation	48
Figure 20: Calibrated horizontal hydraulic conductivity (K_h) distribution map for first layer after calibration in steady-state condition [$m\ day^{-1}$].....	49
Figure 21: (a) Groundwater evapotranspiration in $mm\ day^{-1}$ and (b) UZF recharge in $mm\ day^{-1}$ for the study area for calibrated steady-state condition.....	51
Figure 22. Scatter diagram for modeled and observed groundwater heads with linear correlation coefficient equal to 0.91 for transient model using observation points of 2006.	52
Figure 23. Temporal variation of groundwater level at seven selected observation wells, (a)-(g) comparison between the model simulation and observations; and (h) the locations of the wells.....	54
Figure 24. 3D view of the developed horizontal hydraulic conductivity distribution values for the first and second active cell layer. Deep green color represents inactive cell undefined hydraulic conductivity value. The second layer has a uniform horizontal hydraulic conductivity of 0.001m/d.	55
Figure 26. North-south cross section showing the calculated horizontal hydraulic conductivity (see Figure 2 for the location of cross section point) and refer figure 23 for the legend values).....	56
Figure 27: Simulated Average annual water balance in billion m^3 for the study area	57
Figure 28: Schematic representation of groundwater budget for the entire model (all units are millions of m^3).....	58
Figure 29. Distributions of average simulated river leakage in cubic meters for the year 2006	59
Figure 30. Distribution of simulated drawdown (m.asl) at the end of the modeling period	60
Figure 31. Distribution of simulated head (m.asl) at (a) first and (b) end of study period...	61
Figure 32: The transient calibrated groundwater exfiltration (Ex_{fgw}), groundwater evapotranspiration (ET_g), gross recharge (R_g) and net recharge (R_n) groundwater fluxes for 8-year periods from 01 October 2002 to 30 September 2010.....	62

Figure 33: The transient calibrated unsaturated zone evapotranspiration (ET_{un}) and groundwater evapotranspiration (ET_g) for 8-year periods (01 October 2002 to 30 September 2010)..... 63

PART TWO

Figure 1 Irrigation district 014 and Active cell boundary for MF-FMP modeling 76

Figure 2 Schematic representation of root zone and land surface flow processes simulated by MF-FMP (Schmid and Hanson, 2009b) 81

Figure 3 Change of Crop Consumptive Use Components with varying Head (root zone = Capillary Fringe, Concept1, concept2, left to right)..... 84

Figure 4 Change of Crop Consumptive Use Components with varying Head (root zone <, > Capillary Fringe, Top to Bottom and Concept1, concept2, left to right) 85

Figure 5. Active cell boundary and grids used for MF-FMP modeling 98

Figure 6. Farm Delivery components and the general Inflow and outflow components 99

Figure 7. Identified six water balance subregions (WBS) and delivery canals in irrigation unit 16..... 100

Figure 8: MF-FMP Farm id for irrigation district 16 103

Figure 9: MF-FMP soil id designation for irrigation district 16 104

Figure 10:Surface elevation contour of Irrigation district 16..... 107

Figure 11. Distribution of model cells used for drainage package (DRN)..... 108

Figure 12. Distribution of model cells used for streams flow routing (SFR) package..... 109

Figure 13. Distributions of calibrated horizontal hydraulic conductivity (Kh) for the 1st layer, water sources and grids used for MF-FMP modeling 113

Figure 14 Total annual reported and simulated agricultural pumpage for WBS1 (right) and WBS2 (left) for the period (1995-2006)..... 115

Figure 15 (I) Simulated drawdown (m) and (II) simulated hydraulic heads (m a.s.l.) for irrigation unit 16..... 116

Figure 16 Farm delivery components and the inflows and outflows for two water-balance subregions (WBS1, top, and WBS3, bottom) from 1995 to 2006. Recharge and runoff, refer the second axis..... 117

Figure. 17 Graph showing the percentages of total Landscape (LS) inflows and outflows for two water-balance areas from 1995 to 2006 as part of conjunctive use simulated by MF-FMP 118

List of Tables

PART ONE

Table 1. Percent of wheat, alfalfa, and cotton cultivated areas according to a water source (Calculated from CONAGUA 2006c)..... 29

Table 2. Percentage of the total irrigated area by crop for 3 agricultural years (calculated from CONAGUA 2006c). 29

Table 3: Geohydrologic conditions of the model boundaries..... 31

Table 4: discretization’s of the parent model 37

Table 5: Total water balance of the study area aquifer at steady-state condition (m³/day).. 50

Table 6 Average simulated Groundwater balance obtained from MODFLOW model 57

PART TWO

Table 1. Summary of water balance subregions in irrigation unit 16..... 101

Table 2. Summary of MODFLOW-OWHM with Farm Process (MF-FMP) packages and processes used with the hydrologic flow model of irrigation unit 16, Baja-California 105

Table 3. Summary of MODFLOW-OWHM with Farm Process (MF-FMP) packages and processes used with the hydrologic flow model of irrigation unit 16, Baja-California, Continued 106

Table 4. Summary of agricultural pumpage in thousand cubic meters per year used for this study 110

Table 5. Summary of irrigation unit 16 virtual crop categories and properties..... 111

Table 6. Summary of fractions of transpiration and evaporation by year for irrigation unit 16 crop categories (virtual crops) 112

Table 7 Groundwater balance obtained from the MF-FMP model (whole irrigation unit 16) 115

List of Abbreviations

ΔS	Change in storage
AQUIFEM-1	Finite element aquifer flow model
DEM	Digital Elevation Model
ETg	Groundwater evapotranspiration
ETo	Reference Evapotranspiration
ETss	Subsurface evapotranspiration
ETUn	Unsaturated zone evapotranspiration
ETXWC	Extinction water content
Exfgw	Groundwater Exfiltration
EXTDP	Extinction depth
GHB	General Head Boundary
GSFLOW	Groundwater and Surface Flow
GUI	Graphical User Interface
GW	Groundwater
HBV	Hydrologiska Byråns Vattenbalansavdelning model
HOB	Head Observation package
Kc	Crop Coefficients
KH	Horizontal Hydraulic Conductivity
KV	Vertical Hydraulic Conductivity
m a.s.l	Meters above sea level
MAE	Mean Absolute Error
ME	Mean Error
MODFLOW	Three dimensional finite difference groundwater flow- models
OWHM	One Water Hydrologic Flow Model
PET	Potential Evapotranspiration
PRMS	Precipitation Runoff Modeling System
Rg	Gross recharge (UZF recharge)
RMSE	Root Mean Square Error
SS	Specific Storage
SWAT	Soil and water assessment tool
SY	Specific Yield
UZF	Unsaturated-Zone Flow package of MODFLOW

Preface

The work presented in this thesis was fulfilled at Instituto de Ingenieria, Universidad Autonoma de Baja California (UABC), Baja California, Mexicali, Mexico, under the supervision of Professor Jorge Ramirez Hernandez. Half a year of external research stay was spent at the Texas A&M AgriLife Research Center at El Paso, TX, U.S.A, under the supervision of Prof. Zhuping Sheng.

The PhD. study was financially supported by the Agencia Mexicana de Cooperación Internacional para el Desarrollo de la Secretaria de Relaciones Exteriores del Gobierno Mexicano (SRE).

This Manuscript is divided into two major individuals appended parts; part one, MODFLOW-OWHM modeling of Colorado River delta and part two which presents MODFLOW Farm process analysis for irrigation unit 16 (Modulo 16). The first chapter of part one provides an overview of the present Ph.D. research background, state-of-the-art knowledge of the use of MODFLOW modeling, and the research objectives. Following this, chapter 2, provides a literature review. Chapter 3, briefly describes research methodologies, procedures followed and materials used to come up with the calibrated model. In chapter 4, steady and transient model results obtained including model calibration, head and drawdown analysis and regional water budget of model Colorado River delta. Chapter 5 is a research conclusion and recommendation. Part two also contains about 5 chapters including conclusions and recommendations. It starts with chapter 1 including a general overview of MODFLOW Farm process (MF-FMP); the governing equations. Chapter 2 describes the study area, in chapter 3, MF-FMP development for irrigation unit 16 was presented, in chapter 4 model calibrations and results obtained followed by general conclusion and recommendations was sighted. Finally, chapter 5 includes all the reference cited in the entire document. About 10 Annexes were included for presenting detailed data results ;data for river package (Annex 1), drain package (Annex 2), distribution of simulated head annually from 2003 to 2008 (Annex 3 to 7) , Agricultural related Recharge Annex 8, and farm budgets for Farm 2 and 4 are showed in Annex 9 and 10, respectively.

1: Introduction

1.1. Background of the study

The study of surface water and groundwater interactions has gained special attention in the field of water resources management in recent decades. This is due to the fact that surface water and groundwater flow systems, in many cases, interact with each other. For instance, groundwater abstraction can reduce base flow and adversely affect river hydrology. Conversely, surface water abstraction can reduce groundwater recharge and reduce groundwater potentials of the aquifer system. Moreover, surface water can gain solute from groundwater while the quality of groundwater can be impaired by surface waters. From these facts, the management of surface water and groundwater are hardly inseparable. Krause et al. (2007) pointed out that interactions between surface water and groundwater and the exchange of fluxes between them have high spatial and temporal variability. In that regard, the type of interaction is determined by the direction of flux exchange. For example, a surface water source experiences influent condition when it loses water into an aquifer and experiences effluent condition when it gains water from the aquifer system.

Formerly, the surface water and groundwater flow systems were analyzed separately because the flows take place at different temporal scales (Gupta, 2010) and, thus, its representation was a very difficult undertaking. This approach allowed surface water and groundwater flow regimes to be analyzed in separation using the uncoupled or stand-alone models. For instance, the HBV, PRMS and SWAT codes focus more on modeling surface water and simplify groundwater flow processes. Likewise, the codes like standard MODFLOW and AQUIFEM-1 emphasize more on groundwater flow processes and simplify surface water flow processes. However, the ever-increasing developments in computing facilities have enabled the flow systems to be analyzed together in both spatial and temporal domains. The conjunctive analysis of surface water and groundwater flows is performed through the integrated or coupled models. The typical examples of such models include, among others, MODFLOW-2005, MODFLOW-NWT, GSFLOW and MODFLOW-OWHM.

It should be pointed out that the selection of an appropriate code to deal with a particular problem in hand is of paramount importance. For example, an uncoupled groundwater model can perform better in a particular environment where a coupled model cannot do the same.

The ever-increasing demands of water are largely fulfilled by surface water and/or groundwater resources to satisfy cultural, social and economic uses. In this case, the delta of the Colorado River is no exception that the water demand is fulfilled by the diversions of Colorado River and aquifer pumping; the over increasing of the groundwater wells in the area may cause a negative effect on the groundwater source.

Previous researches related to groundwater in the Colorado River delta has largely centered on the area which lies within the United States, particularly Yuma, Arizona. Some of these reports have included analysis of small areas of the north and/or a northeast portion of the Colorado River delta in Mexico. In 1988 the Arizona Department of Water Resources (ADWR) published the results of two finite difference numerical groundwater models that focused on Yuma, Arizona over the 1983-84 time periods (Mock et al. 1988). Although these models did not consider any part of the Colorado River Delta within Mexico, they provide insight into the parameterization of the Delta hydrogeology to develop the groundwater model for the agricultural regions of the Mexicali Valley. The Mexicali Valley has been different research efforts. The latest groundwater modeling effort in the Mexican part of Colorado River were made in 2008 and 2012 by the University of Arizona, U.S.A, and Universidad Autonoma de Baja California, Mexico, respectively.

Less than 100 years ago, the Colorado River Delta was a 3,000-square-mile expanse of riparian, marsh, and estuarine habitat that supported a multitude of plant, bird, and marine life. Since the mid-1900s however, the Colorado River has not regularly flowed into the sea due to upstream dams and diversions (Figure 1), causing the Delta to gradually be reduced to less than 10 percent of its original size. The introductions of many upstream Colorado River impoundments and the transformation of the Colorado River Delta from wilderness to the highly productive agricultural region brought significant water stress in the Delta which calls better water management strategies for sustainable development. This study was proposed to simulate the groundwater behavior and to study the aquifer response to agricultural pumping by using a MODFLOW numerical modeling for a better

understanding of agricultural water uses. Figure 1, shows how the historic Colorado River flow at U.S.-Mexico border influenced by upstream dam constructions and diversions.

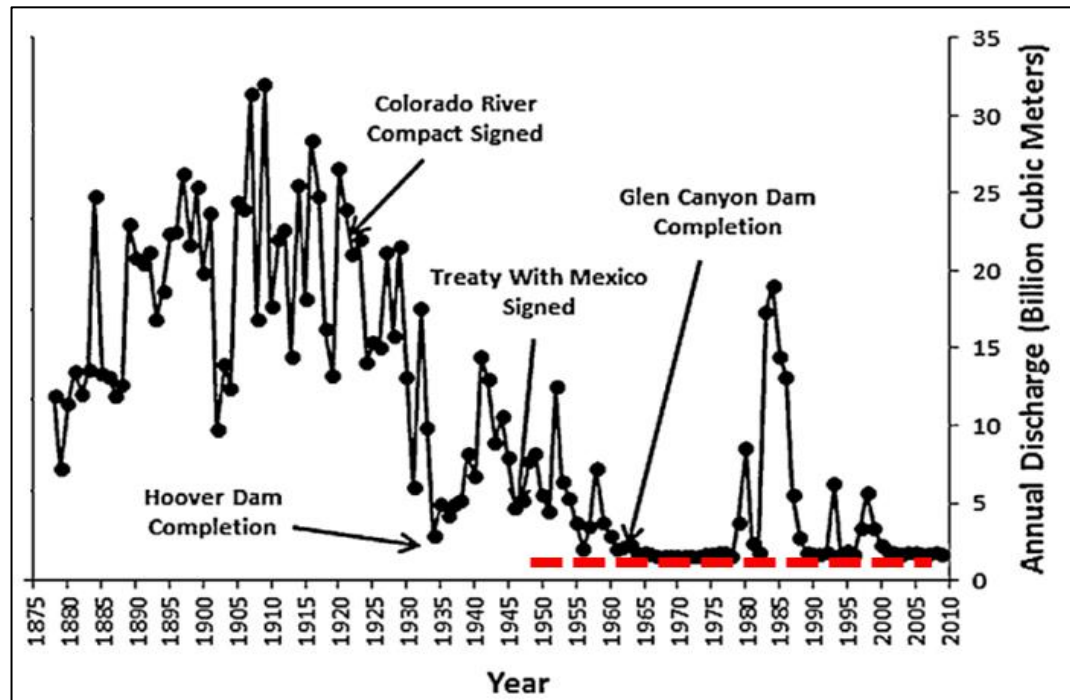


Figure 1. Colorado River Flow at the U.S. – Mexico border from 1878 to 2009. The red dotted line indicates 1944 U.S. – Mexico treaty obligation. International Boundary and Water Commission (IBWC, 2011).

The ultimate aim of this research is to improve the understanding of surface water and groundwater by using MODFLOW modeling in Colorado River Delta for sustainability and to influence effective decision making in water resource management in the Delta and specifically in the Colorado River irrigation district 014. A MODFLOW farm process analysis was done at irrigation unit 16 which is presented in part two of this paper.

In order to be able to model the water in the Delta, this research practices the MODFLOW-OWHM codes running under ModelMuse as the graphic user interphase. The stress packages, among others, will employ the Unsaturated Zone Flow (UZF), River package (RIV), Well package (WEL), Drain package (DRN), General Head boundary package (GHB) and head observation package (HOB) to facilitate the study of surface water-groundwater and to detect the effects of pumping on aquifer storage and to calculate the final water balance in the study area.

1.2. Problem Definition

The transformation of the Colorado River Delta to the highly productive agricultural region that exists today, construction of upstream impoundments, and the installation of many large-scale groundwater wells that have been in place cumulatively brought a significant change in the region. However, despite those cumbersome changes, little has been done to investigate its imposed effects in the hydrogeological regime of the Delta mainly effect of agricultural activities on groundwater levels and groundwater recharge.

1.3. Research objectives

1.3.1. Main objectives

To simulate groundwater flow dynamics and groundwater flow components of the Mexicali Valley (Irrigation District 014) aquifer for better water management strategies applying MODFLOW One-Water Hydrologic Flow Model (MODFLOW-OWHM).

1.3.2. Specific objectives

- I. To perform MODFLOW Farm process (MF-FMP) modeling at irrigation unit 016, which is found in part two of this document.
- II. To develop conceptual model for the Colorado River Delta.
- III. To better understand the impact of groundwater pumping on aquifer storage.

1.3.3. Research hypothesis and assumptions

It is hypothesized that the calibration of integrated steady and transient numerical model could give a realistic estimate of the groundwater flow and groundwater budget of the Delta provided that the following assumptions are met:

- The interaction between the Delta aquifer and the streams can be realistically simulated using the RIV (River) and DRN (Drain) packages of MODFLOW-OWHM;
- The fluxes interacting between surface water and groundwater domains, i.e. recharge, groundwater evapotranspiration and groundwater exfiltration, can be

realistically simulated using the UZF1 (Unsaturated-Zone Flow) package of MODFLOW.

1.3.4. The novelty of the study

The findings of this thesis will amplify the existing data and will contribute to the understanding of integrated surface water and groundwater modeling in the study area by including the following novelties.

1. Application of the new concept of MODFLOW one water hydrologic model (MODFLOW-OWHM) not tested in the Delta study area yet.
2. Application of modeling tools that was not used before in the model area; so far MODFLOW under NWT solver was used. In this study, MODFLOW-OWHM under Model Muse environment and MODFLOW farm process (MF-FMP) is applied.
3. Uses of MODFLOW packages not tested in the area before: unsaturated zone flow package (UZF), Streamflow routing package (SFR), and head observation package (HOB).

1.4. Study Area

In the arid Northwest of Mexico, the Colorado River sustains its southernmost agricultural development in the upper portion of its Delta (Figure 2). The northern boundary of the Irrigation District 014 is the international border between Mexico and the US; 89 km in the Baja California (MX)-California (US) border region and 3.3 km in the Sonora (MX)-Arizona (US) border region. To the south, lie the coastal estuaries of the northern portion of the Gulf of California. The fields of this agricultural valley spread across the borders of the Mexican States of Sonora and Baja California surrounded by Mexico's driest desert, the Sonoran Desert (East), and the coastal desert of the Baja California Peninsula (West). The Colorado River meandered and deposited fertile sediments before reaching the sea. In between the levees that protect Mexicali's agricultural valley are the river and its associated wetlands. On the eastern margin of the river floodplain, farmers cultivate 27,980 hectares that lie within the Municipality of San Luis Rio Colorado, Sonora. On the western margin, there are 180,280 cultivated hectares

within the Municipality of Mexicali, Baja California (Conagua, 2008c). The State of Baja California is located to the Northwest of Mexico, bounded on the north by the State of California, U.S.A, to the east by the State of Sonora, Mexico, to the west by the Pacific Ocean and south by the State of Baja California Sur (Carrillo-Guerrero, 2009).

Within the limits of the States of Baja California and Sonora, is located the section of the Colorado river corresponding to Mexico, where the territorial boundary between the two States, which begins its journey in the diversion dam diverter Jose Maria Morelos up reach the Gulf of California. The areal extent of the proposed model domain proposed to include most of the agricultural areas within the Mexicali and San Luis Valley's (also known as Colorado River Irrigation District 014) (Figure 2).

The region is hot and dry: precipitation averages less than 7.5 cm annually, while maximum daily temperatures may exceed 38° Celsius for more than 5 months each year. The climate generates a significant net outflow of water, with pan evaporation rates in the region exceeding 2.7 m per year. Precipitation tends to fall in two distinct seasons, with winter precipitation generated by moisture from the Pacific Ocean and summer rainfall, often occurring in brief, high-intensity storms, generated by moisture from the Gulf of California. Brief storms can produce substantial runoff from surrounding mountains, though most of this runoff tends to be absorbed by the sandy alluvial soils of the basin floor (Olmsted et al. 1973).

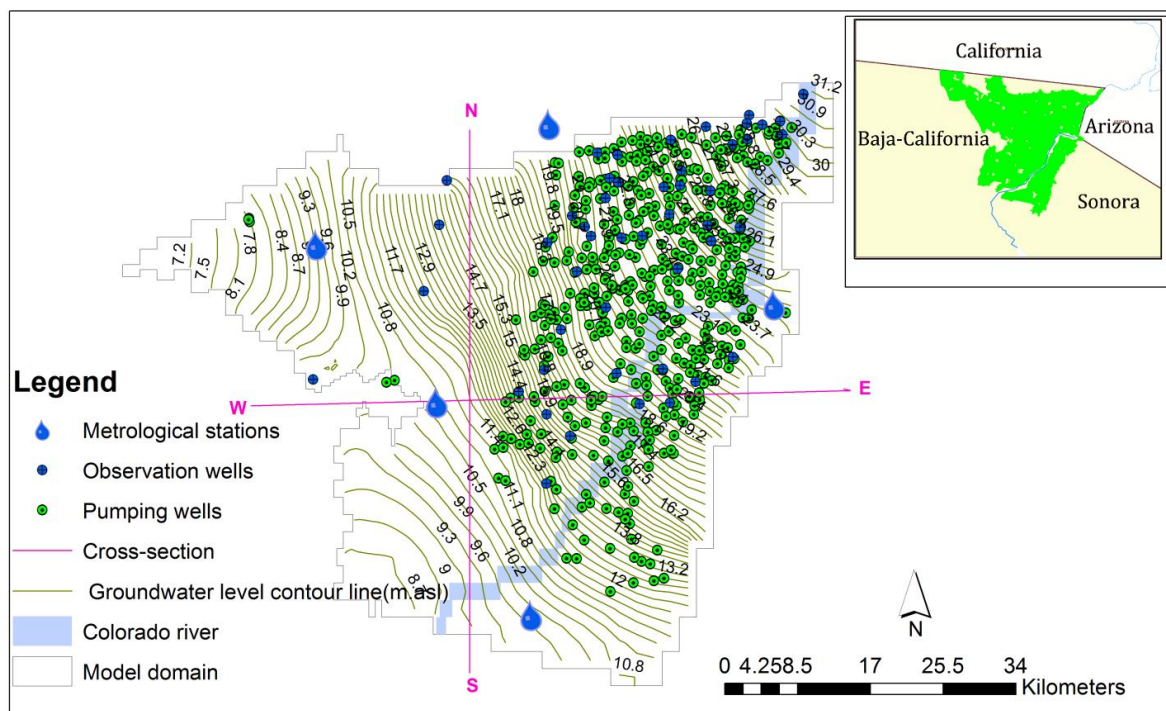


Figure 2. Location of the study area in the Mexicali Valley; US–Mexico border along with pumping wells, climate stations, observation wells and NS-WE cross section lines. Initial groundwater level contour lines in the study area showing the groundwater flow direction following the path of Colorado River.

1.4.1. Water Use in the Irrigation District 014

The Baja California-California border region is bonded by a common geography characterized by its booming population, scarce water supply, and arid land. The natural rivers of this region are among the most regulated, used, and contaminated watercourses in the world. These rivers are currently used to the extent that they often no longer discharge to their respective termini, i.e. the Colorado River, whose billions of cubic meters of annual flow no longer reach, the Gulf of California. This situation is largely driven by upstream diversions and economic forces that make the border region one of the most productive geographic regions in México. This is also one of the driest regions in the country and its explosive growth has put tremendous strain on the limited water resources. The increase in agriculture land brought an increased demand for groundwater in the valley. In general, the water consumption of the valley is fulfilled by diversions from the Colorado River and groundwater pumping, the distributions of main water sources for irrigation district 014 is

shown in Figure 3. For administrative purpose District 014 was divided in 22 irrigation units for administrative purposes, each of them receives a fixed amount of surface water and the administration of each irrigation unit distributes the water to the final agriculture user.

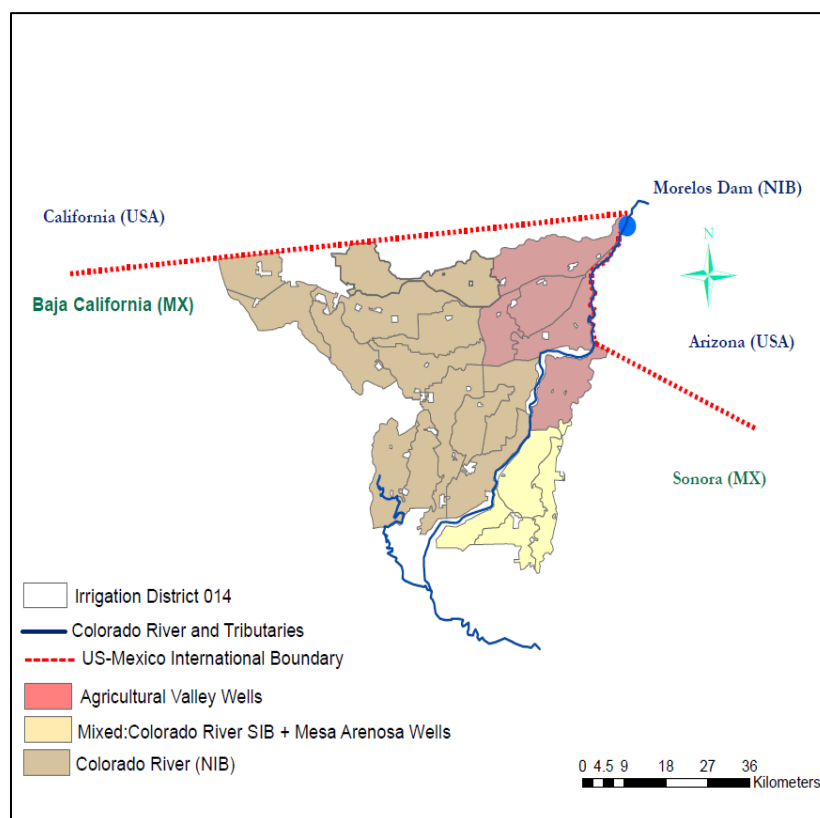


Figure 3. Distribution of Main water sources for Irrigation District 014. NIB and SIB are Northerly international boundary and Southerly international boundary respectively.

The total water available in the district varies accordingly to the US-to-Mexico Colorado River deliveries; usually, 87% of the available volume is consumed by agriculture, 10% is consumed in cities, and 3% is used by industries. The programmed water supply of the District for all users is 2,747.594 million cubic meters, 69% of this volume is Mexico's entitlement to Colorado River flows, 25% of the district's water supply is withdrawn from Mexicali's aquifer in the agricultural valley, and the rest is withdrawn from the wells located in the Mesa Arenosa de San Luis (CONAGUA, 2006a).

The International Water Treaty signed in February of 1944 by the United States of America (U.S.A) and Mexico (Figure 1) established the allocation of flows for each country for 3 of their shared river systems. One of these is the Colorado River. The main stem of the Colorado River meanders more than 2,250 km (nearly 1,400 miles) in a watershed that extends more than 625,000 km² (SRE 1944) and supports 2 million acres of croplands and more than 30 million inhabitants in both countries (Anderson, L. 2002). Mexico has an annual allocation of 1,850.234 million cubic meters (Mm³) of water per year (SRE, 1944); about 10% of the average annual Colorado River flows. The Colorado River flows received at the international boundaries is presented in Figure 4.

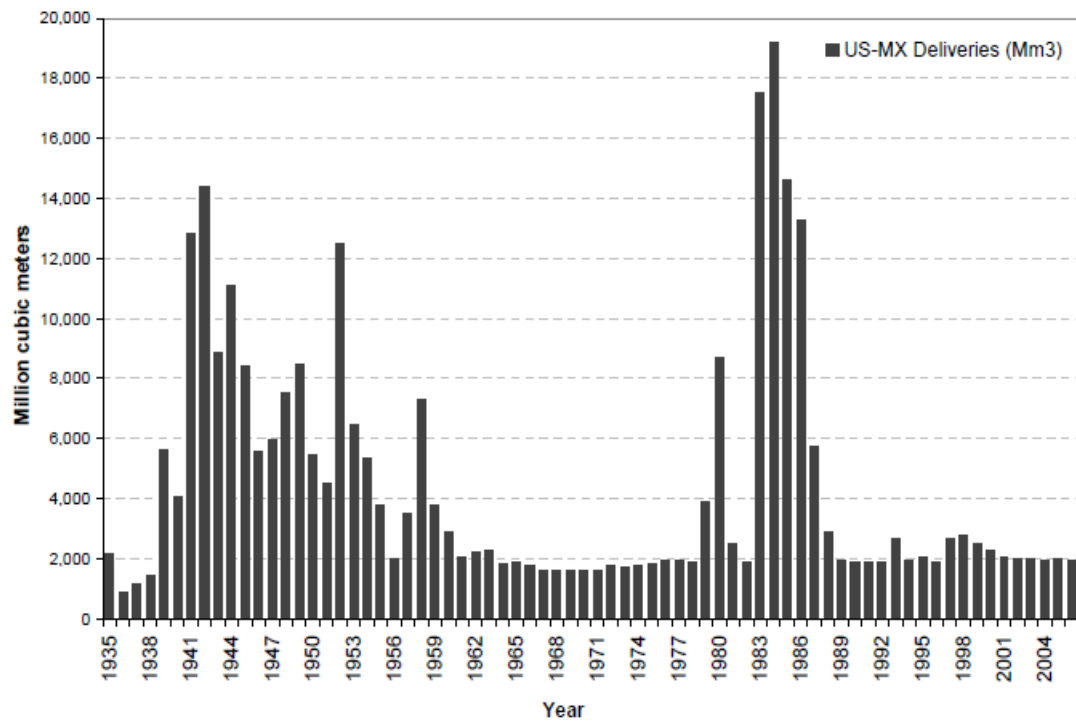


Figure 4. Colorado River flows received at Northernly international boundary(NIB) and Southerly international boundary(SIB) during the period 1935-2006 by Mexico's Irrigation District 014-Rio Colorado (calculated from CONAGUA (2007a), reprinted from Carrillo-Guerrero (2009)).

Agriculture in the Mexicali Valley withdraws approximately 2.5×10^9 m³ of water annually (Roman-Calleros and Ramírez-Hernández, 2003). Pumping of groundwater for

supplementary irrigation in the valley has reduced groundwater levels significantly in some areas (Roman-Calleros and Ramírez-Hernández, 2003).

The study area includes about 489 large production pumping wells, all positioned in layer 1 (Figure 2 and Figure 6). These large-scale production wells are unevenly distributed and are primarily located in the eastern portion of the model domain (Figure 2). Pumping wells are monitored by CONAGUA which maintains records of the monthly volume pumped from each well, and takes a water level measurement from many of the wells once each year.

The well package is designed to simulate the inflow or outflow through recharge or pumping wells. Wells are handled in the package by specifying the location of each well and its rate (positive for recharge and negative for extraction). In the study area, more than 489 water wells are tapping the upper aquifer. The official records of groundwater extraction (Figure 5) for irrigation were used to calculate the annual artificial discharge for each individual well in the study area. The shapefile which contains extraction rate and groundwater well location was prepared and imported into ModelMuse graphical user interface and analyzed using well package.

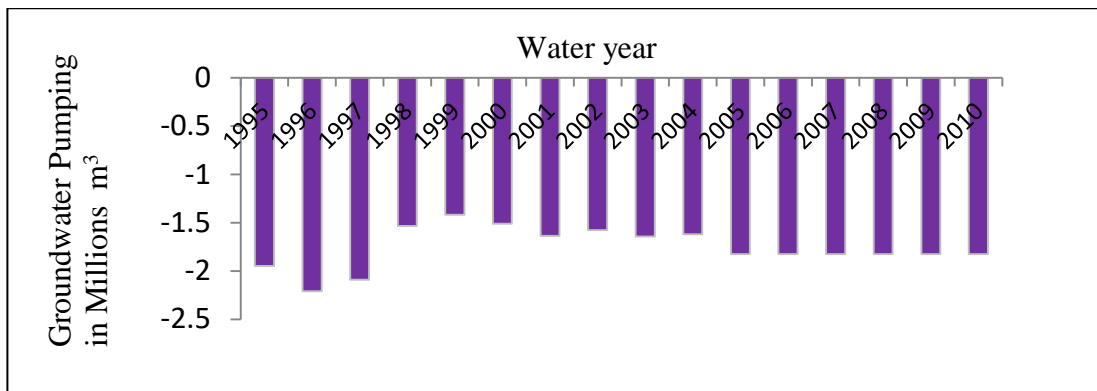


Figure 5. Total annual groundwater extraction for MODFLOW model development

Well pumping rates developed (Figure 5) in the conceptual model were applied to cells that contained point shapefiles representing the location of each wells (Figure 6) using the well-package in MODFLOW.

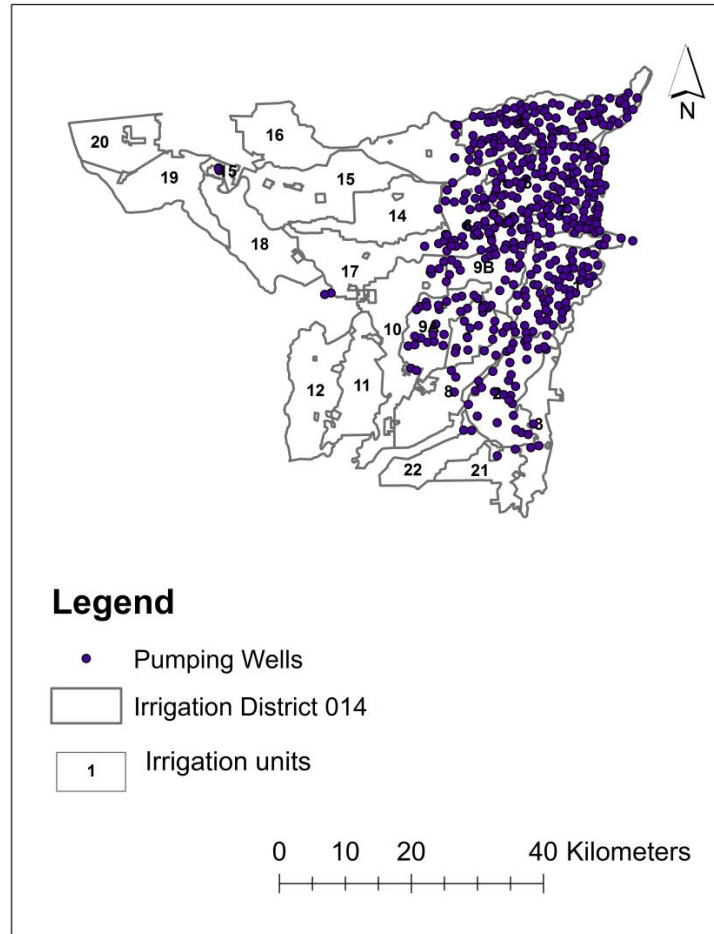


Figure 6. Distribution of large production wells within the study area.

2. Literature Review

2.1. Introduction

Understanding the distribution and the dynamics of the interaction between surface water and groundwater is necessary and essential for assessment or quantification of the contribution of one component to another. Another essential element is conceptual knowledge of the structural and system controls that govern the occurrence and movement of water from the groundwater to the surface water component and vice versa.

It is accordingly essential to begin this literature review by providing a general overview of system components (i.e. various aspects of the spatial distribution of surface water and subsurface water including groundwater) and the dynamics of flow across the

interface between the two components. The overview of the system components is followed by a focus on the nature of linkages between these systems and a discussion on ways of identifying the interaction, and finally a literature review of methodologies for surface water and groundwater interaction (MODFLOW).

2.1.1 Various components of surface water and groundwater

The surface water component comprises of water in the rivers, lakes, dams and overland flow, while the unsaturated zone component constitutes that part of the subsurface where the infiltrating water from rainfall or leakage from runoff does not completely fill the voids in between the soils and rocks. Although flow in the unsaturated zone is generally downwards in response to gravity, relatively impermeable rock layers often impede infiltration to layers below causing horizontal flow that could discharge as seepage to the surface or streams. Such flow is called interflow. The groundwater component comprises the saturated zone that is replenished or recharged by the infiltrating water from rainfall and overlying layers. Seepage from groundwater storage, particularly during extended drought periods sustains streams and such a contribution to surface water is called base flow. Streams that are often observed flowing even long after it had rained are invariably fed by springs and groundwater leakages. Figure 7 conceptually depicts various components of both the surface and subsurface water. However, in real hydrological settings, the system is more complex due to the heterogeneity of the host rocks, where various factors such as climate, geohydrology, ecology and human-induced impacts modify the process of interaction between surface water and groundwater.

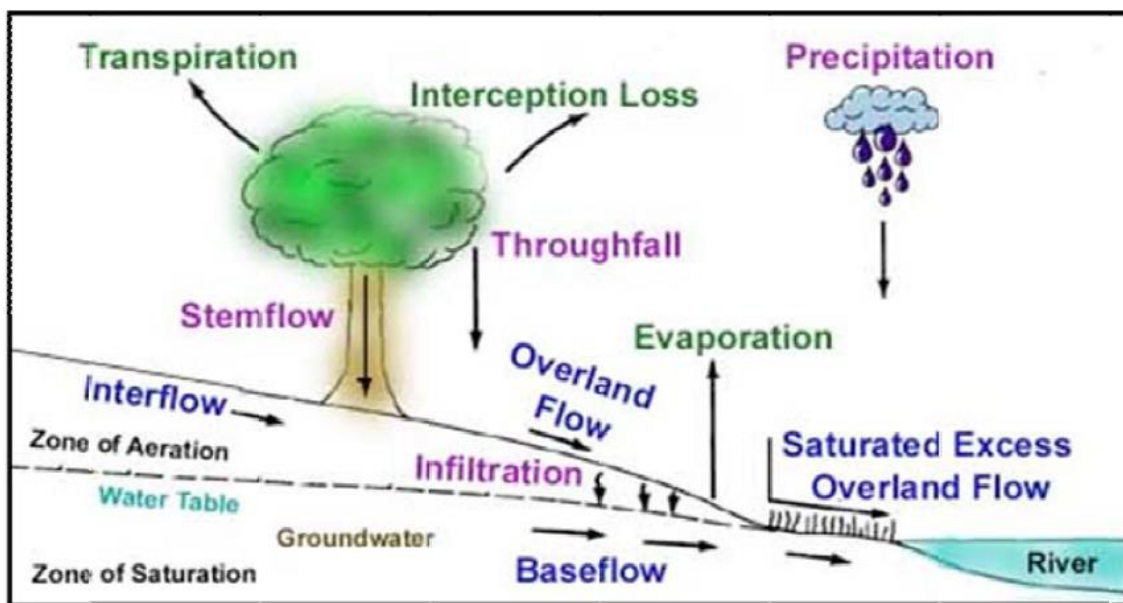


Figure 7. Various components of surface water and groundwater (Berner and Berner, 1987)

Surface water and groundwater have long been considered separate entities, and have been investigated individually (Kalbus et al., 2006). However, hydrologists have always recognized that groundwater and surface water are closely linked, yet studies have mostly been carried out largely by single disciplines. A number of authors (Winter, 1999, Sophocleous, 2002, and Weidong et al., 2007) maintained that surface water and groundwater are undivided components of the hydrologic system since development or contamination of one component commonly affects the response or water quality of the other.

2.2 Detailed literature Review

Movement of water in the atmosphere and on the land surface is relatively easy to visualize, but the movement of groundwater is not. As illustrated in Figure 8, groundwater moves along flow paths of varying lengths from areas of recharge to areas of discharge. The generalized flow paths in Figure 8 start at the water table, continue through the groundwater system and terminate at the stream or at the pumped well. The source of water to the water table (ground-water recharge) is infiltration of precipitation through the unsaturated zone. In the uppermost, unconfined aquifer, flow paths near the stream can be tens to hundreds of meter in length and have corresponding travel times of days to a few years.

The longest and deepest flow paths in Figure 8 may be thousands of meters to tens of miles in length, and travel times may range from decades to millennia. In general, shallow groundwater is more susceptible to contamination from human sources and activities because of its close proximity to the land surface.

Small-scale geologic features in beds of surface-water bodies affect seepage patterns at scales too small to be shown in Figure 8. For example, the size, shape, and orientation of the sediment grains in surface-water beds affect seepage patterns. If a surface-water bed consists of one sediment type, such as sand, inflow seepage is greatest at the shoreline, and it decreases in a nonlinear pattern away from the shoreline. Geologic units having different permeability's also affect seepage distribution in surface water beds. For example, a highly permeable sand layer within a surface-water bed consisting largely of silt will transmit water preferentially into the surface water as a spring.

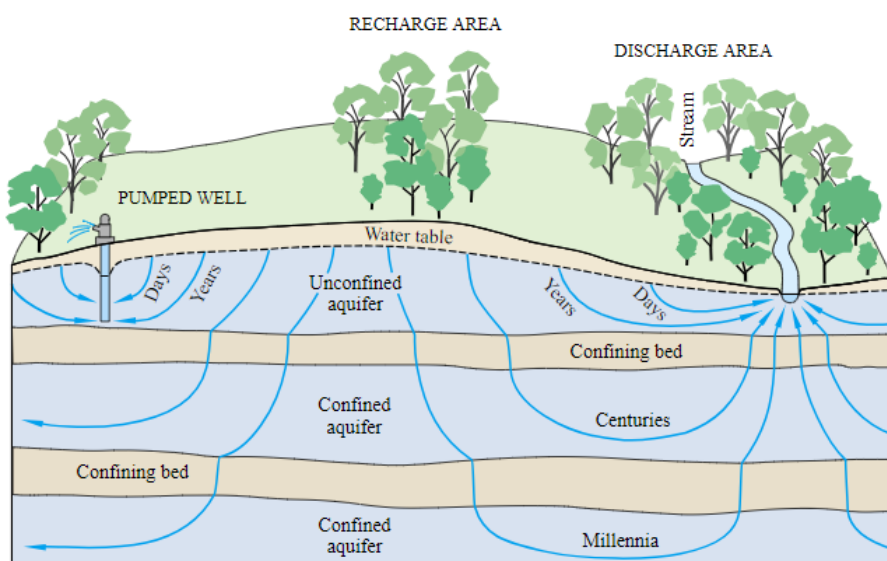


Figure 8. Groundwater flow paths vary greatly in length, depth, and travel time from points of recharge to points of discharge in the groundwater system (Anderson & Woessner, 1992).

Different methods of assessing the interaction between surface water and groundwater have over the years been developed by various investigators. There is a number of approaches used ranging from Darcian flux based methods through chemistry approaches, isotopic hydrology, hydrograph separation methods, to analytical and numerical methods.

A number of authors (e.g. Sophocleous, 2002; Malcolm et al, 2005; Kalbus et al., 2006; and McCallum et al., 2009) discuss various methods of investigating stream-aquifer interactions.

Typical approaches often entail statistical analyses of hydrological data (i.e. rainfall, stream flow and hydrograph) in order to establish connectivity (i.e. whether the river is gaining water from or losing water to the aquifer); application of Darcy's Law, which states that water flux is a function of hydraulic gradient and conductivity; slug and pumping tests to determine hydraulic properties, and field measurements using seepage meters.

Streams interact with groundwater in all types of landscapes. The interaction takes place in three basic ways: streams gain water from inflow of groundwater through the streambed (gaining stream, Figure 9A), they lose water to groundwater by outflow through the streambed (losing stream, Figure 9B), or they do both, gaining in some reaches and losing in other reaches. For groundwater to discharge into a stream channel, the altitude of the water table in the vicinity of the stream must be higher than the altitude of the stream-water surface. Conversely, for surface water to seep to groundwater, the altitude of the water table in the vicinity of the stream must be lower than the altitude of the stream-water surface. Contours of water-table elevation indicate gaining streams by pointing in an upstream direction (Figure 9c), and they indicate losing streams by pointing in a downstream direction (Figure 9d) in the immediate vicinity of the stream. Losing streams can be connected to the ground-water system by a continuous saturated zone (Figure 9A) or can be disconnected from

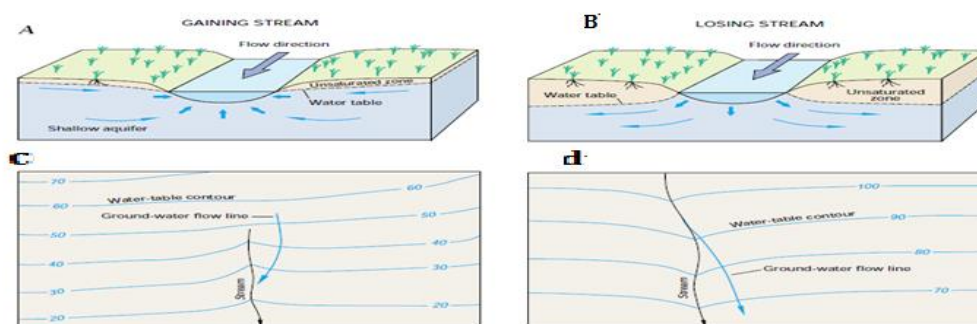


Figure 9. Gaining and losing streams situations which receive water from the Groundwater system and Losing streams lose water to the groundwater system (Anderson & Woessner, 1992)

the ground-water system by an unsaturated zone. Where the stream is disconnected from the groundwater system by an unsaturated zone, the water table may have a discernible mound below the stream (Figure 10) if the rate of recharge through the streambed and unsaturated zone is greater than the rate of lateral groundwater flow away from the water-table mound. An important feature of streams that are disconnected from groundwater is that pumping of shallow groundwater near the stream does not affect the flow of the stream near the pumped wells.

In some environments, streamflow gain or loss can persist; that is, a stream might always gain water from groundwater, or it might always lose water to groundwater. However, in other environments, flow direction can vary a great deal along with a stream; some reaches receive groundwater, and other reaches lose water to groundwater. Furthermore, flow direction can change in very short timeframes as a result of individual storms causing focused recharge near the streambank, temporary flood peaks moving down the channel, or transpiration of groundwater by streamside vegetation.

A type of interaction between groundwater and streams that takes place in nearly all streams at one time or another is a rapid rise in stream stage that causes water to move from the stream into the streambanks. This process, termed bank storage (Figures 10), usually is caused by storm precipitation, rapid snowmelt, or release of water.

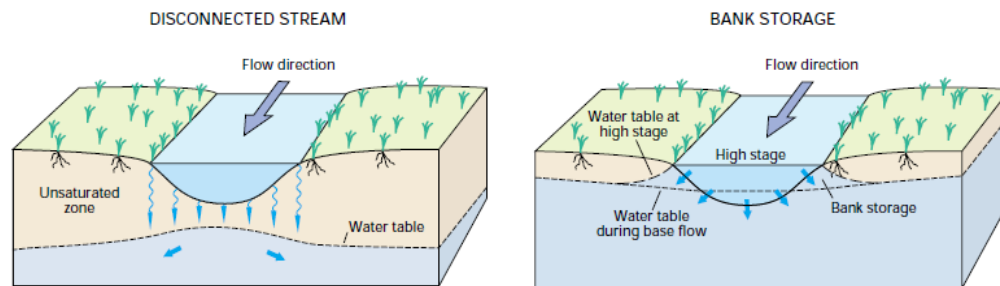


Figure 10. Typical Examples of disconnected streams and Bank storage system (Anderson & Woessner, 1992)

2.3. Evaluation of surface water-groundwater interaction using Numerical Models

There are two main categories of numerical modeling methods, namely the gridded or discretized method that entails grids or a mesh of small elements, and the non-gridded or mesh-free method, also called the boundary element method which is only discretized at

boundaries or along flow elements. In this study only gridded method (MODFLOW) will be used to develop surface water-groundwater model.

The gridded methods such as the finite element or finite difference methods solve the groundwater flow equation by breaking the problem domain into small elements such as squares and blocks. The flow equation is then solved for each element where all material properties are assumed constant or linearly variable within an element, and then linking together all elements using conservation of mass across boundaries between elements.

2.4. Flow Model

Groundwater flow is a process that is controlled by the properties of the fluid (water) and the properties of the substrate through which the fluid moves. The three-dimensional flow of water of constant density through a porous, anisotropic, heterogeneous subsurface medium can be described by the following partial differential equation:

$$\frac{\partial}{\partial x} \left(K_h \frac{\partial h}{\partial x} \right) + \frac{\partial}{\partial y} \left(K_h \frac{\partial h}{\partial y} \right) + \frac{\partial}{\partial z} \left(K_v \frac{\partial h}{\partial z} \right) \pm W = S_s \frac{\partial h}{\partial t} \quad (1)$$

Where x , y , and z represent the coordinate axes parallel to the major axes of hydraulic conductivity;

h is the hydraulic head;

K is hydraulic conductivity [L/t];

W is a volumetric flux per unit volume of aquifer representing sources and/or sinks of water [t^{-1}];

t , represents time [t]; and S_s is specific storage [1/t].

The groundwater flow system is described by applying equation (1) to a system that has specified boundary and initial conditions (McDonald and Harbaugh 1988, Freeze and Cherry 1979).

Because of the inherent complexities of groundwater systems, analytical solutions of equation (1) are time-consuming and difficult to obtain for large-scale real-world scenarios. The application of a finite difference approach simplifies the problem so that an approximate solution may be attained with numerical methods. This simplification is achieved by breaking the model domain into a finite number of three-dimensional cells.

A node at the center of each cell (node-centered cell) is the point for which hydraulic head and a mass balance is calculated at each time step as water flows from cell to cell within the model. Each cell in the finite difference grid can be independently parameterized allowing for the development of a simplified representational system.

2.4.1 MODFLOW

MODFLOW is one of the most widely used surface water/groundwater models. MODFLOW solves the three-dimensional equation (1) for groundwater flow using a finite difference grid representation of the flow system. The MODFLOW user defines the boundary and initial conditions, the number of iterations the model should run through and the convergence criteria for each iteration. The basic model output is an array of values of the hydraulic head with one value per MODFLOW cell. The discretization approach used in MODFLOW requires that the model domain is broken into a grid of three-dimensional cells each with a unique row, column, layer (i, j, k) identifier (Figure 11).

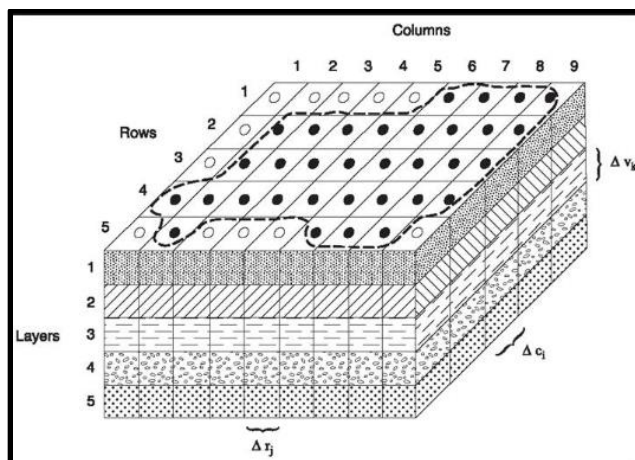


Figure 11. A discretized hypothetical aquifer system (Harbaugh et al. 2000)

Choice of an appropriate numerical method for simulation of surface water-groundwater interaction is informed by the conceptual model of the system in the study area. In other words the first approach should be the development of the physical and the mathematical conceptual model of the system. Any groundwater flow simulation requires a good conceptual hydrogeological model and the development of a systematic database accounting for all the model input parameters (Ayenew and Tilahun, 2008).

This task may require collection field data and information, as well as a reference to published information products such as maps and databases. The conceptual model is a descriptive representation of hydrogeological understanding of how water flows in to, through and out of a ground water system (Ayenew and Tilahun, 2008).

This is usually presented in the form of diagrams and maps of the physical characteristics of the geological formation geometry and the flow systems/directions. The mathematical model is the assembly of numerical data sets that reflect the conceptual model, and the computer coded package of equations that enable calculation of changes in water level or pressures in the various geological strata to be calculated. Then with all the input parameters, meteorological and hydrological data considered and available, one may identify an appropriate numerical models to use for simulation, calibration, and prediction or for use as required.

2.4.1.1. MODFLOW Packages

The modular structure of MODFLOW consists of a Main Program and a series of highly-independent subroutines called modules. The modules are grouped in packages. Each package deals with a specific feature of the hydrologic system which is to be simulated such as flow from rivers or flow into drains or with a specific method of solving linear equations which describe the flow system such as the Strongly Implicit Procedure or Preconditioned Conjugate Gradient. The division of MODFLOW into modules permits the user to examine specific hydrologic features of the model independently. This also facilitates the development of additional capabilities because new modules or packages can be added to the program without modifying the existing ones. The input/output system of MODFLOW was designed for optimal flexibility. MODFLOW-2005 version includes the following functionality that is documented in Harbaugh (2005).

BAS	: Basic Package
BCF	: Block-Centered Flow Package
LPF	: Layer-Property Flow Package
HFB	: Horizontal Flow Barrier Package
CHD	: Time-Variant Specified-Head Option
RIV	: River Package

DRN	: Drain Package
WEL	: Well Package
GHB	: General Head Boundary Package
RCH	: Recharge Package
EVT	: Evapotranspiration Package
SIP	: Strongly Implicit Procedure Package
PCG	: Preconditioned Conjugate Gradient Package
DE4	: Direct solver

The following functionalities are also included. This functionality is documented in separate reports for use in earlier versions of MODFLOW. Conversion of this functionality to work with MODFLOW-2005 is documented in separate files that are provided with the MODFLOW-2005 distribution.

FHB	: Flow and Head Boundary Package
IBS	: Interbed Storage Package
GMG	: Geometric MultiGrid Solver Package
HUF	: Hydrogeologic-Unit Flow Package
MNW1	: Version 1 of Multi-Node Well Package
MNW2	: Version 2 of the Multi-Node Well Package
ETS	: Evapotranspiration with a Segmented Function Package
DRT	: Drains with Return Flow Package
RES	: Reservoir Package
SUB	: Subsidence Package
OBS	: Observation Process
SFR	: Streamflow-Routing Package
LAK	: Lake Package
UZF	: Unsaturated Zone Package
GAG	: Gage Package
SWT	: Subsidence and Aquifer-System Compaction Package
LMT	: Link to the MT3DMS contaminant-transport model
HYDMOD	: Hydrograph capability

PCGN : Preconditioned Conjugate Gradient solver with improved nonlinear control

The One-Water Hydrologic Flow Model (MF-OWHM) (Hanson and others, 2014) is a MODFLOW-based integrated hydrologic flow model (IHM) that is the complete version, to date, of the MODFLOW family of hydrologic simulators needed for the analysis of a broad range of conjunctive-use issues. Conjunctive use is the combined use of groundwater and surface water. MF-OWHM allows the simulation, analysis, and management of nearly all components of human and natural water movement and its use in a physically-based supply-and-demand framework.

MF-OWHM is based on the Farm Process for MODFLOW-2005 (MF-FMP2, Schmid and Hanson, 2009) that is now combined with Local Grid Refinement (LGR, Mehl and Hill, 2013) for embedded models to allow use of the Farm Process (FMP) and Streamflow-Routing (SFR) within embedded grids. MF-OWHM also now includes new features such as the Surface-water Routing Process (SWR, Hughes and others, 2012), Seawater Intrusion (SWI, Bakker and others, 2013), and Riparian Evapotranspiration (RIP-ET, Maddock III and others, 2012). MF-OWHM contains all the previously available solvers and the new solvers such as Newton-Raphson (NWT, Niswonger and others, 2011) and the nonlinear preconditioned conjugate gradient (PCGN, Naff and Banta, 2008).

What makes MF-OWHM unique is that it allows the simulation of head-dependent flows, flow-dependent flows, and deformation dependent flows that collectively affect the conjunctive use of water resources. The supply-constrained and demand-driven framework combined with the linkages between packages and processes provides relations of water use and movement, and helps to prevent mass loss to an open system thus facilitating the accounting for "all of the water everywhere and all of the time."

2.4.2. Setting up a finite difference numerical model

In constructing a finite difference numerical model to represent the spatial variability in the system being modeled, the area is overlain by a rectangular grid, with each cell in the grid representing a point at the center of that cell (block centered grid) or at the intersection of the grid lines (mesh-centered grid). These are node points at which the solution of the

unknown values, such as the water fluxes is sought or determined. The choice of the type of the grid mainly depends on boundary conditions.

For instance, it is more convenient to use block centered grids in cases where the flux is specified while mesh centered types could be more useful where values of the head are specified. The grid can be applied to a number of layers if the hydraulic characteristics of the geological section vary with depth.

Each layer can represent the various formations that occur within the model domain. Each individual cell, within each layer is then assigned a range of properties determined from the investigation work, such as the ability to store water, the ability to transmit water (horizontally and vertically), the vertical thickness of the formation at that point, and water level or pressure (Ayenew and Tilahun, 2008).

Hence, the general assumption is that all discharge from or recharge to the nodal area occurs at the node point and that water levels in the entire nodal area are the same as at that node point. In fact each cell is a hydrologic response unit (HRU) and the discretization is based on hydrologic and physical characteristics such as drainage boundaries, land-surface altitude, slope, and aspect; plant type and cover; land use; distribution of precipitation, temperature, and solar radiation; soil morphology and geology; and flow direction. Each HRU is assumed to be homogeneous with respect to these hydrologic and physical characteristics and to its hydrologic response (Markstrom et al., 2008).

As part of the discretization process, rivers or streams are divided into reaches and segments where a reach is defined as a section of a stream that is associated with a particular finite difference cell. More than one stream reach can be assigned to a particular finite difference cell, but only one finite-difference cell can be assigned to a single reach.

Reaches are grouped into segments that represent lengths of the stream between connections with another stream or tributary, a lake, or a watershed boundary. User-specified inflows to a stream that are external to inflows calculated by the model are added to the stream at the upstream end of a segment. Specified outflow at the upstream or downstream end of a segment can be used to divert water from a stream to a pipeline or lined canal; the water that is diverted in this way is removed from the modeled area without surface water-groundwater interaction.

2.4.3. The initial conditions, boundary conditions and model input parameters

Initial conditions for changes in hydraulic head or drawdown are often assumed zero everywhere since these are caused usually by pumping and computed drawdown can be superimposed on natural flow system. In water-table conditions, a head distribution should be specified as an initial condition. If available observation data are limited, interpolation techniques using the relationship between water levels and altitude may be used to estimate initial hydraulic head values. On the other hand, a transient simulation should start from a steady state position.

The nature or type of boundary conditions can be deduced from field evidence or a hydrogeological conceptual model of the system. Cells used for simulation of boundary conditions may either be specified head (i.e. constant head) such as is the case in the boundary between the aquifer and the river, or no flow cells (where flow into cells or flow out of cells is not allowed).

The rest of the cells are variable-heads where groundwater head, vary with time and are thus computed. Time-variant inflow and (or) outflow boundary conditions can be assigned to variable-head cells using MODFLOW stress packages such as the Well Package, where the stress rates can only be change at the beginning of a stress period. Another type of possible boundary condition applied to variable-head cells is the head-dependent flow boundary condition. Interaction of groundwater with streams and lakes is an example of a head-dependent flow boundary condition (Markstrom et al., 2008).

The input data is often estimated from pump testing results, previous studies, and observation measurements or adjusted through calibration.

2.5. Uncertainty in the Conceptual Model

All conceptual models are qualitative and uncertain due to our inability to represent the full complexity of even a simple hydrogeological system. Moreover, the field data on which the conceptual model is based are always incomplete and provide only an approximate description of true hydrologic condition.

Two approaches can be used to address uncertainty in the conceptual model.

1. The conceptual model is updated and revised as new information becomes available. The new information includes new field data as well as information gained during model calibration and uncertainty.

2. Alternative versions of the conceptual models are developed. Wuolo (1993) likened this approach to T.C. Chamberlin's (1897) well-known concept of multiple working hypotheses on which a geologist formulates several possible hypothesis that could account for the phenomenon being studied, but with a better understanding of the system, some of the hypothesis are eliminated and a new one may be proposed. In groundwater modeling, the alternative conceptual models are tested during calibration and forecast uncertainty.

In practice, the Project Budget and modeling purpose determine how much effort is devoted to identifying alternative conceptual models. A favored conceptual model might be updated and revised during the modeling process and retained as the final conceptual model if the numerical model on which it is based is satisfactorily calibrated and judged to perform well during uncertainty analysis. If a numerical model fails either of these criteria, one or more alternative conceptual models can then be tested.

2.6. Common Modeling Errors

- The modeler constructs a model to learn something about the system without defining a specific purpose or framing specific questions. Although modeling without a well-defined propose might be helpful in the initial stage of an interpretive generic modeling exercise, even a generic model benefits from a well-defined purpose. The purpose helps the modeler select the purpose, parameters, and level of detail to include in the conceptual and numerical models.
- The modeler becomes enamored with a conceptual model. Field data alone rarely support the selection of a single conceptual model, especially after project resources are depleted. Yet, a single conceptual model is often selected for convenience and the modeler might be reluctant to let go of favored model, especially after significant investment of resources. However, during model calibration, the presence of recalcitrant misfit and optimal calibrated parameter values those are at the extreme of a hydrogeologically reasonable range may require revising the conceptual model, or selecting an alternative conceptual model, and repeat the modeling process.

- The modeler builds a detailed "real-world" conceptual model that is inappropriately complex for constructing a numerical model given the modeling purpose, budget, and time available. In some scientific applications constructing the conceptual model is the sole objective; in those cases, the conceptual model appropriately includes every possible process and parameter that might influence the outcomes. However, in groundwater modeling, the purpose of constructing a conceptual model is to distill the real world to a representative set of processes and parameters that can be simulated in a groundwater flow code and is appropriate to the modeling purpose.

3. Research Methods and Materials

3.1. Methodology flow chart

The methodology applied to answer the research question and to come up with the targeted objective is summarized in the flowchart in and the model calibration process step followed (Figure 12).

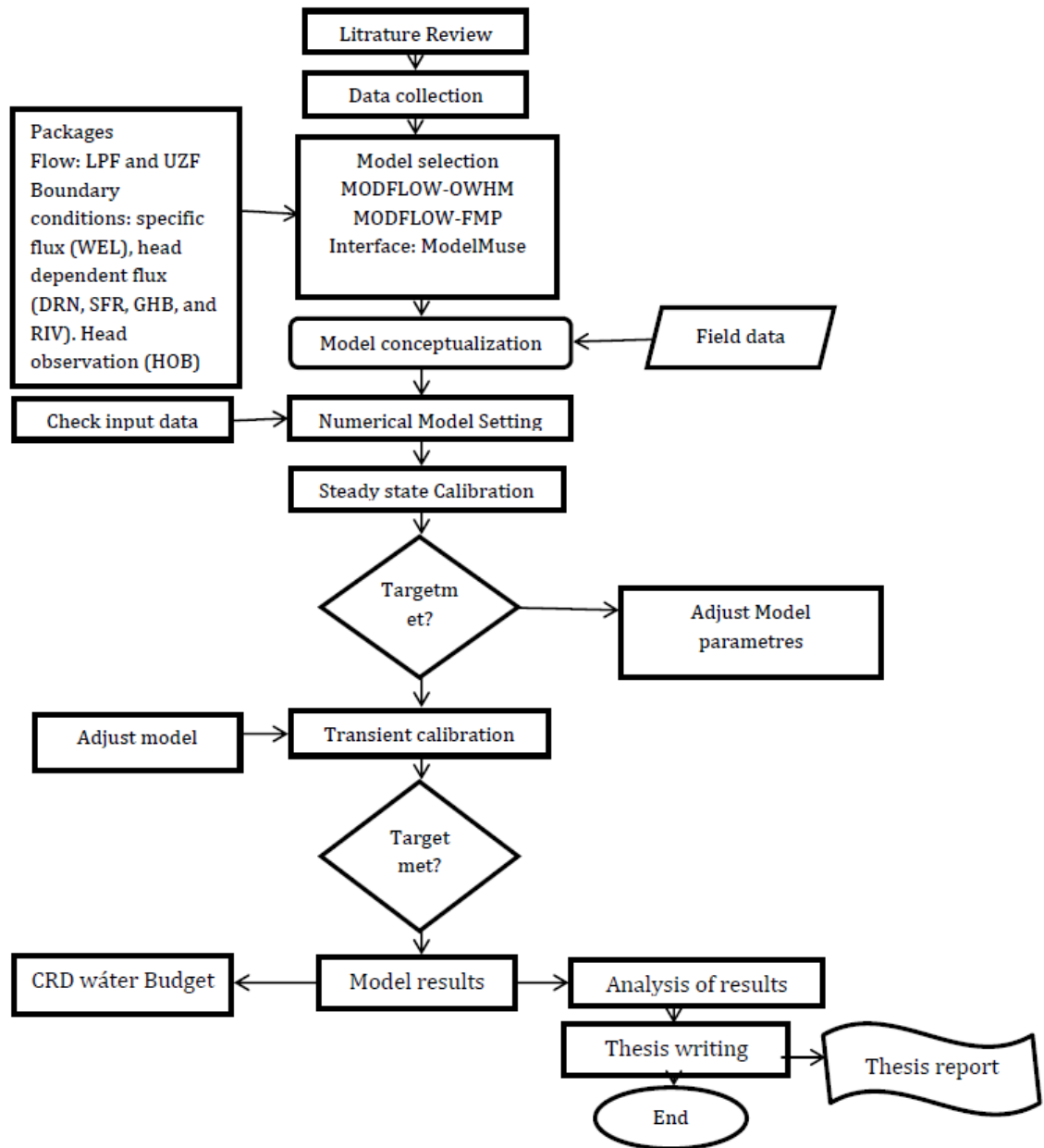


Figure 12: Flowchart showing methodologies applied and the processes followed during the study

3.2. Data collection and model input preparation

Data analysis and input preparation is a pre-calibration activity, which is needed to provide the base for effective model simulation. Meteorological and hydrogeological data were collected, analyzed and pre-processed according to the model requirement to

facilitate model simulation. The model was simulated for 8 hydrological years from October, 01, 2002 to September, 30, 2010.

3.2.1. Precipitation

Precipitation is the most important input for hydrological models. Precipitation at land surface is partitioned in the UZF1 package (Niswonger et al., 2006) into runoff, infiltration, evapotranspiration, unsaturated-zone storage, and recharge.

Andrade, San Luis, Zacatecas, Nuevo Leon and Mexicali, stations (Figure 2) were used to estimate the meteorological data, such as precipitation, evapotranspiration, temperature, etc. This data was aggregated to annual time step in order to match the UZF1 package input requirement.

3.2.2. Potential evapotranspiration

McMahon et al. (2013) defined PET as the rate at which evapotranspiration would occur from a large area completely and uniformly covered with growing vegetation which has access to an unlimited supply of soil water, and without advection or heat storage effects. PET is one of the driving forces in the applied modeling solution involving UZF1 package. In UZF1, the PET is applied at the land surface and decreases linearly with depth down to the assigned extinction depth where evapotranspiration no longer occurs (Allander et al., 2014).

There are two methods to convert ET_o to PET. The first is the single crop coefficient, in which the evapotranspiration differences between reference grass and the crop is combined into one single coefficient and depends only on crop characteristics, crop type, and growth stage. The second is the dual crop coefficient which requires detailed data of the crop and soil. In this approach, the crop coefficient is split into two factors describing separately the differences in evaporation and transpiration between the crop and reference surface (Allen et al., 1998). Since detailed data about the crop/vegetation and soil of the area is not available, the single crop coefficient (K_c) method was applied in this study. Following that method, PET is calculated using Equation 2.

$$PET = ET_0 * Kc \dots\dots\dots(2)$$

Where: ET_0 - reference evapotranspiration [mm day^{-1}] and Kc - crop coefficient [-]

ET_0 values for different years in the model area were taken from the freely available web page of <http://www.simarbc.gob.mx/>. Those values of ET_0 were converted into PET as per the crop cover and the respective crop coefficient in the irrigation District 014. The water sources and the crop coverage for irrigation District 014 are presented below.

Table 1. Percent of wheat, alfalfa, and cotton cultivated areas according to a water source (Calculated from CONAGUA (2006)).

Crop	Colorado River	Gw wells_Federal	Gw wells_Private
Wheat	48%	46%	42%
Alfalfa	16%	18%	18%
Cotton	11%	23%	16%
% Total Irrigated Area	74%	86%	76%

Table 2. Percentage of the total irrigated area by crop for 3 agricultural years (calculated from CONAGUA (2006)).

Crop	1999-1998	2004-2005	2005-2006
Wheat	29%	39%	47%
Alfalfa	17%	24%	17%
Cotton	34%	15%	14%

3.2.3. Infiltration rate

Infiltration rate is the amount of water per surface area per time that percolates to the soil. It is an input for UZF1 package applied at the surface. The infiltration rate was calculated from the recharge which is applied to each irrigation fields at the different season as required by UZF1 package.

The average infiltration rate over the 8 year simulation period applied for steady-state was 1.687 mm day⁻¹. In the transient model, the infiltration rate input was calculated annually for each time step in order to account for the temporal variability of subsurface fluxes. The calculated PET and Infiltration rates are found in Figure 16.

3.3. Conceptual Hydrological Model

Anderson and Woessner (1992) defined the conceptual model in the context of groundwater studies as a pictorial representation of the groundwater flow system. Its ultimate objective is to configure the field problem in a simple but meaningful schema to ease analysis procedures and the field data organization. The representation could be in the form of a block diagram or a cross-section of the model area. Moreover, it is an important tool that determines the numerical model dimensions and design of grids. To sum up, the conceptual model is a foundation of a numerical model and its closer representation to the field situation influences the accuracy of numerical model results. In order to build a conceptual model, the authors mentioned three important steps to be followed, namely; defining hydrostratigraphic units, preparing water budget and defining the flow system. These steps for the study area are more elaborated in the following Subsections.

3.3.1. The Areal extent of the Model Domain

The first step in the formation of the model is defining the area of interest; it includes defining the flow domain, identifying the natural hydrologic boundaries, etc. The areal extent of the Colorado River Delta model in this study is designed to include almost all of the agricultural areas within the Mexicali and San Luis Valley, Colorado River irrigation district 014. Inside the model domain, there are 22 existing irrigation units which have an overall area of more than 247,118 hectares (Figure 2).

3.3.2. Geo-hydrological conditions at the model borders

Groundwater flow in the main aquifer layer is governed by conditions at the boundaries of the regional system. The geohydrological borders considered in this model are to the W and SW, the Cucapá Mountain Range and El Mayor which is impermeable regions, that is the flow of underground water may not cross this border and it is considered as a no-flow boundary.

In the NW, the Rio Nuevo is considered as one of the outflow Zone. In the north, the Drain Mesa can be considered as inflow zone for the model. In the East, the Sonora/Arizona may be considered as a zone of inflow to the aquifer system. In the south, the Gulf of California is considered as a border of constant potential that is a zone where outflow from the aquifer is considered to occur. The boundaries of the study are summarized in Table 3 and Figure 13.

Table 3: Geohydrologic conditions of the model boundaries

s. no	Direction	Features	Expected Geohydrologic condition	Boundary
1	SW&W	Mountain range El mayor and Cuapá	Impermeable	No flow
2	NW	Rio Nuevo /Mexicali	Outflow	GHB
3	NE and E	Arizona/Sonora	Inflow	GHB
4	S	Gulf of California	Inflow/Outflow	GHB

When a head dependent boundary; GHB, is implemented, the code calculates flow across the boundary using the hydraulic gradient between a user specified boundary head and model calculated head at boundary node. The boundary which is impermeable may be represented using no flow conditions.

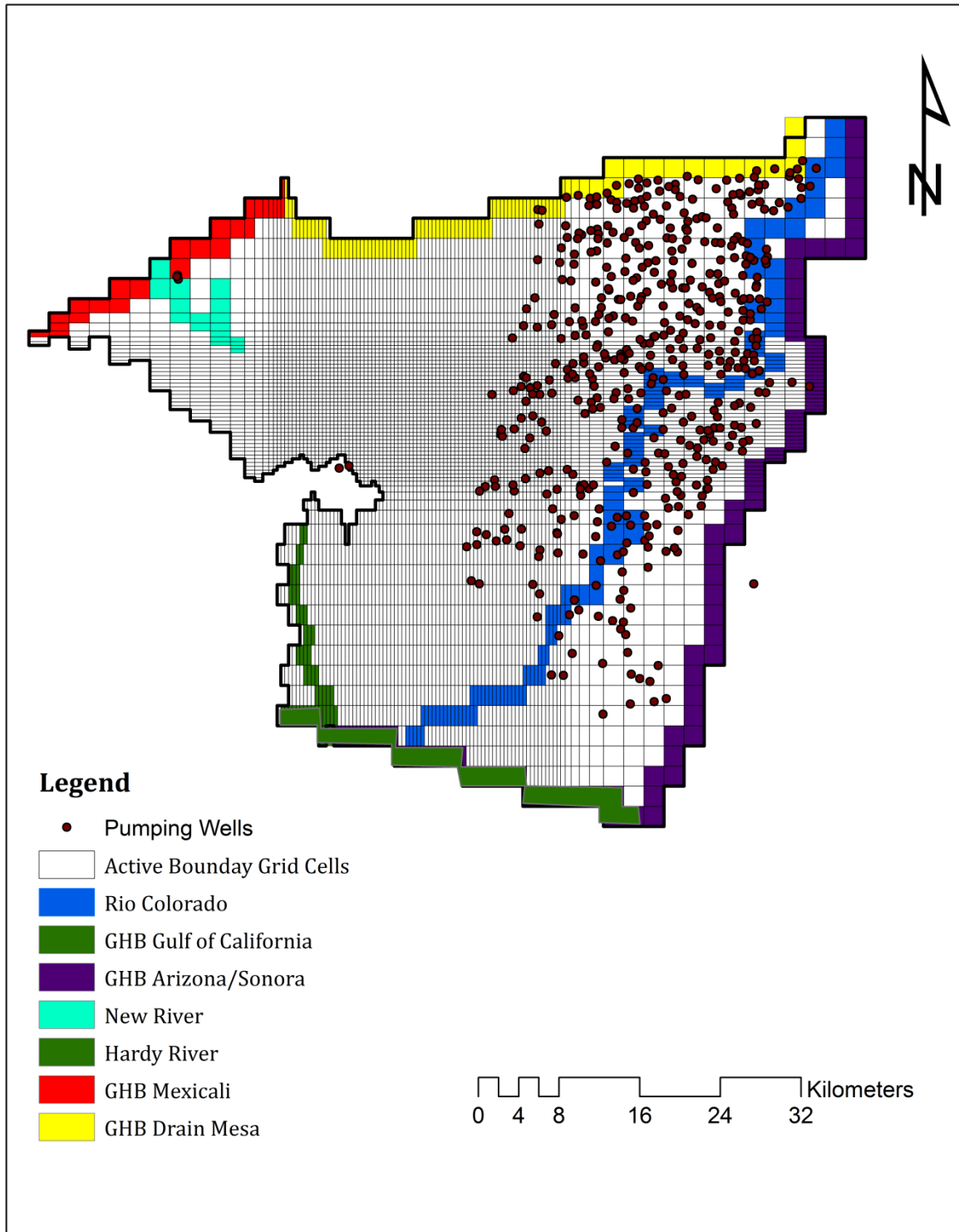


Figure 13: Boundary conditions and hydrologic features used for MODFLOW simulation.

3.4. Geology and hydrogeology

Geologic mapping and an aquifer testing campaign in the Colorado River Delta would greatly increase the applicability of the Yuma (U.S.A) data to the portion of the Colorado River Delta within Mexico. The two areas coevolved through the scouring and depositional processes associated with the evolution of the Colorado River Basin and they are considered to be hydrologically connected (Feirstein et al., 2008).

Older areas of the basement rock in the modeled Colorado River Delta are overlaid by upper Cretaceous granite and early Tertiary sequences of sedimentary rock with areas of volcanic intrusions and meta-sediments primarily associated with geothermal activity in the west. These sedimentary rocks constitute the lower of two sedimentary units in the modeled Colorado River Delta and are composed of consolidated to semi-consolidated mudstone-siltstone and well-sorted sandstone of continental origin overlying marine sedimentary rocks such as siltstone and shale. The lower sedimentary unit roughly correlates to the poor water-bearing rocks of Tertiary age as defined by (Mock.et.al, 1988), and is hydrologically less significant than the upper sedimentary unit above it.

The upper sedimentary unit is composed of fluvial and alluvial non-consolidated sediments of Pleistocene to recent ages. This unit composition includes thick Quaternary deltaic sediments of clays, sands, and gravels periodically interstratified by volcanic deposits. In Yuma Arizona, NE of the study area, the upper unit has been further divided into three layered hydrologic zones which are known (from the bottom to the top) as the Wedge zone, the Coarse Gravel zone, and the Upper Fine-Grained zone.

The wedge zone which has an average thickness of 760m is considered a single heterogeneous water-bearing hydrostratigraphic unit composed of irregularly layered sands, gravels, silts, and clays. In the lower 300m of the wedge zone, hydraulic conductivity and porosity decrease as clay and silt deposits become more prevalent.

Above the wedge zone, there is a 30m highly permeable coarse gravel zone composed primarily of irregularly layered coarse gravel and sand. This unit constitutes the main pathway for horizontal groundwater flow in the system (Olmsted.et.al, 1973).

The upper sediments of the Mexican Colorado River Delta basin with a composition of fluvial and alluvial non- consolidated sediments of Pleistocene to Recent ages may be represented by the wedge zone and the coarse gravel zone together. Horizontal hydraulic

conductivity values for the wedge zone and coarse gravel zone combined were determined to range up to 400 m/d. The vertical hydraulic conductivity of 0.03 m/d, a storage coefficient of 10^{-3} , and a specific yield between 0.18 and 0.35 were estimated and reported by Feirstein et al. 2008.

The Upper Fine-Grained zone which has a thickness ranging from 0 to 75 m consists primarily of floodplain alluvium and windblown sand. Horizontal hydraulic conductivities were calculated to range from 15 to 150 m/day. Vertical hydraulic conductivities were undetermined for the Upper Fine-Grained zone, but a storage coefficient of 10^{-3} and specific yield of between 0.18 to 0.35 were estimated (Mock et al., 1988).

In terms of regional hydrogeological significance, the primary source of groundwater in the Colorado River Delta is agriculturally related infiltrated Colorado River water. The majority of subsurface flow moves towards the Gulf of California in Mexico following the path of the Colorado River. The flow is easily influenced by local pumping from irrigation wells, because of the high transmissivity of the basin sediments (Olmsted et al., 1973).

Water flow in the subsurface occurs primarily in the Coarse-Grained zone and the sandy layers of the Upper Fine Grained zone above it. Together these units behave as a semi-confined aquifer. The principal source of surface water in the study area is the Colorado River which, when it is flowing, meanders between its levees through the low relief terrain of the Delta. Surface water is also transmitted in the research area via canals, drains, and the main tributary of the Colorado River. The Colorado River flows crossing the international boundary are regulated in accordance with the 1944 U.S.-Mexico treaty which states that no less than 1,850,234,000 m³/yr of Colorado River water is to be released into Mexico each year (U.S.A-Mexico Joint Projects 1944 treaty). The water from Colorado River water is diverted into Mexico at Morelos Diversion Dam 1.8 km downstream of the Northern International Border (NIB) and approximately 25 km upstream of the Southern International Border (SIB) (See Figure 1). Downstream of Morelos Dam water is diverted into agricultural fields throughout the research area using Distribution canals.

A conceptual model is constructed from hydrostratigraphic units. These are units with similar hydrogeological properties that may be combined into a single unit or a geologic

formation may be subdivided into aquifers and confining units depending on the hydrogeological characteristics (Anderson and Woessner 1992).

3.4.1. Model Layer 1

The upper unconfined layer was designed to reflect a combination of the hydrologically important units of the region including the Upper Fine Grained zone, and the Coarse Gravel zone and part of wedge zone from the land surface to a depth of 120 m. Based on aquifer test values of hydraulic conductivity for the first layer vary from a minimum of 30 m/day (3.47×10^{-4} m/s) to a maximum of 550 m/day (6.36×10^{-3} m/s) while the regional specific yield ranges between 0.18 and 0.35. These values were later verified through manual calibration.

The first layer is the layer where most water extraction occurs for agricultural use, and also detail lithology of this layer was defined by many authors that the geohydrologic properties of this layer was clearly defined.

3.4.2. Model Layer 2

This layer represents the less hydrologically significant thick lower unit of consolidated to semiconsolidated mudstone-siltstone and well-sorted sandstone of marine and continental origin. Layer 2 has a thickness of 680 m. In second layer a uniform horizontal and vertical hydraulic conductivity of 0.001 m/d and 0.03 m/d respectively was considered (Feirstein et al., 2008). A specific storage of 3×10^{-5} 1/m was also assigned.

3.4.3. Surface water features

The surface water features included in this model are the Colorado River and multiple drains. In this model, New River and the Hardy River were considered as drains (Figure 14).

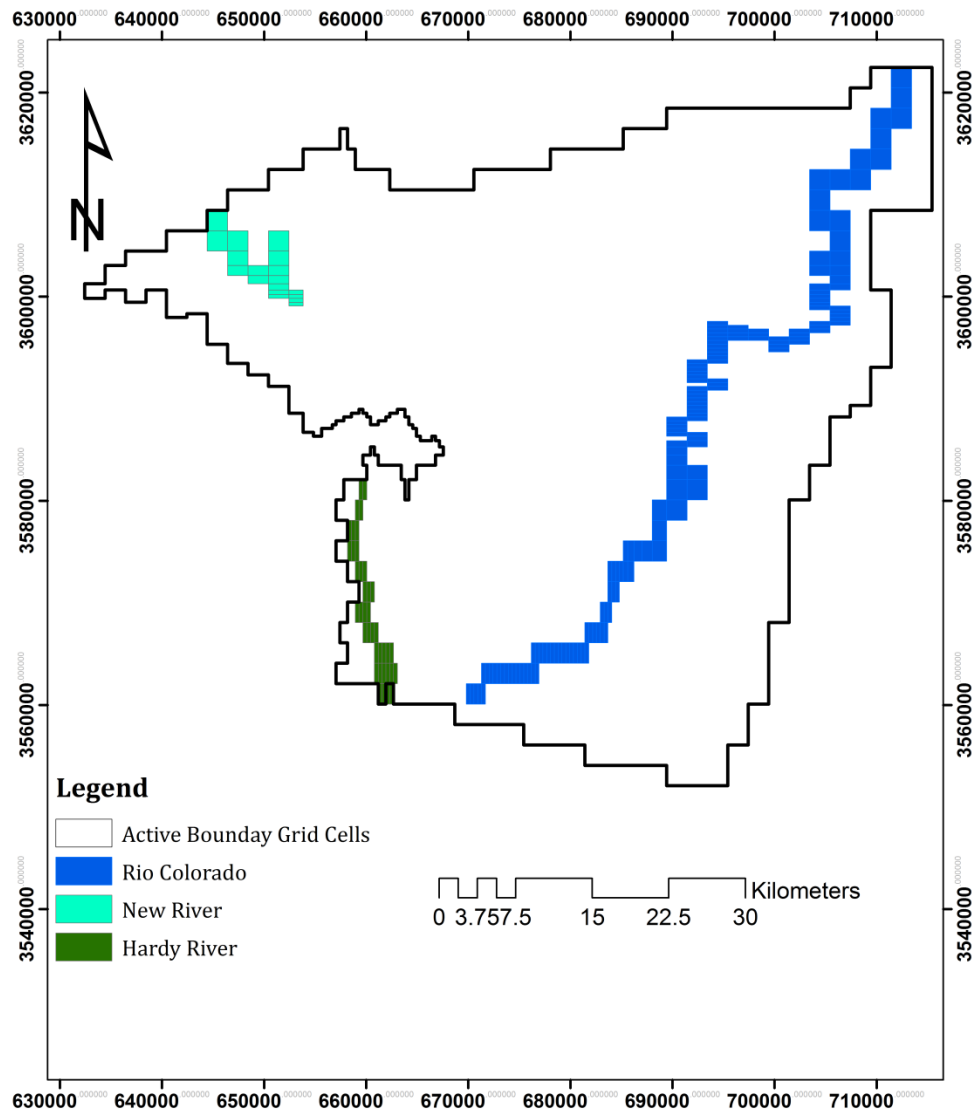


Figure 14 Representation of rivers and drains in the model

Each feature was represented by a series of line segments connected by nodes that were assigned elevations for both the top and bottom of the channel feature. Annex 1 and Annex 2; show the basic parameterization of the surface water features.

3.5. Parent model grid design

The regional stratigraphy was conceptualized in two layers as explained in section 3.4.1 and 3.4.2. The first layer has a thickness of 120 m from the ground surface and this layer is a zone where most extraction of water for irrigation occurs. The second layer has a thickness of 680 m from the first layer down.

The mesh starts at the coordinates of 624420 E and 3626461.998 N (UTM WGS84 zone 11) and was discretized in 113 columns and 73 rows following the recommendations of USGS MODFLOW.

The dimensions of the grid cells are variable. The criterion to achieve the refinement followed the recommendations of MODFLOW (Harbaugh, 2005) preventing size difference between adjacent cells which should not be more than 1.5. The grid cells are ranging from 2000 m x 2000 m to the refining area 375 x 375 m. The grid size and their locations are presented below (Table 4 and figure 15).

Table 4: discretization's of the parent model

Column	Row	Longitude(m)
1 up to 14	1 up to 11	2000
15	12	1400
16	13	1000
17	14	800
18	15	600
19	16	450
20 up to 95	17 up to 53	375
96	54	450
97	55	600
98	56	800
99	57	1000
100	58	1400
101 up to 113	59 up to 73	2000

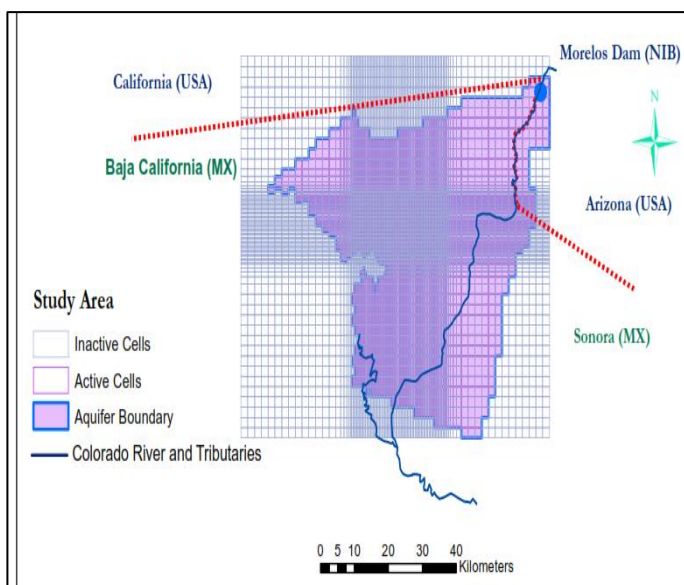


Figure 15: Model domain showing a grid and active cell boundary

3.6. Software selection

The groundwater flow was simulated with the three-dimensional finite difference block centered groundwater model code MODFLOW-OWHM.

MODFLOW-OWHM with RIV, WELL, DRN and UZF1 and for calibration Head observation package (HOB) are among the models in which link dynamic of flows between groundwater and surface water through the unsaturated zone.

The model was applied under the ModelMuse Graphical User Interface (GUI) (Winston, 2009) to pre-process input data and post-process output. The One-Water Hydrologic Flow Model (MF-OWHM) is a MODFLOW-based integrated hydrologic flow model (IHM) that is the complete version, to date, of the MODFLOW family of hydrologic simulators needed for the analysis of a broad range of conjunctive-use issues. Conjunctive use is the combined use of groundwater and surface water. MF-OWHM allows the simulation, analysis, and management of nearly all components of human and natural water movement and use in a physically-based supply-and-demand framework. The model incorporates the Unsaturated Zone Flow (UZF1) (Niswonger et al., 2006) and River package (RIV) (Niswonger & Prudic, 2005) packages among others. The Preconditioned Conjugate Gradient Package (PCG) was selected to solve the finite difference equations in each step of a MODFLOW-OWHM stress period. In PCG solver the maximum absolute change in head and maximum absolute residuals was set to 0.01 m for convergence. The model units of length and time were assigned as meters and days respectively.

3.7. Numerical model

Groundwater and surface water are interrelated components of the hydrologic system through different physiographic and climatic conditions. The interaction process occurs through the vertical and lateral exchange of fluxes between surface water and groundwater systems through the unsaturated zone and infiltration to or exfiltration from the saturated zone (Sophocleous, 2002).

The UZF1 package is a recently developed package that replaces the Recharge and Evapotranspiration Packages of MODFLOW-2005 (Niswonger et al., 2006). It uses a

kinematic-wave approximation of vertical, 1D variably saturated flow by applying the kinematic-wave approximation equation:

$$\frac{\partial \theta}{\partial t} + \frac{\partial K(\theta)}{\partial z} + a = 0$$

where:

θ - The volumetric water content (L^3L^{-3}); t is time (T), z - the distance in the vertical direction (L); $K(\theta)$ - unsaturated hydraulic conductivity (LT^{-1}); a - evapotranspiration rate per unit length of roots (T^{-1}); and L and T denote length and time units.

UZF1 calculates groundwater evapotranspiration (ETg), unsaturated zone evapotranspiration (ETun), gross recharge (Rg), storage change (ΔS) and groundwater exfiltration (Exfgw) as a function of the inputs assigned to the package including extinction water content (EXTWC), extinction depth (EXTDP), PET and infiltration rate. In principle, UZF1 recharged groundwater from precipitation after satisfying the evapotranspiration demand based on the given input values of EXTWC, EXTD, and PET (Viridi et al., 2013).

Previous groundwater modeling efforts for areas within the United States in close proximity to the Colorado River Delta (CRD) have used the assumption of zero mountain front, or precipitation related, recharge. For the ADWR Yuma groundwater model, as reported in Feirstein et al., (2008) noted that previous estimates of the annual total un-gaged local runoff from precipitation were less than 1,233,482 m³/yr. Olmsted et al., (1973) indicated that the majority of this water which infiltrated the ground surface was not recharged to the aquifer, but evaporated or transpired out of the system leaving moisture content at less than 5 percent between the top few meters of surface soil and the groundwater table outside of irrigated areas.

Therefore, the precipitation related recharge for the model area is accounted as zero and the recharge for the aquifer is from the applied irrigation water to the agricultural lands (Colorado River Irrigation District 014).

Agriculture is the main water user within the modeled Colorado River Delta and recharges associated with agriculture, mainly irrigation, may be considered a primary

source of recharge to the modeling area aquifer (Olmsted et al., 1973). The agriculture-related recharge for each Irrigation units based on the irrigation seasons was obtained from previous studies and the available agriculture-related recharge is converted into infiltration rate and prepared as an input for the UZF1 package. The infiltration rate was assigned as $1.687 \text{ mm day}^{-1}$; the evapotranspiration demand (PET) $1.6387 \text{ mm day}^{-1}$; extinction water content was fixed to $0.06 \text{ m}^{-3} \text{ m}^{-3}$ as spatially uniform to all cells and the extinction depth, below which no more water will be removed by evapotranspiration, was assigned a weighted average of 1.2 m. The weight of extinction depth is given according to the main seasonal crops in the area and their coverage of the study area. The main crop types identified are wheat, cotton, and alfalfa and the average extinction depth of those crops were taken as 1.2 m.

The infiltration rate and PET values for steady-state simulation were assigned as the average values for the 8 years of simulation period and for the transient state, time series data aggregated on annual was applied. The “Number of trailing waves” (NTRAIL2) was set to 16 (the recommendable range is between 10 and 20) and “Number of wave sets” (NSETS2) was set to 20 since the infiltration rate varies with time and also options “Route discharge to streams and lakes” (IRUNFLG) and “Simulate evapotranspiration” (IETFLG) were selected. The Brooks-Corey-Epsilon was assigned as 3.5 which define the relation between unsaturated hydraulic conductivity and water content (Niswonger & Prudic, 2005); spatially uniform maximum unsaturated vertical hydraulic conductivity 0.35 m day^{-1} and saturated water content 0.3 m^{-3} were assigned to all cells. The model top was taken as the land surface where the infiltration was applied. “The recharge and discharge location option” (NUZTOP) was selected as “Top active cell”.

3.8. Hydraulic properties

The hydraulic properties including hydraulic conductivity (Kh), specific storage (SS) and specific yield (SY) data was calculated from previous studies (Feirstein et al., 2008, Rodríguez-Burgueño., 2012) as described in section 3.4.1 and 3.4.2. Those values were used as initial values and adjusted during the model calibration.

3.9. Head observations (HOB)

The locations of head observation points (Figure 2, part one) were imported as shapefile to ModelMuse and the piezometer ID, time step and observed heads were assigned as an input to each piezometer using point object. The observed heads were used as a reference in the model calibration to and graph the observed versus simulated head during steady-state and transient simulation.

3.10. Water budget

Water budget shows the fluxes of groundwater within the aquifer system. In the steady-state model, the average water budget of 8-year simulation periods was estimated. In the transient model, water budget was estimated for each time step, i.e., annually. No external source of groundwater recharge other than direct infiltration from agriculture was considered. In water budget assessment, the incoming and outgoing flux should balance exactly or within acceptable limit at the end of the simulation period. After each run, the MODFLOW-OWHM model gives the overall budget of the model, not for the individual model layers. The water balance of the entire model and the fluxes for the surface, unsaturated and saturated zone were calculated using the following equations:

Water balance of the entire catchment (aquifer) was calculated using Equation 4, modified after Hassan et al. (2014)

$$P = ET + q + q_g \pm \Delta S \dots\dots\dots (4)$$

Where P- precipitation; ET - total evapotranspiration; q- stream discharge at the outlet of the catchment; qg - lateral groundwater outflow across the northern catchment boundary and ΔS is the change in the catchment storage.

The ET and ΔS component of Equation 4 was explained in detail in Equations 5 and 6.

$$ET = ET_g + ET_{un} + I \dots\dots\dots (5)$$

$$\Delta S = \Delta S_g + \Delta S_{un} \dots\dots\dots (6)$$

Where ET_g - groundwater evapotranspiration, ET_{un} - unsaturated zone evapotranspiration from UZF1 package, ΔS_g - change of storage in the saturated zone, ΔS_{un} - change of storage in the unsaturated zone and I - canopy interception, no accounted for this study.

The water balance of the land surface and the unsaturated zone is expressed in Equation 7

$$P + EXf_{gw} = I + R_o + R_g + ET_{un} + \Delta S_{un} \dots\dots\dots (7)$$

Where EXf_{gw} - groundwater exfiltration, R_o - the total runoff to streams and R_g – gross recharge

Actual infiltration rate in the unsaturated zone and gross recharge can be computed as (Equation 8):

$$P + EXf_g = I + R_o + P_e \dots\dots\dots (8)$$

Where P_e the actual infiltration rate and can be further divided into (Equation 9):

$$P_e = R_g + ET_{un} \pm \Delta S_{un} \dots\dots\dots (9)$$

The water balance of the groundwater (saturated) zone is expressed as (Equation 10)

$$R_g + q_{sg} = ET_g + EXf_{gw} + g_{gs} + q_g \pm \Delta S_g \dots\dots (10)$$

Where, Q_{sg} - stream leakage into the groundwater, Q_{gs} - groundwater leakage into the stream and ΔS_g - change in the groundwater storage

Net groundwater recharge controls the sustainability of groundwater resources and enables to understand the behavior of changes in groundwater storage better than using the total recharge (Hassan et al., 2014; Sophocleous, 2005) and it is estimated by Equation 11:

$$R_n = R_g - EXf_{gw} - ET_g \dots\dots\dots(11)$$

Where, R_n - net recharge, R_g - total recharge, EXf_{gw} - groundwater exfiltration and ET_g - groundwater evapotranspiration.

The net recharge is the actual amount of water that recharges the groundwater after the loss of water by evapotranspiration and exfiltration. Groundwater net recharge originates from net agricultural related recharge that reaches the water table through the unsaturated zone and was applied in the model using UZF1.

3.11. Model calibration

Model calibration is the modification of model input data to match observed and simulated heads and flows (Reilly & Harbaugh, 1999), so to minimize average error in calibration (Anderson & Woessner, 1992). The calibration process of the model was completed in two different but interrelated processes. Initially, steady-state model calibration was undertaken, followed by the transient model calibration. Groundwater heads were monitored at different observation points. In this study, the calibration was performed using the trial-and-error adjustment method. In some aspects, that type of calibration is advantageous as compared to automated calibration as it is much faster and enables to understand the model behavior during the calibration process and in consequence to incorporate hydro (geo) logical knowledge of the area in the calibrated model (Hassan et al., 2014). The results of calibration run after parameter adjustment were evaluated applying Root Mean Square Error (RMSE). The trial-and-error adjustment was conducted till the RMSE became small and no more model improvement was observed.

The driving forces in this study area were agriculture-related infiltration and potential evapotranspiration; the state variables were heads and the calibrated variables are K_h , K_v , S_y , and S_s . Additionally, the water table was controlled whether in any cell, it does not rise above the topographic surface and also the budget consistency and realism were assessed in every model run.

3.11.1. Steady-state model calibration

A steady-state model was calibrated based on trial and error procedure. Seven internally homogenous, uniform K_{hx} zones were defined for first layers based on previous studies. The vertical hydraulic conductivity for steady-state calibration was assigned by uniform homogeneous K_v -zone for both first and second layer. The K_h and K_v were assigned initially on the basis of the previous studies on the area. The initial hydraulic conductivity values were assigned and adjusted during model calibration till model error assessment criteria suggested by Anderson & Woessner (1992) and Mason & Hipke (2013) was met.

3.12. Error assessment

In this study, error assessment was carried out to evaluate the performance of the calibrated model. Error assessment of the model calibration was demonstrated by statistical and graphical comparisons of simulated and observed data. The observed time series data set of groundwater levels at 27 piezometers and 45 piezometers were used as a reference to compare with simulated heads for steady period and for transient simulation period respectively. The residual error was analyzed by Mean Error (ME), Mean Absolute Error (MAE) and Root Mean Square Error (RMSE) (Anderson & Woessner, 1992) and the ratio of the RMSE to the total head loss (less than 10 % error) was also used for further assessment of the errors. Equations 12 to 14 were used to facilitate the error assessment analysis. Scatter plot of observed head versus simulated head was used for graphical comparison of the model simulation result.

ME that is the difference between the observed head (Head_{obs}) [m] and model-calculated (Head_{sim}) [m] result and calculated as (Equation 12):

$$ME = \frac{1}{n} \sum_{i=1}^n (Head_{obs} - Head_{sim})_i \dots\dots\dots (12)$$

Mean absolute value is the mean of the absolute differences of the observed head (Head_{obs}) [m] and model calculated (Head_{sim}) [m] result and calculated as (Equation 13):

$$MAE = \frac{1}{n} \sum_{i=1}^n |(Head_{obs} - Head_{sim})_i| \dots\dots\dots (13)$$

Root means square error (RMSE) is calculated as (Equation 14):

$$MAE = \left(\frac{1}{n} \sum_{i=1}^n |(Head_{obs} - Head_{sim})_i|^2 \right)^{0.5} \dots\dots\dots (14)$$

Where *n* is the number of calibration values

Discrepancy error in the volumetric budget was assessed for error analysis of the water balance closure. In most cases, percent discrepancy of 0.1% is recommended and it was applied in this study (Konikow, 1996).

4. Results and Discussions

4.1. Metrological and Hydrological analysis result

4.1.1. Metrological data analysis

The only external sources of recharge considered in the modeling area are, Agriculture related water that infiltrates into the aquifer and lateral inflows. Extremely low precipitation rates in the area, on average below 55 mm/yr., preclude the inclusion of mountain-front recharge as a source of recharge for this model.

Methods for calculating mountain front recharge typically involve thresholds for minimum precipitation that exceed this average amount. The Maxey and Eakin method (as described in [Feirstein et al., 2008](#)) for example, calculate mountain front recharge by multiplying the average annual precipitation by a coefficient to determine “annual excess” precipitation- the recharge value. This coefficient is equal to zero for a precipitation amount less than 0.2 m supporting the application of zero mountain front recharge to this model domain.

4.1.2. Infiltration rate

In this study, the actual infiltration rate was calculated using equation (9) by assuming that there is no change in storage in unsaturated zone. High infiltration rate was observed during the periods with a high rate of irrigation application, the estimated infiltration was the highest in May 2006 with 4.5 mm day^{-1} (Figure 16). The estimated infiltration rate ranged from 0 to 4.5 mm day^{-1} with an average of $1.687 \text{ mm day}^{-1}$. That average infiltration rate was applied in the steady-state model calibration. Calculated annual infiltration rates were applied for transient MODFLOW modeling.

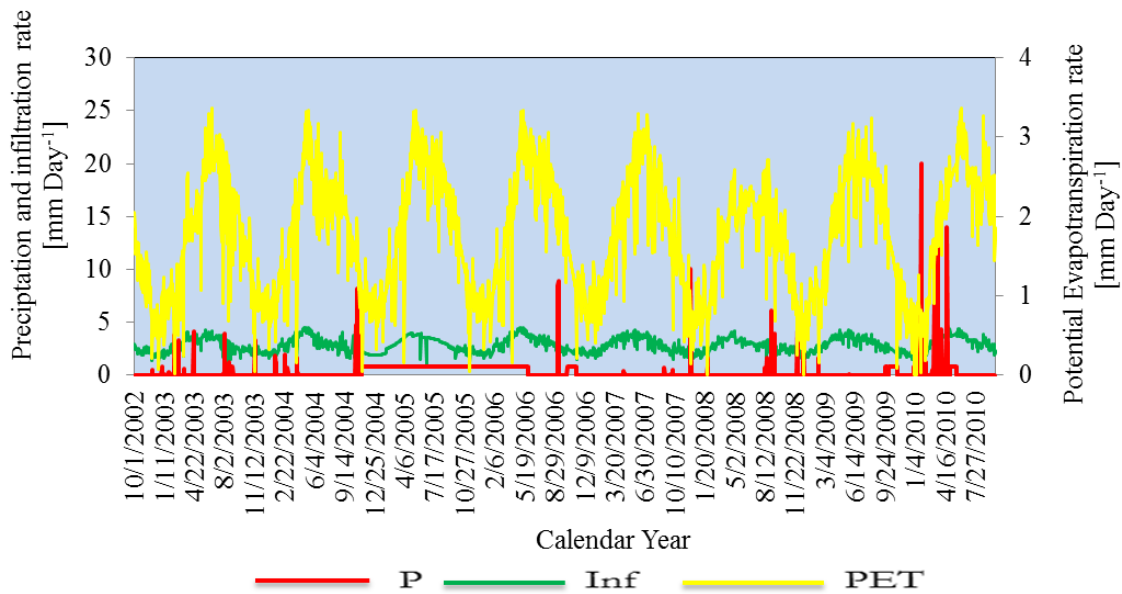


Figure 16: Precipitation (P), infiltration rate (Inf), and potential evapotranspiration (PET) for 8-year periods (hydrologic years 2002 to 2010) for the study area

4.2. Steady-state model calibration

4.2.1. Calibrated head and error assessment

In this study, it was decided that only the most uncertain parameters (Horizontal hydraulic conductivity and specific yield) will undergo calibration. Both parameters were changed individually, followed by a visual comparison of observed and modeled piezometer heads (Figure 17), correlation coefficient, and standard deviation. The steady-state simulated and observed heads were examined for correlation using a scatter plot and by calculating the coefficient of correlation (r). A quantitative comparison of the head data in all the observation points after multiple trials indicates a reasonable match between the observed and simulated head values (Figure 17). The residuals calculated as the difference between observed and simulated heads in all observation points are indicated in Figure 18 and the coefficient of correlation was high ($R^2=0.93$) as shown in Figure 17. The residual varied from the lowest -1.1 m to the highest 2.3 m (Figure 18). The overall residual error was negative that indicates there was a slight overestimation of water level rise by the model. The result agrees with the suggestion of Hill (1998) who stated that, when

observed heads are plotted against simulated heads they should fall close to a line with a slope of 1 and the correlation between them should be greater than 0.90. The mean error (ME), Root Mean Squared error (RMS) and Mean Absolute Error (MAE) metrics for the calibrated residuals were -0.08,0.5,0.03 m respectively.

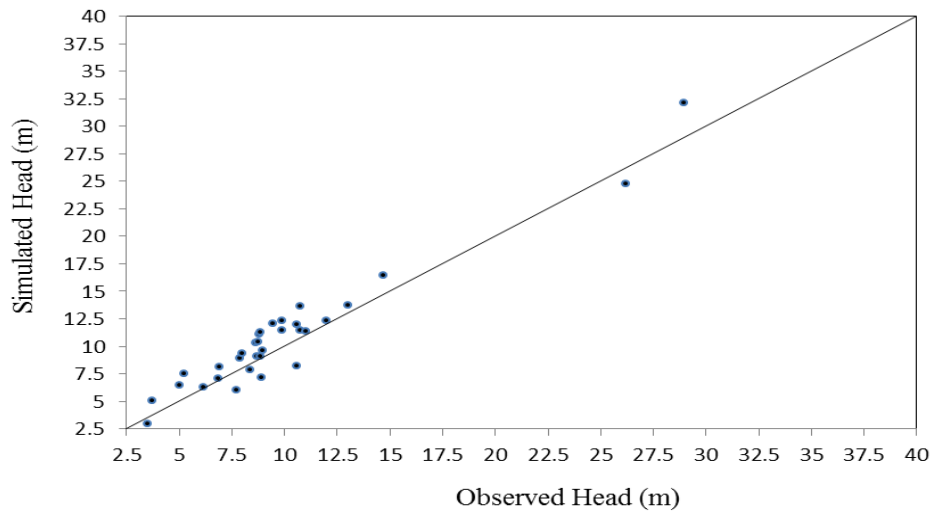


Figure 17: Relationship between simulated and observed head in the study area for steady-state condition.

Plotting residuals against hydraulic head help to check for bias in a groundwater (GW) flow model (Hill, 1998). Figure 18 shows that the residuals randomly and uniformly distributed hence the model were reasonably not biased.

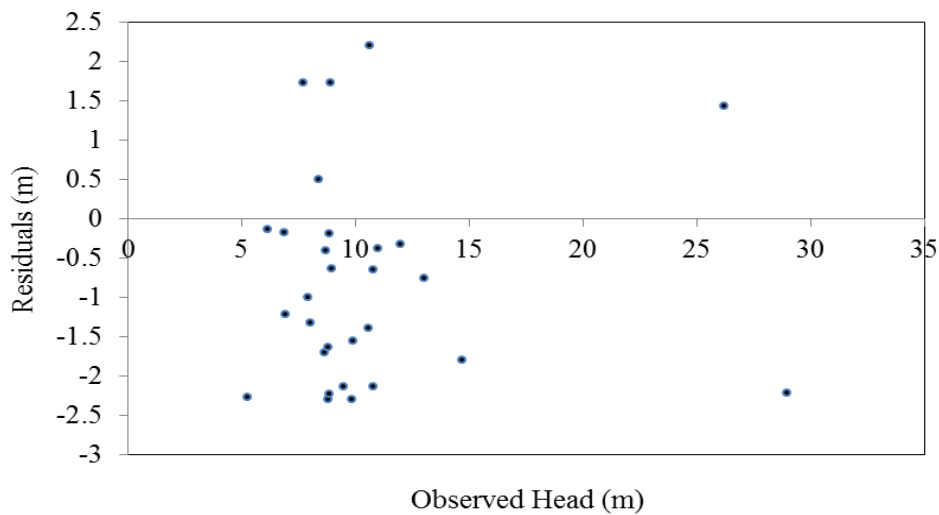


Figure 18: Residuals vs. Observed head of steady-state simulation

Figure 19 shows the distribution of the calibrated heads of the first and second layer after the steady-state model calibration. From the two figures, it can be observed that the water flows from all directions of the model towards the gulf of California at the southern border of the model, match the course of the Colorado River. The first and second layers showed nearly the same potentiometric surface.

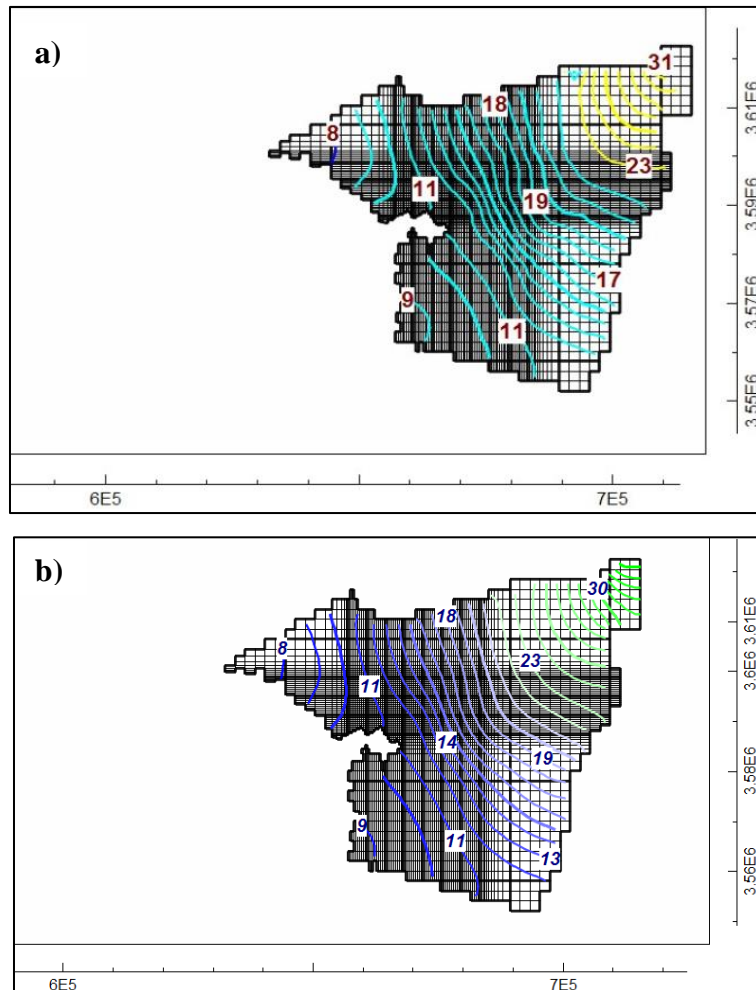


Figure 19: Calibrated head distribution (a) first layer (b) second layer of the steady-state model simulation

As additional calibration control, the Water Table Depth (WTD) was compared to the topographic surface to check if it did not rise above the ground surface. In all cells of the model, the water table was below the ground surface and the WTD varied from 0.1 m to 30 m depth.

4.2.2. Hydraulic conductivities

The initial hydraulic conductivity values were taken from previous studies and calibrated throughout the model using trial and error. The resulting hydraulic conductivity values after steady state calibration are shown in Figure. 20. In general, conductivity is low in the central model Colorado River Delta and high in the north west and south west due to coarse alluvial piedmont sand and gravel sediments derived from the Cucapah mountain.

The calibrated steady state horizontal hydraulic conductivity of the first layer was ranged from the highest hydraulic conductivity of 539.2 m/d (6.241×10^{-3} m/s) to the lowest hydraulic conductivity of 96.4 m/d (1.1×10^{-3} m/s). The horizontal hydraulic conductivity for the second layer was assigned a constant value of 0.001 m/d (1.15×10^{-8} m/s). The vertical hydraulic conductivity K_v , was assigned a uniform value of 0.03 m/d for both layers. The calibrated specific yield (Sy) and storage coefficient (Ss) were 0.2 and $1e^{-5}$ respectively.

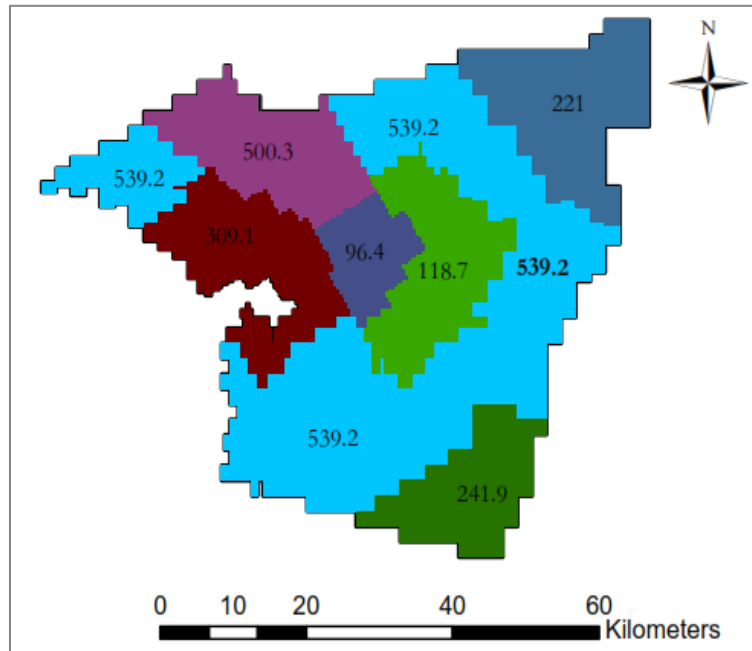


Figure 20: Calibrated horizontal hydraulic conductivity (K_h) distribution map for first layer after calibration in steady-state condition [m day^{-1}]

The MODFLOW model for the study area is highly sensitive to the horizontal hydraulic conductivity. Figure 20, shows the calibrated hydraulic conductivity which

produces an acceptable head, equivalent to the observed piezometric head. The model is less sensitive to change in vertical hydraulic conductivity.

4.2.3. Water budget of the steady-state simulation

Water budgets were constructed to explore the relationship between the sources and sinks to the groundwater system. The main sources to the model groundwater system include losses from stream flow, agricultural recharge, and cross-boundary sub-surface flows from the Drain Mesa and across the eastern domain boundary from Sonora. The main sinks of groundwater include gaining stream conditions, evapotranspiration, groundwater pumping, and cross-boundary sub-surface flows to the Gulf of California and Mexicali.

The OUT components of water balance: Ground Water Evapotranspiration contributed 87.5 %, stream discharge at the outlet of the model 3.1 %, pumping from groundwater wells 3.09% and lateral groundwater outflow 6.31 % of the total outflow from the model area (Table 5).

Table 5: Total water balance of the study area aquifer at steady-state condition (m³/day)

Budget component	IN	Budget component	OUT
River Leakage	102640.87	Pumping	92379.39
Head Dependent Bounds	96654.04	Head Dependent Bounds	185035.34
UZF Recharge	2787929.0	GW Evapotranspiration	2614900
		Surface Leakage	94968.93
Total	2987224.00	Total	2987283.75

4.2.4. Groundwater fluxes spatially

The groundwater fluxes show spatial variation as shown in Figure 21a for the steady-state model simulation. The simulated groundwater evapotranspiration loss from groundwater in MCRD in the steady-state condition varied from 0 mm day⁻¹ to 2.1 mm day⁻¹ (Figure 21a). The negative sign indicates the water is removed from the groundwater budget. Highest GWET was observed in North West aligned with the stream courses of Rio Nuevo, where the groundwater was the shallowest and similarly near to the Gulf of California where the groundwater was similarly expected to be shallowest. UZF recharge for the steady-state mode simulation is shown in Figure 21b.

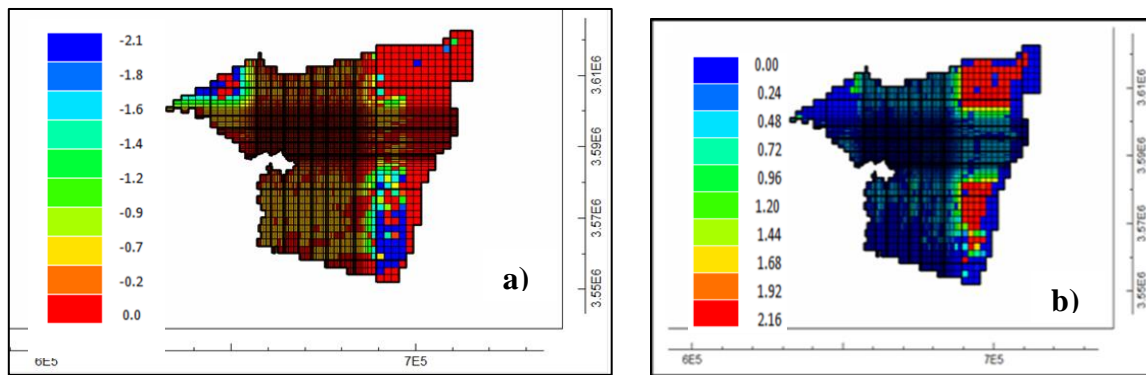


Figure 21: (a) Groundwater evapotranspiration in mmday⁻¹ and (b) UZF recharge in mmday⁻¹ for the study area for calibrated steady-state condition

4.3. Transient state model Calibration

4.3.1. Initial Condition

Initial conditions refer to the hydraulic head distribution everywhere in the system at the beginning of the simulation and thus are boundary conditions in time. It is a standard practice to select as the initial condition a steady state head solution generated by the calibrated model (Franke et al. 1987). A steady-state calibrated model (Figure 19) was developed for the study area; the developed steady-state simulation head was used as initial head for this transient simulation.

4.3.2. Calibration Results

The observed and simulated average groundwater levels at the 45 monitoring wells were compared in Figure 22. A scatter plot and a regression analysis of the measured head against the calibrated head are analyzed (Figure 22) in which a reasonable fit between these two datasets can be recognized.

In this study, it was decided that the only the most uncertain parameters (horizontal hydraulic conductivity and specific yield) undergo calibration. The mean error (ME), Root Mean Squared error (RMS) and Mean Absolute Error (MAE) metrics for the calibrated residuals were -1.38,1.1,1.59 m respectively.

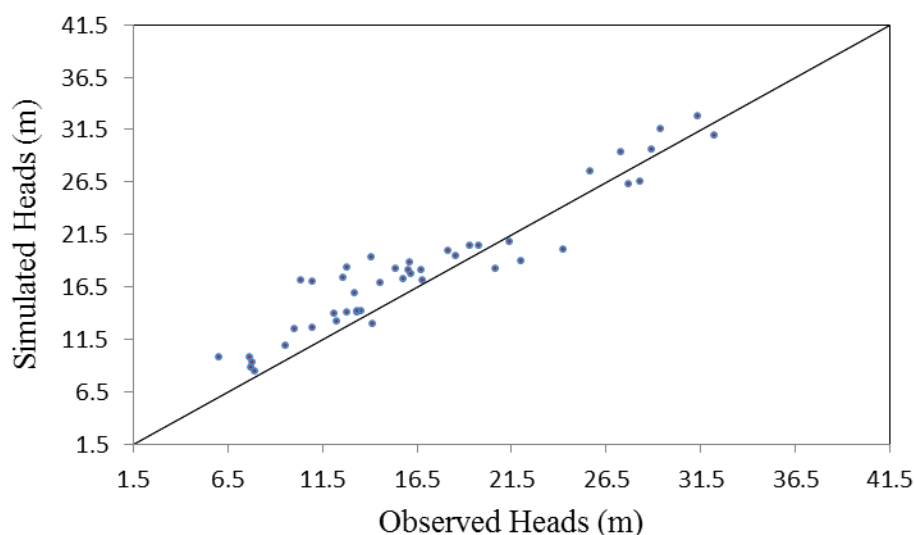


Figure 22. Scatter diagram for modeled and observed groundwater heads with linear correlation coefficient equal to 0.91 for transient model using observation 45 points of 2006

Both parameters were changed individually, followed by a visual comparison of observed and modeled piezometric heads (Figure 22), correlation coefficient, and standard deviation.

The horizontal hydraulic conductivity and specific yield values were finally considered as acceptable when standard deviation reached 0.35 m and the correlation coefficient was equal to 0.91.

Next, the model was checked for validation on the basis of continues groundwater levels measured throughout 2002 to 2006 on 7 piezometer points which are located near the Colorado River (Figure 5) where the groundwater fluctuation is controlled by the surface

water-groundwater interaction in addition to pumping. In the simplest manner, we estimated the quality of the model by visual comparisons (Figure 5) and also by calculating correlation coefficients between modeled and observed heads for all piezometers. The achieved values (0.7–0.82) do not indicate good or very good quality, but rather suggest a satisfactory (or acceptable) one.

Figure 23, shows the graphical comparison of hydrographs for observed and simulated groundwater heads for the transient model calibration. There was fluctuation in rising and recession of the heads in response to irrigation in most of the monitoring points. The rise of the hydrographs is due to the recharge of the groundwater during the irrigation seasons and recession can be due to pumping and evapotranspiration which are the main outflow components in the Mexicali Valley in all simulation periods. The graphs also depict that there is an acceptable match in trend of the rise and recession between the simulated and observed heads even though the lines do not match perfectly in some of the monitoring points.

There are different reasons for the mismatch of the observed and simulated heads. This can be caused by poor boundary conditions, poor conceptualization of the geology resulting in incorrect hydraulic properties (vertical and horizontal hydraulic conductivity, specific storage and specific yield), and error in numerical solution and problem in parameterization (Konikow & Bredehoeft, 1992). Unaccounted heterogeneity, uncertainty in the measured water level records, unaccounted water extraction, grid size and sub-grid-scale altitude variability can be also reasons for fluctuation in results (Hassan et al. (2014)).

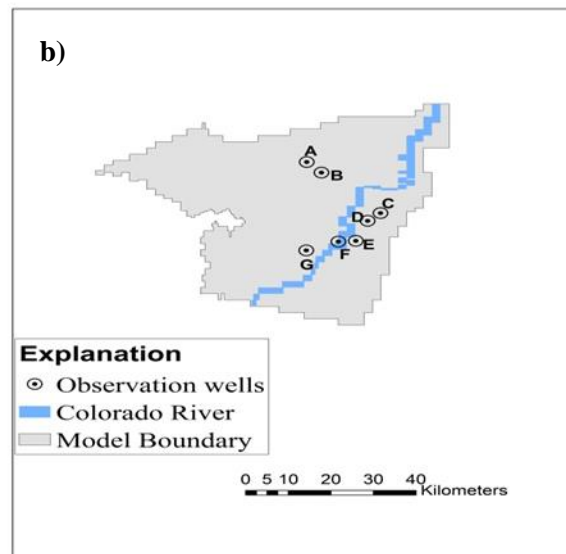
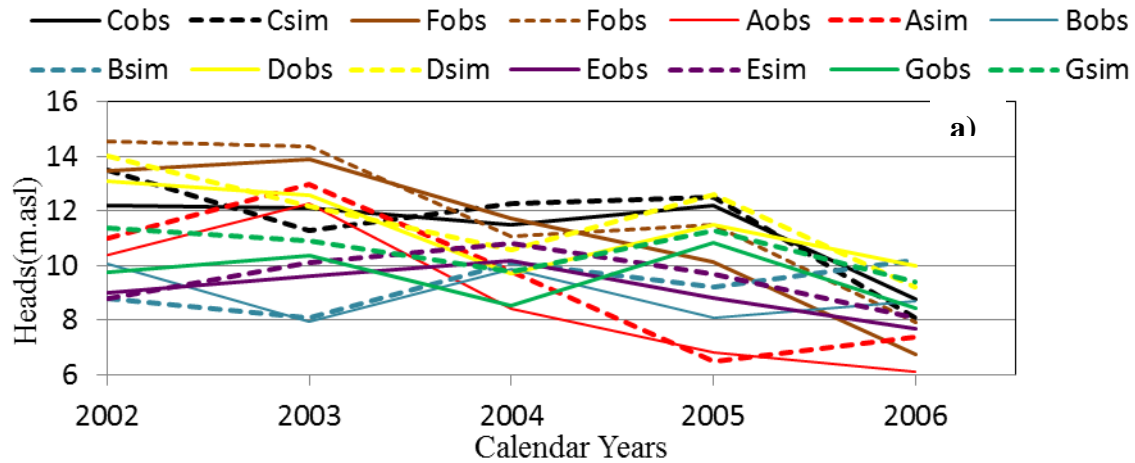


Figure 23. (a) Hydrographs between simulated and observations heads at 7 piezometric points; and (b) locations of the piezometric points

4.3.3. Hydraulic Conductivity

The distributions of calibrated horizontal hydraulic conductivity values for the first layer (Figures 24-26) shows seven zones of hydraulic conductivity. The uppermost sediment vary spatially and include coarse alluvial piedmont sand and gravel sediments derived from the Sierra Cucapah mountain, which dominate in the south-west portion of the modeling area which has the highest calibrated hydraulic conductivity (544.4 m/d), while the north-central part of the modeling area, has the lowest calibrated hydraulic conductivity

(77.7 m/d). The horizontal hydraulic conductivity of the second layer and the vertical hydraulic conductivity values were 0.001 m/d and 0.03 m/d respectively. The specific yield of the modeling area varies from 0.18 and 0.35 in which the calibrated specific yield value was 0.2.

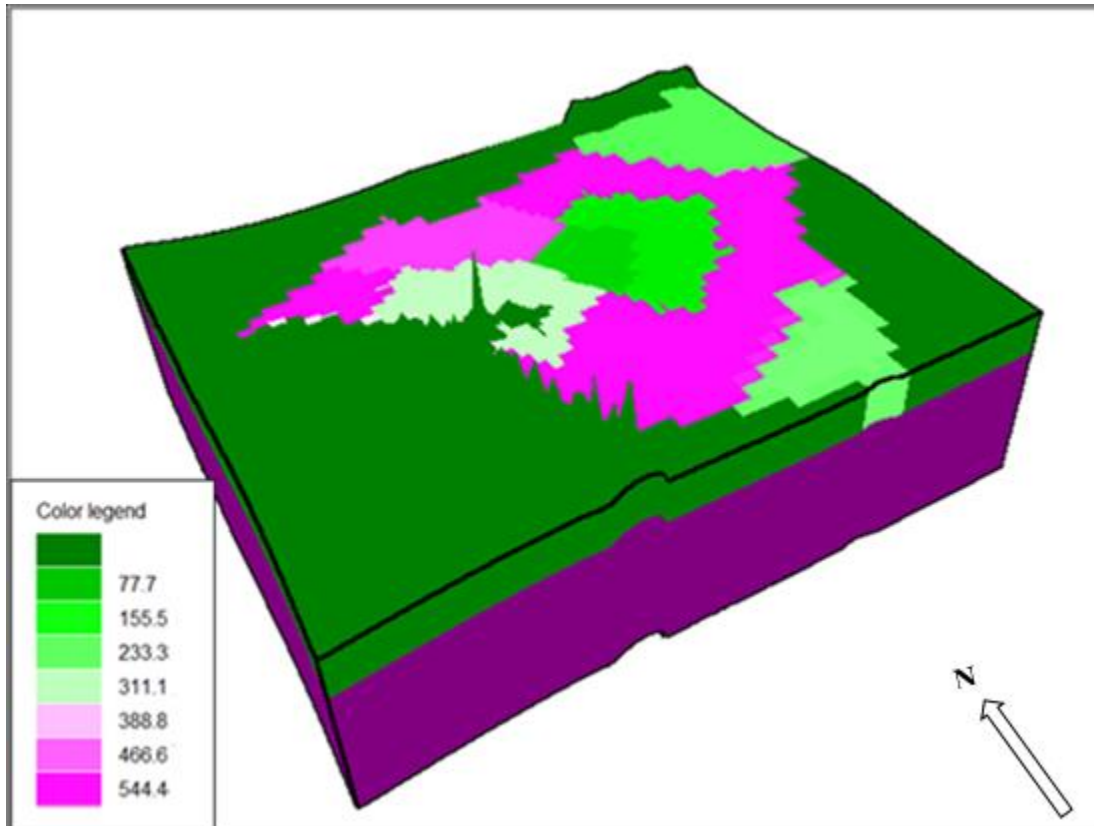


Figure 24. 3D view of the developed horizontal hydraulic conductivity distribution values for the first and second active cell layer. Deep green color represents inactive cell undefined hydraulic conductivity value. The second layer has a uniform horizontal hydraulic conductivity of 0.001m/d.

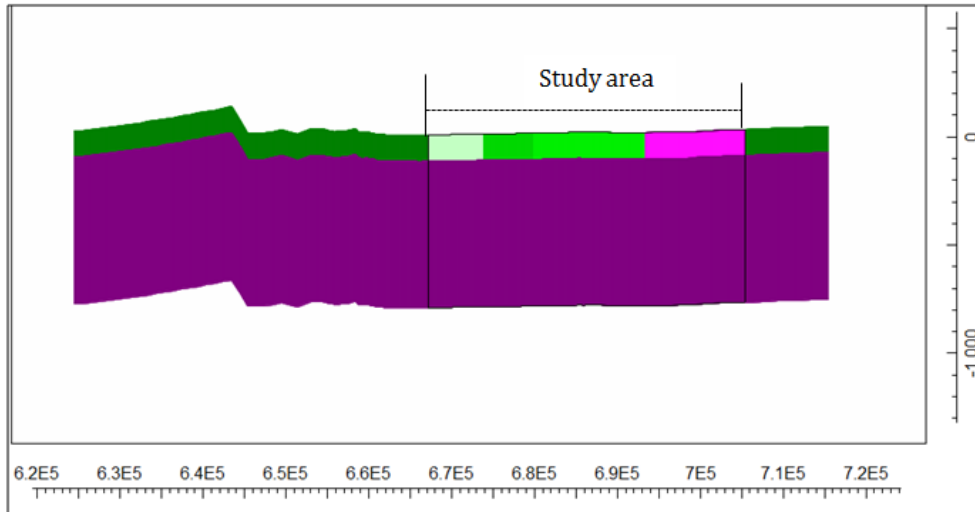


Figure 25. East-west cross section showing the calculated horizontal hydraulic conductivity (see Figure 2 for the location of cross section point) and refer figure 23 for the legend values)

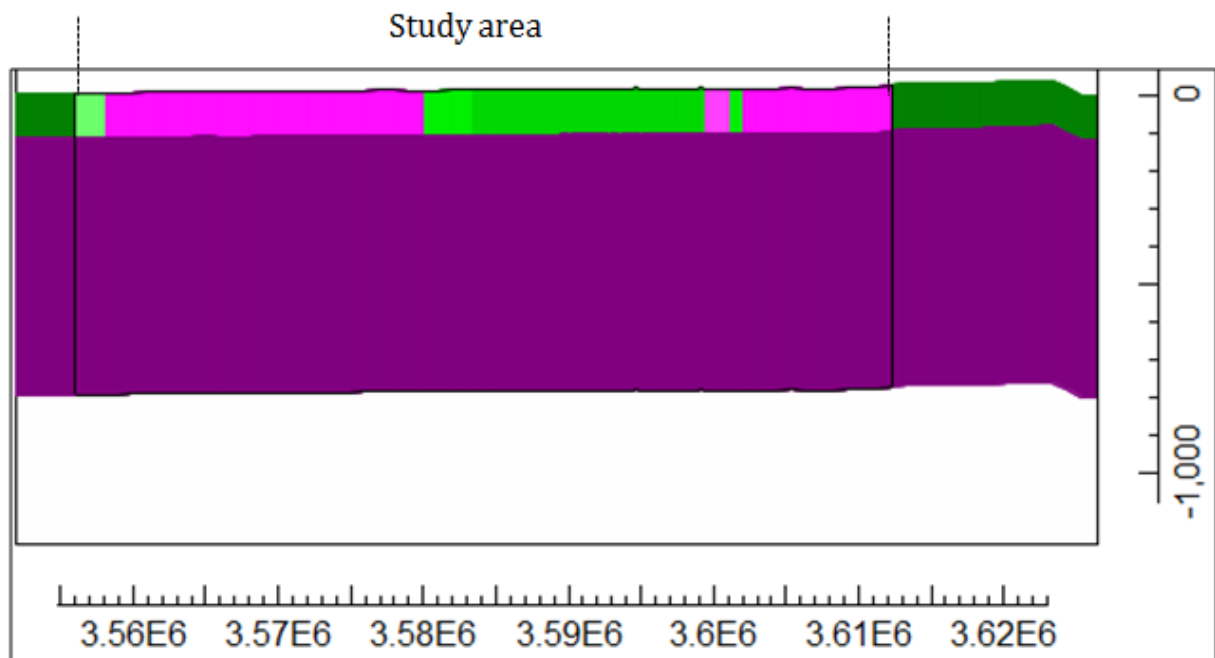


Figure 26. North-south cross section showing the calculated horizontal hydraulic conductivity (see Figure 2 for the location of cross section point) and refer figure 23 for the legend values)

4.3.4. Regional water Budget

MODFLOW model has been adequately calibrated to simulate the general behavior of the surface water-groundwater system in Mexicali Valley, which was confirmed by the model calibration. Table 1 and Figure 27-28 shows the simulated annual water balance (averaged over 2002-2010). The average simulated Groundwater balance shows that the groundwater inflow which is mostly from agricultural recharge ($302.81 \times 10^6 \text{ m}^3$) is the top input after lateral inflows ($578.66 \times 10^6 \text{ m}^3$). From the averaged water budget (Figure 27), it can be concluded that the surface water-groundwater exchanges in both directions are significant with higher budget magnitudes. The net exchange, from groundwater to surface water was $610.22 \times 10^6 \text{ m}^3$. In the simulated period, more subsurface flows ($578.66 \times 10^6 \text{ m}^3$) appear to enter the system than leave ($189.54 \times 10^6 \text{ m}^3$). Groundwater pumpage (P) was $400.50 \times 10^6 \text{ m}^3$ in the water budget.

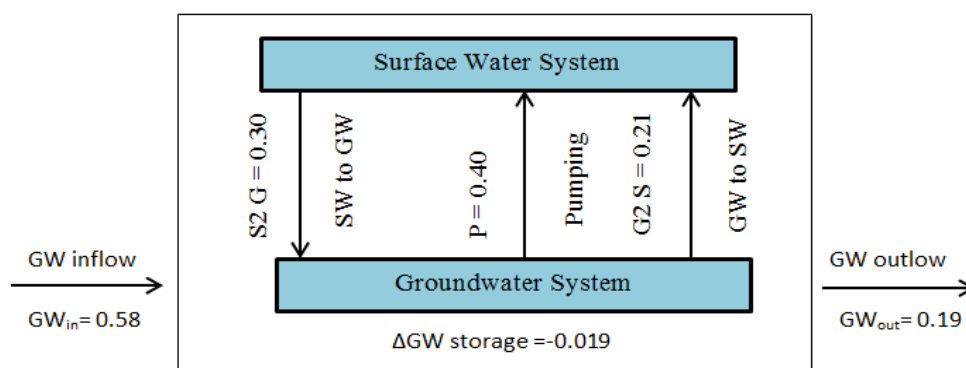


Figure 27: Simulated average annual water balance in billion m^3 for the study area

Table 6 Average simulated Groundwater balance obtained from MODFLOW model

Inflow	Amount(10^6 m^3)	Outflow	Amount(10^6 m^3)
Storage	1315.44	Storage	1335.35
Lateral inflow	578.66	Pumping	400.50
Agricultural Recharge	302.81	Drain	111.20
		River Leakage	3.55
		Lateral outflow	189.54
		GW-ET	78.32
		Surface Leakage	94.97
Total	2196.92		2213.45
Inflow-Outflow			-16.53×10^6
Percent discrepancy			0.075%

The total groundwater discharge (Figure 27 and Figure 28 and Table 6) consisted of the groundwater evaporation (GWE, equal to $78 \times 10^6 \text{ m}^3$) and exfiltration to land surface (GE, equal to $94.97 \times 10^6 \text{ m}^3$) in addition to pumping and lateral outflow.

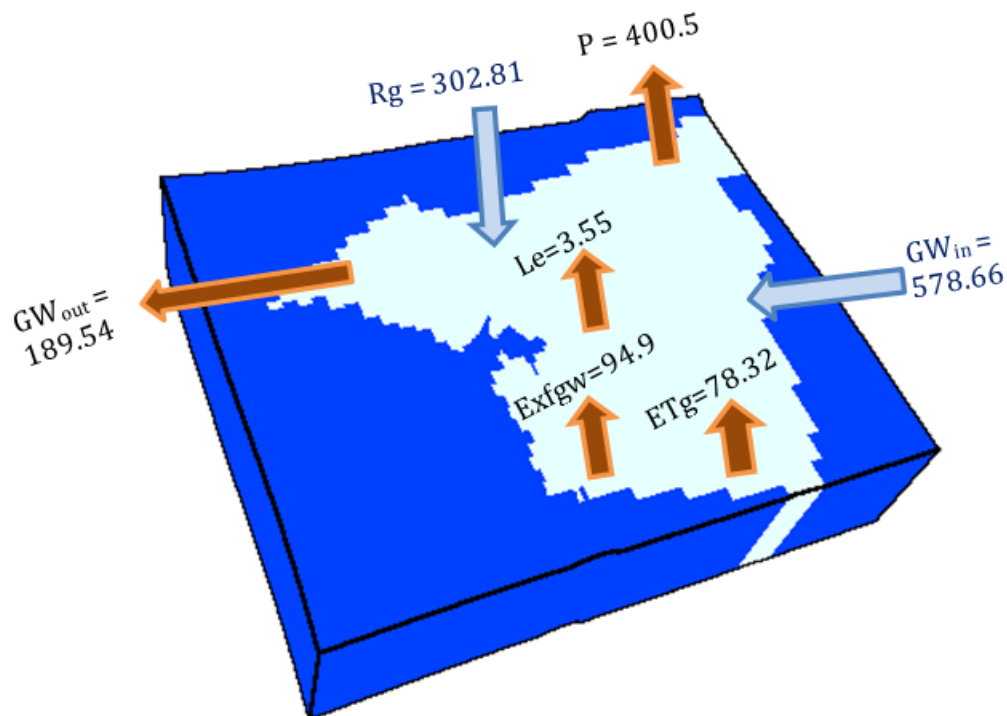


Figure 28: Schematic representation of groundwater budget for the entire model (all units are millions of m^3)

Figure 27 show schematic representation of the water budget for the entire model. The water budget components that contribute to the groundwater INPUT are (in % of IN): gross recharge (34.35 %), lateral inflow (65.64%). The discharges that contribute to groundwater OUTPUT are (in % of OUT): pumping (45.61%), groundwater evapotranspiration (8.9 %), outflow through drain boundary (12.66 %), storage out from the groundwater aquifer (21.58 %), and groundwater exfiltration (10.81 %), and leakage from groundwater to streams (0.44 %).

The average negative change in storage was mainly due to the depletion of the groundwater storage ($\Delta\text{GW} = -19.91 \times 10^6 \text{ m}^3$), which implied that the current water use might not be sustainable in the long term and proper management measures are desired.

This research simulates the river leakage which might assist the Colorado River restoration efforts. There is no surface water left in the stretch of Colorado River in the Mexican part after Morelos dam in which all water is diverted into irrigation fields. Colorado River Delta is under different restoration program to conserve the fauna and flora of the basin. A U.S. and Mexico binational team of government officials, conservation organizations and scientists have been identified conservation priorities in the Delta. The river leakage was simulated in this research (an average of $3.55 \times 10^6 \text{ m}^3$) and the river leakage distribution for the year 2006 is presented in Figure 29. The simulated river leakage (Figure 29) shows a negative value which indicated that the river is a gaining stream in which in some stretch of the river, shallow groundwater conditions have maintained different populations of birds and animal species.

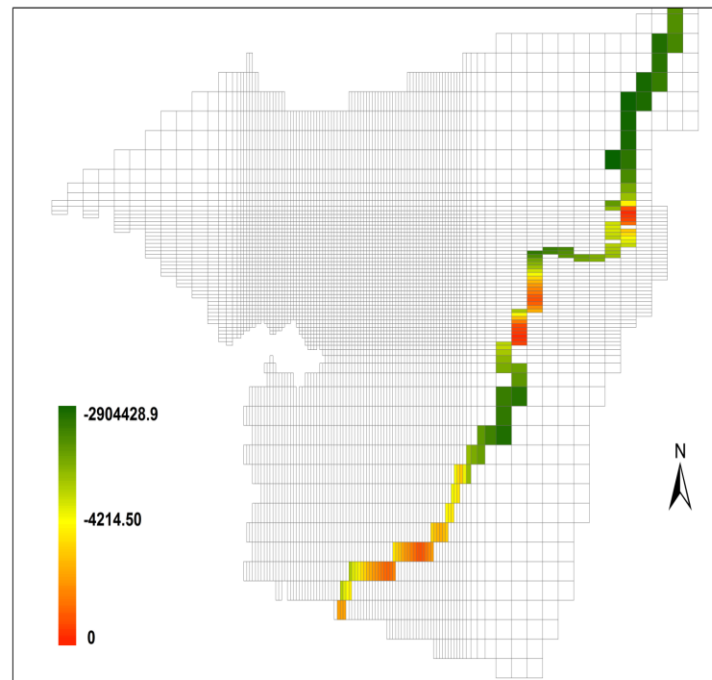


Figure 29. Distributions of average simulated river leakage in cubic meters for the year 2006

The only available water in the river stretches after the Morelos dam is shallow groundwater. The simulated river leakage showed that in some stretch of the river, the Colorado River gained up to 2904428.9 m^3 of water from groundwater and some stretches were still dry.

The decline of the water table surface is another indication of aquifer response to pumping and/or climate change effects; Figure 31 shows the simulated hydraulic head at the first and last period of simulation. The result of steady state modeling was used as an initial condition.

The temporal head distribution shows the drawdown of water levels from first simulation year to other points in the transient model. As indicated by the simulated potentiometric level, groundwater flows laterally from the highlands to the lowlands toward the Gulf of California. Simulated water levels range from 21.6 m in the highland areas to less than 5 m in the lowland (Figure 31) at the 2010 simulation period. The three-dimensional modeling of groundwater in the study area shows aquifer drawdown for the study period. Drawdown is seen to increase from year to year, with drawdown for each year observed to be highest in the northeast portion of the modeling area where there is a concentration of pumping wells (Figure 30).

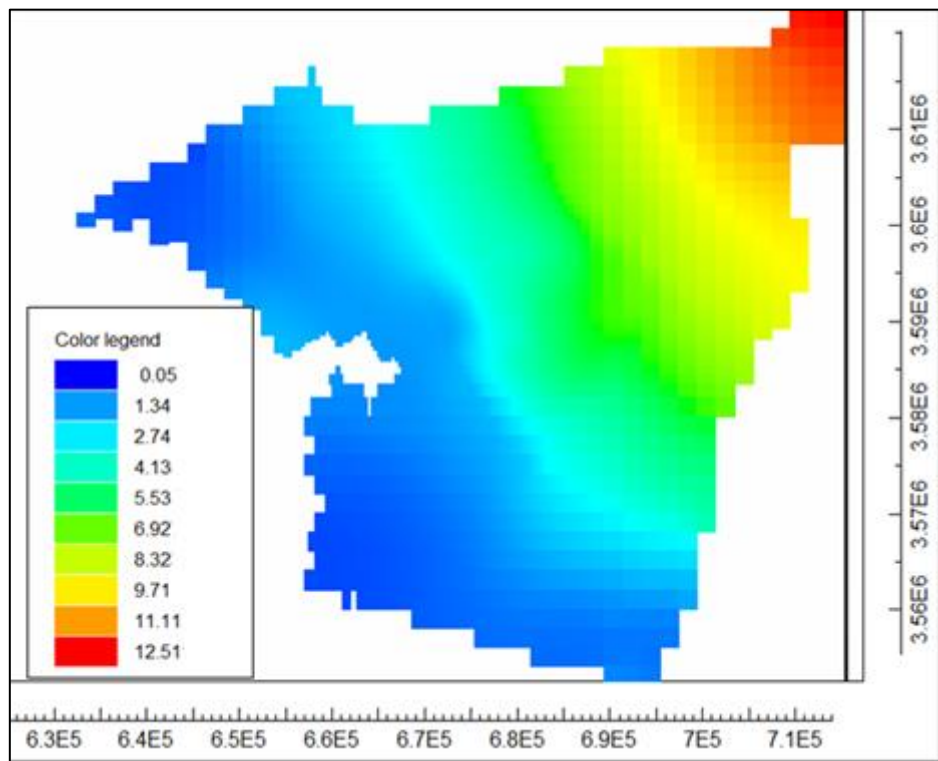


Figure 30. Distribution of simulated drawdown (m.asl) at the end of the stress period

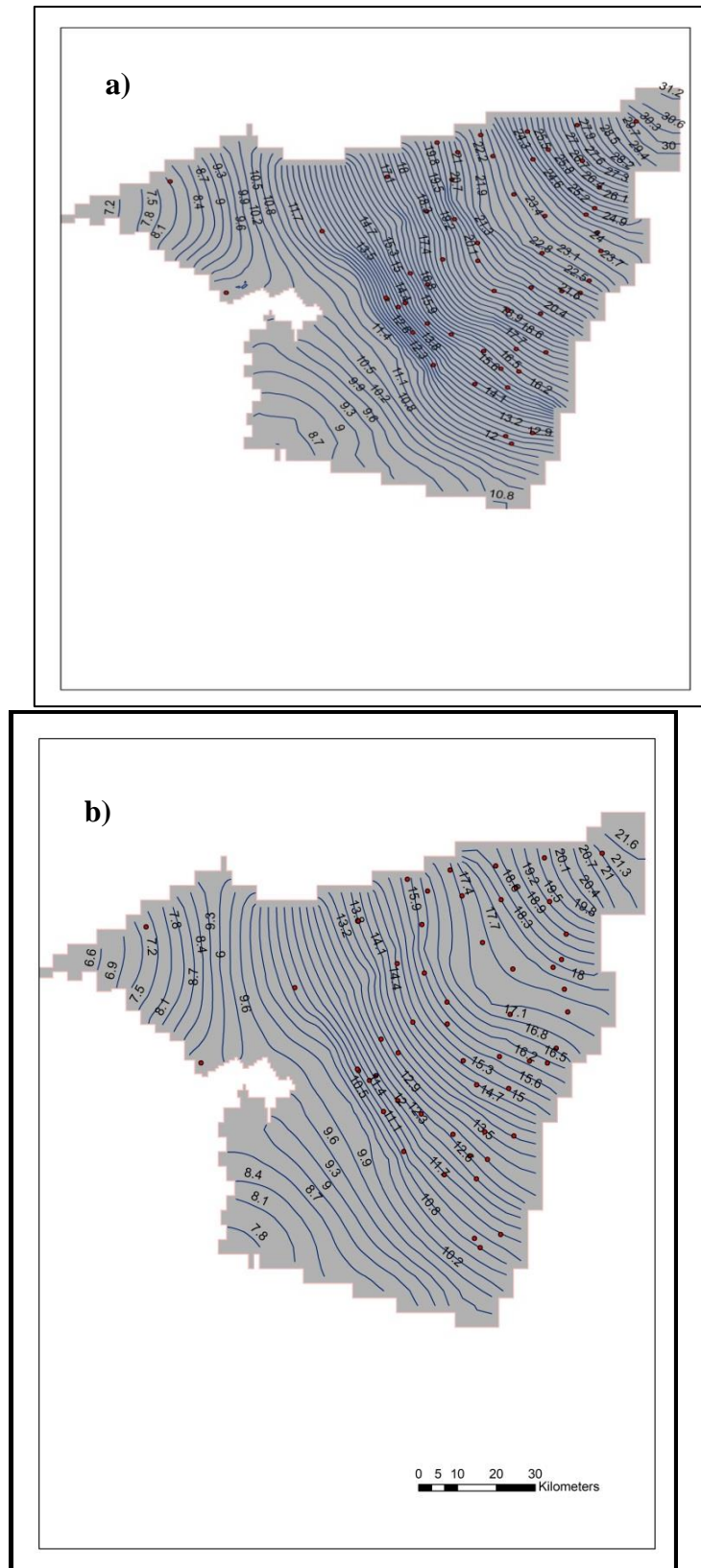


Figure 31. Distribution of simulated head (m.asl) at (a) first and (b) end of study period.

4.3.5. Groundwater fluxes spatially

The gross recharge, groundwater evapotranspiration, groundwater exfiltration, and the resultant net recharge (Equation 11), all showed large temporal variability (Figure 32). The gross recharge and the net groundwater recharge indicated the same trend. The difference between gross recharge and Exfiltration is referred (Hassan et al. 2014) as effective recharge ($R_e = R_g - \text{Exfgw}$).

Summarizing groundwater flux variability within the simulated period (01 October 2002 to 30 September 2010): the ET_g ranged from $-40.2 \text{ Mm}^3 \text{ year}^{-1}$ at the end of the transient modeling period to $-100.4 \text{ Mm}^3 \text{ year}^{-1}$ in the year 2004 with an average of $-78.32 \text{ Mm}^3 \text{ year}^{-1}$; the Exfgw ranged from $93.5 \text{ Mm}^3 \text{ year}^{-1}$ in 2003 to $104.4 \text{ Mm}^3 \text{ year}^{-1}$ in the year 2008 with an average of $94.9 \text{ Mm}^3 \text{ year}^{-1}$; The net recharge, R_n which is calculated using equation 11, was ranged from $95.78 \text{ Mm}^3 \text{ year}^{-1}$ to $212.2 \text{ Mm}^3 \text{ year}^{-1}$ (Figure 32).

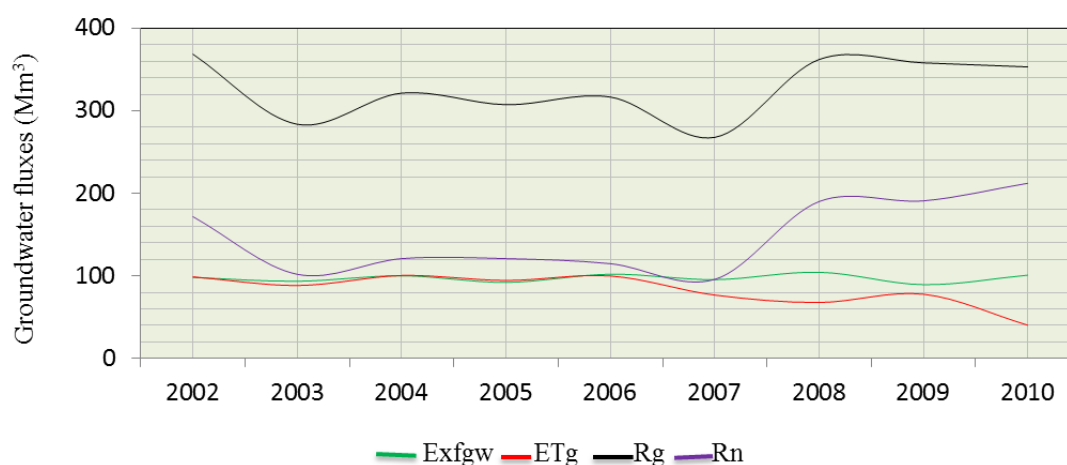


Figure 32. The transient calibrated groundwater exfiltration (Exfgw), groundwater evapotranspiration (ET_g), gross recharge (R_g) and net recharge (R_n) groundwater fluxes for 8-years stress period from 01 October 2002 to 30 September 2010.

The ET_g and ET_{Tun} rates from UZF1 output showed a yearly variability as shown in Figure 33. The maximum ET_{Tun} of $185.63 \text{ Mm}^3 \text{ year}^{-1}$ was observed in 2004 and the minimum ($158 \text{ Mm}^3 \text{ year}^{-1}$) in 2006. The graph shows also that the ET_{Tun} was typically higher than ET_g during the modeling period when PET demand was satisfied by the

available soil moisture of unsaturated zone, which come from infiltrated agricultural recharge preventing or at least restricting ETg. Evapotranspiration simulated over a specified depth in the unsaturated zone. The rate of groundwater evapotranspiration is dependent on the quantity of water stored in the unsaturated zone above the assigned extinction depth and on extinction water content. The ETg of this study was ranged from $100.4 \text{ Mm}^3 \text{ year}^{-1}$ to $40 \text{ Mm}^3 \text{ year}^{-1}$.

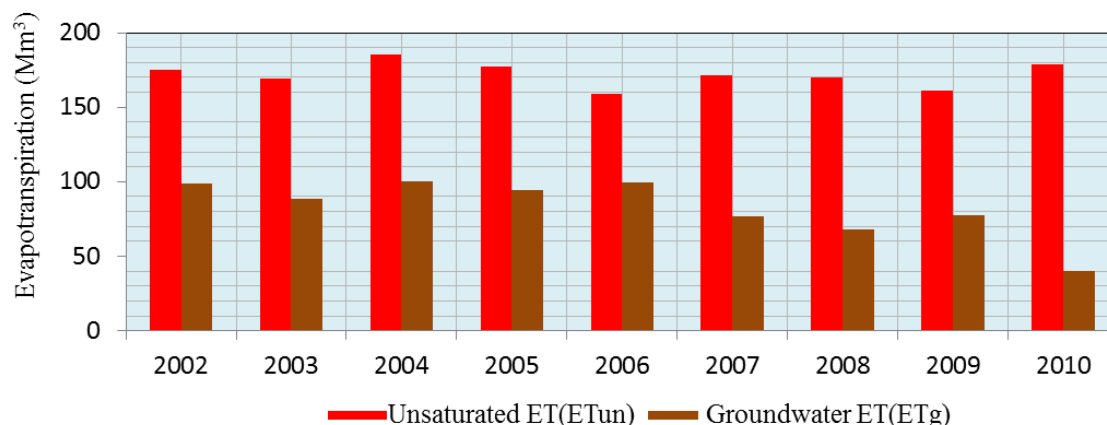


Figure 33. The transient calibrated unsaturated zone evapotranspiration (ETun) and groundwater evapotranspiration (ETg) for 8-years period from 01 October 2002 to 30 September 2010.

5. Conclusion and Recommendations

5.1. Conclusions

In this study, MF-OWHM numerical model utilizing its RIV and UZF1 Packages was successfully used to model the conjunctive surface water and groundwater interaction and to study the temporal aquifer response to groundwater pumping. The new model effectively addresses the study objectives in Mexicali valley; an irrigation system with both surface water diversion and groundwater pumping

Steady state and transient simulations show that groundwater flows axially from almost all directions of the model towards the Gulf of California at the southern border of the model, match the course of the Colorado River and laterally towards new river in the North-west, with a larger portion flowing out to south than north-west. Inflow takes place

in the east and north, showing that the modeling area is not merely draining water to groundwater (longitudinally), but also receives inflow from (lateral) recharge.

. The most important findings of this study that satisfy the research objectives and answer the research questions are listed below:

- The estimated infiltration rate was ranged from 0 to 4.5 mm day⁻¹ with an average of 1.687 mm day⁻¹. High infiltration rate was observed during the periods with a high rate of irrigation application, the estimated infiltration was the highest in May 2006 with 4.5 mm day⁻¹. That average and annual infiltration rate were applied in the steady-state model calibration and transient MODFLOW modeling respectively.
- A steady state simulation was built based on average values and calibrated ($R^2 = 0.93$). The transient simulation was calibrated for the years 2006. Calibration of the transient state model using the available observations of groundwater levels gives a relatively reasonable fit with a correlation coefficient of 0.91.
- The calibrated steady state horizontal hydraulic conductivity of the first layer was ranged from the highest hydraulic conductivity of 539.2 m/d (6.241×10^{-3} m/s) to the lowest steady state calibrated hydraulic conductivity of 96.4 m/d (1.1×10^{-3} m/s). The horizontal hydraulic conductivity for the second layer was assigned a constant value of 0.001 m/d (1.15×10^{-8} m/s). The vertical hydraulic conductivity K_v , was assigned a uniform value of 0.03 m/d for both layers. The calibrated specific yield (Sy) and storage coefficient (Ss) were 0.2 and 1×10^{-5} respectively.
- The uppermost sediments vary spatially and include coarse alluvial piedmont sand and gravel sediments derived from the Sierra Cucapah mountain, which dominate in the south-west portion of the modeling area which has the highest transient calibrated hydraulic conductivity (544.4 m/d), while the north-central part of the modeling area, has the lowest transient calibrated hydraulic conductivity (77.7 m/d).
- The specific yield of the modeling area varies from 0.18 and 0.35 in which the calibrated specific yield value was 0.2.
- Steady-state was calibrated using 27 years of average hydraulic heads. In the steady-state calibration, gross recharge contributed 93.3%, lateral inflow 3.2% and stream leakage 3.4% of the total groundwater inflow. The groundwater outflow

consisted of groundwater evapotranspiration 87.5%, surface leakage 3.1%, groundwater pumping 3.09% and lateral outflow 6.31%.

- In the transient model calibration, the following 8-years average (01 October 2002 to 30 September 2010) groundwater fluxes were obtained: the ETg was ranged from $-40.2 \text{ Mm}^3 \text{ year}^{-1}$ at the end of the transient modeling period to $-100.4 \text{ Mm}^3 \text{ year}^{-1}$ in the year 2004 with an average of $-78.32 \text{ Mm}^3 \text{ year}^{-1}$; the Exfgw ranged from $93.5 \text{ Mm}^3 \text{ year}^{-1}$ in 2003 to $104.4 \text{ Mm}^3 \text{ year}^{-1}$ in the year 2008 with an average of $94.9 \text{ Mm}^3 \text{ year}^{-1}$; The net recharge Rn, was ranged from $95.78 \text{ Mm}^3 \text{ year}^{-1}$ to $212.2 \text{ Mm}^3 \text{ year}^{-1}$.
- The ETg and ETun rates from UZF1 output showed a yearly variability. The maximum ETun of $185.63 \text{ Mm}^3 \text{ year}^{-1}$ was observed in 2004 and the minima ($158 \text{ Mm}^3 \text{ year}^{-1}$) in 2006. The calculated ETg of this study was ranged from $100.4 \text{ Mm}^3 \text{ year}^{-1}$ to $40 \text{ Mm}^3 \text{ year}^{-1}$.
- The water budget components that contribute to the groundwater INPUT are (in % of IN): gross recharge (34.35 %) and lateral inflow (65.64). The discharges that contribute to groundwater OUTPUT are (in % of OUT): pumping (45.61%), groundwater evapotranspiration (8.9 %), outflow through drain boundary (12.66 %), storage out from the groundwater aquifer (21.58 %), groundwater exfiltration (10.81 %). and leakage from groundwater to streams (0.44 %).
- MODFLOW-OWHM with UZF1 and RIV in the steady-state model simulation does not have capability to simulate ETg and ETun separately; as a result high ETg was obtained in the steady state model calibration, 87.5 % of the groundwater outflow; this value can be considered as sub-surface evapotranspiration that incorporates the ETun and ETg.
- The simulated potentiometric level at the end of the modeling period, 2010, showed a hydraulic head range from 21.6 m in some areas to less than 5 m in the lowlands and groundwater flows toward the Gulf of California following Colorado River.
- The three-dimensional modeling of groundwater in the study area showed aquifer drawdown for the study period. Drawdown is seen to increase from year to year, with drawdown for each year observed to be highest in the northeast portion of the modeling area where there is a higher number of pumping wells.

- The average negative change in storage was mainly due to the depletion of the groundwater storage ($\Delta GW = -19.91 \times 10^6 \text{ m}^3$), which implied that the current water use might not be sustainable in the long term and proper management measures are desired.

Results of multiple model parameterizations led to a better understanding when compared to simpler water balance models, while at the same time preventing unsubstantiated claims about system behavior as is the case in more complex models.

In this study, MF-OWHM was successfully used to model the dynamics of surface water and groundwater uses and to study the aquifer response to groundwater pumping. The developed regional groundwater model and these findings would help decision makers to have a better understanding of the groundwater budget components

5.2. Recommendations

This PhD study represents the first known large scale numerical groundwater model of the Colorado River Delta which try to implement the newest versions and package of MODFLOW .MODFLOW-OWHM was implemented in Colorado river delta, a region that is increasingly at the center of regional scientific and social research. For better development of MODFLOW model on the study area, this model will form the basis with the following recommendations:

- Agriculture is the leading user of water in the study area, but data related to agricultural information are limited. An effort to produce a detailed water budget for the agriculture sector in Colorado River Irrigation District 014, and perhaps development of the Farm Package (FMP) which is only implemented on irrigation unit 16 in this study, could greatly enhanced by availability of sufficient data. Therefore, developments of database in relation to agriculture sectors are highly recommended.
- The hydrogeological units for this study were based on the previous studies in which their work was using the hydrogeological properties of the Yuma area assuming that they are hydrologically connected. Further study should be conducted

to confirm the hydrological connectivity of Yuma and model Colorado River Delta and developing a detail geological log analysis of the Delta aquifer.

- The numerical implementation of the hydrological conceptual model is reliable but more spatio-temporal data and smaller grid size (less than 100 x 100 m) would make that solution better, enabling to understand better the dynamics of the water uses in the Delta aquifer.
- The stress period discretization for transient model simulation was conducted yearly and hasn't considered seasonal variations and the seasonal water requirements of regional agricultural crops. It might produce a better model if the time discretization is based on a seasonal framework and daily or monthly analysis.

6: References

- Allander, K. K., Niswonger, R. G., & Jeton, A. E. (2014). Simulation of the Lower Walker River Basin Hydrologic System, West-Central Nevada, Using PRMS and MODFLOW Models Scientific Investigations Report 2014 – 5190.
- Allen, R.G., Pereira, L.S., Raes, D., Smith, M. (1998) Crop evapotranspiration guidelines for computing crop water requirements. FAO Irrigation and drainage paper 56. Food and Agriculture Organization, Rome.
- Anderson, M. P. y Woessner, W. W. 1992. "Applied Groundwater Modeling simulation of Flow and Advective Transport". Academic Press, Estados Unidos. 373 p.
- Ayewew, T and Tilahun, N. (2008) Assessment of Lake-groundwater interactions and anthropogenic stresses, using numerical groundwater flow model, for a Rift lake catchment in central Ethiopia. *Lake & Reservoirs: Research and management* 2008 13:325- 345.
- Bakker, M., Schaars, F., Hughes, J.D., Langevin, C.D., and Dausman, A.M., 2013, The seawater intrusion (SWI2) package for modeling vertically-integrated variable-density groundwater flow in regional aquifers using the U.S. Geological Survey Modular Groundwater Flow Model (MODFLOW-2005): U.S. Geological Survey Techniques in Water Resources Investigations, Book 6, Chapter A46, 47 p.
- Berner, E.K., and Berner, R.A. (1987) *the Global Water Cycle. Geochemistry and Environment*; Englewood Cliffs; NJ: Prentice Hall Inc.
- Carrillo-Guerrero, Y.K., 2009. *Water Conservation, Wetland Restoration and Agriculture in the Colorado River Delta, Mexico*, Ph. D., The University of Arizona., Tucson, AZ.
- Comisión Nacional del Agua (CONAGUA), 2006, *Rehabilitación y Modernización del Distrito de Riego 014, Rio Colorado, Baja California y Sonora. V.1.* Mexicali, B.C., Mexico.
- Comision Nacional del Agua (CONAGUA), 2008. *Características Generales del Distrito de Riego 014, Rio Colorado-Anexo1. Jefatura del Distrito de Riego 014, Departamento de Estadística Agrícola.* Mexicali, B.C., Mexico.

- Feirstein, E., Zamora-Arroyo, F., Vionnet, L. y Maddock, T. 2008. Simulation of groundwater conditions in the Colorado River Delta, Mexico. Tesis de Maestría. Tucson, AZ.
- Franke, O.L., Reilly, T.E., Bennett, G.D., (1987). Definition of boundary and initial conditions in the analysis of saturated ground-water flow systems – An introduction. Techniques of Water-Res. Invests. of the U.S. Geol. The survey, Book 3, Ch. B5: 15 pp.
- Gupta, S. K., (2010) Surface and Groundwater Flow Modelling, in Modern Hydrology and Sustainable Water Development, John Wiley & Sons, Ltd, Chichester, UK. doi: 10.1002/9781444323962.ch5.
- Harbaugh, A. W., E. R. Banta, M. C. Hill, and M. G. McDonald (2000), MODFLOW 2000, the U.S. Geological Survey modular groundwater model-user guide to modularization concepts and the groundwater flow process, U.S. Geological Survey Open-File Report 00-92, Reston, VA, USA.
- Harbaugh, A. 2005. MODFLOW-2005, The U.S. Geological Survey modular ground-water model—the Ground-Water Flow Process: U.S. Geological Survey Techniques and Methods 6- A16, variously p.
- Hassan, S. M. T., Lubczynski, M. W., Niswonger, R. G., & Su, Z. (2014). Surface-groundwater interactions in hard rocks in Sardon Catchment of western Spain: An integrated modeling approach. *Journal of Hydrology*, 517, 390–410. doi:10.1016/j.jhydrol.2014.05.026
- Hely, A.G., & Peck, E.L. 1964. Precipitation, Runoff and Water Loss in the Lower Colorado River-Salton Sea Area. U.S. Geological Survey Professional Paper 486-B. Washington, D.C.: U.S. Government Printing Office. 16 pp.
- Hill, B. M., (1993), Hydrogeology, numerical model and scenario simulations of the Yuma area groundwater flow model Arizona, California, and Mexico, Modeling Report no. 7, Arizona Department of Water Resources, Phoenix AZ, USA.
- Hill, M. (1998). Methods and guidelines for effective model calibration: US Geological Survey Water-Resources Investigations Report 98-4005, 90 p. US Geological Survey, Water Resources Investigations Report 98-4005, 1–98. Retrieved from [http://ascelibrary.org/doi/pdf/10.1061/40517\(2000\)18](http://ascelibrary.org/doi/pdf/10.1061/40517(2000)18)
[http://scholar.google.com/scholar?hl=en
&btnG=Search&q=intitle:](http://scholar.google.com/scholar?hl=en&btnG=Search&q=intitle:)
Methods+and+guidelines+for+effective+model+calibration, U.S.

+GEOLOGICAL+SURVEY+WATERRESOURCES+INVESTIGATIONS+REPO
RT+98-4005#1

- Hughes, J.D., Langevin, C.D., Chartier, K.L., and White, J.T., 2012, Documentation of the Surface-Water Routing (SWR1) process for modeling surface-water flow with the U.S. Geological Survey Modular Ground-Water Model (MODFLOW-2005): U.S. Geological Survey Techniques and Methods, book 6, chap. A40, 113 p.
- Kalbus, E.; Reinstorf, F. and Schirmer, M. (2006) Measuring methods for groundwater-surface water interactions: a review. *Hydrol. Earth System Sci.* 10(6), 873–887
- Konikow, L. F. (1996). Use of numerical models to simulate groundwater flow and transport. *Ground Water Techniques of Water-Res. Invests. of the U.S. Geol. The survey*, (1996), 75–116.
- Konikow, L. F., & Bredehoeft, J. D. (1992). Groundwater Models Cannot Be Validated. *Advances in Water Resources*, 15(1), 75–83. doi:10.1016/0309-1708(92)90033-x
- Krause, S., Bronstert, A., Zehe, E., 2007. Groundwater-surface water interactions in a North German lowland floodplain -Implications for the river discharge dynamics and riparian water balance. *Hydrol.* 347, 404-417. doi:10.1016/j.jhydrol.2007.09.028
- Maddock III, T., Baird, K.J., Hanson, R.T., Schmid, Wolfgang, and Ajami, H., 2012, RIP-ET: A riparian evapotranspiration package for MODFLOW-2005, U.S. Geological Survey Techniques and Methods 6–A39 p. 39
- Markstrom, S.L., Niswonger, R.G., Regan, R.S., Prudic, D.E., and Barlow, P.M., (2008) GSFLOW-Coupled ground-water and surface-water flow model based on the integration of the Precipitation-Runoff Modeling System (PRMS) and the Modular Groundwater Flow Model (MODFLOW-2005): U.S. Geological Survey Techniques and Methods 6 D1, 240 p.
- Mason, D., & Hipke, W. (2013). Regional groundwater flow model of the Tucson Active Management Area, Arizona, (24), 97. Retrieved from <http://www.azwater.gov/azdwr/default.aspx>.
- McMahon, T. A., Peel, M. C., Lowe, L., Srikanthan, R., & McVicar, T. R. (2013). Estimating actual, potential, reference crop and pan evaporation using standard meteorological data: a pragmatic synthesis. *Hydrology and Earth System Sciences*, 17(4), 1331–1363. doi:10.5194/hess-17-1331-2013

- McDonald, M. G., and A. W. Harbaugh (1988), Techniques of water-resources investigations of the United States Geological Survey: Chapter A1, Book 6, A modular three-dimensional finite-difference groundwater flow model, U.S.G.S., Reston VA, USA.
- Mehl and Hill, (2013), MODFLOW-LGR—Documentation of Ghost Node Local Grid Refinement (LGR2) for Multiple Areas and the Boundary Flow and Head (BFH2) Package
- Niswonger, R. G., Panday, S., & Ibaraki, M. (2011). MODFLOW-NWT, A Newton Formulation for MODFLOW-2005. Ground Water - Modeling Techniques, 56.
- Niswonger, R. G., & Prudic, D. E. (2005). Documentation of the Streamflow-Routing (SFR2) Packages to Include Unsaturated Flow Beneath Streams—A Modification to SFR1. U.S. Geological Survey, (Techniques and Methods 6-A13), 50. Retrieved from <http://pubs.er.usgs.gov/publication/tm6A13>
- Niswonger, R. G., Prudic, D. E., & Regan, S. R. (2006). Documentation of the Unsaturated-Zone Flow (UZFI) Package for Modeling Unsaturated Flow Between the Land Surface and the Water Table with MODFLOW-2005. Book 6, Modeling Techniques, Section A, Ground Water, 71.
- Olmsted, F., Loeltz, O. y Irelan, B. 1973. Geohydrology of the Yuma Area, Arizona, and California, Geological Survey Professional Paper 486-H, United States Government Printing Office Washington, DC.
- Owen-Joyce and Raymond 1996. An accounting system for water and consumptive use along the Colorado River, Hoover Dam to Mexico.
- Naff, R.L. and Banta, E.R., 2008, The U.S. Geological Survey modular ground-water model—PCGN: A preconditioned conjugate gradient solver with improved nonlinear control: U.S. Geological Survey Open-File Report 2008–1331, 35 p.
- Reilly, B. T. E., & Harbaugh, A. W. (1999). Guidelines for Evaluating Ground-Water Flow Models Different Modeling Approaches to Address. Retrieved from <http://pubs.usgs.gov/sir/2004/5038/PDF/SIR20045038part2.pdf>
- Rodríguez-Burgueño, J., (2012). Modelación geohidrológica transitoria de la relación acuífero-río de la zona FFCC -vado Carranza del río Colorado con propósito de manejo de la zona riparia., Master Eng., Universidad Autónoma de Baja California, Mexicali, B.C.

- Roman-Calleros, J., Ramírez-Hernández, J. 2003. Interdependent Border Water Supply Issues: The Imperial and Mexicali Valleys. In: Michel S. (Eds.), The U.S.-Mexican border environment: Binational water management planning. San Diego State University Press, San Diego, California, Chap: 2, pp. 95-144.
- Schmidt, W., R. T. Hanson, and T. Maddock (2004), Simulation of Conjunctive Agricultural Water Use with the new FARM package for MODFLOW-2000.
- Schmid, W., and R.T. Hanson (2009), The Farm Process Version 2 (FMP2) for MODFLOW-2005: Modifications and Upgrades to FMP1. U.S. Geological Survey Techniques in Water Resources Investigations, Book 6, Ch. A32.
- Secretaria de Relaciones Exteriores de Mexico (SRE), 1944. Tratado sobre la Distribución de Aguas Internacionales entre los Estados Unidos Mexicanos y los Estados Unidos de America.
- Sophocleous, M. (2002) Interactions between groundwater and surface water: the state of the science. *Hydrogeol. J.* 10, 52–67.
- Sophocleous, M. (2005). Groundwater recharge and sustainability in the High Plains aquifer in Kansas, USA. *Hydrogeology Journal*, 13(2), 351–365. doi:10.1007/s10040-004-0385-6
- Virdi, M. L., Lee, T. M., Swancar, A., & Niswonger, R. G. (2013). Simulating the effect of climate extremes on groundwater flow through a lakebed. *Ground Water*, 51(2), 203–18. doi:10.1111/j.1745-6584.2012.00969.x
- Winston, R.B. 2009. Model Muse: A graphical user interfaces for MODFLOW–2005 and PHAST: U.S. Geological Survey Techniques and Methods 6–A29, 52 p., available only online at <http://pubs.hical User Interface for MODFLOW–2005 and PHAST>.
- Winter, T.C. (1999) Relation of streams, lakes, and wetlands to groundwater systems. *Hydrogeology J*, 7. 28- 45.
- Wuol (1993). Applied Groundwater Modeling: Simulation of Flow and Advective Transport

PART TWO

**Modeling and Simulations of Conjunctive use with
MODFLOW'S Farm process in Irrigation Unit 16 (Modulo 16).**

Abstract

This study identified the effects of agricultural activities on groundwater levels and groundwater recharge in irrigation unit 16 by comprehensive MODFLOW Farm process (MF-FMP) numerical modeling. The source of water to the groundwater reservoirs in the study area is through net-agricultural recharge, which amounts a total of $97.84 \times 10^4 \text{ m}^3$. The study area experienced high groundwater evaporation amount of about $123.16 \times 10^4 \text{ m}^3$. Calibration of the model using the available observations of groundwater levels gives a relatively good fit with an RMS of 0.02 m and a normalized RMS of 2.1% with a correlation coefficient of 0.97. The reported agricultural pumpage located at WBS1 and WBS2 were used as an additional calibration target that, the simulated pumpage is within the range of uncertainty of the reported pumpage. The average annual differences (reported minus simulated) for total agricultural were $-671 \text{ m}^3/\text{yr}$. and $-570 \text{ m}^3/\text{yr}$. which represents average differences of about -0.54 and -0.49 percent of the reported agricultural pumpage for WBS1 and WBS2 respectively. The average negative change in storage is indicating that outgoing groundwater from the study area is higher than incoming groundwater (recharge) which shows aquifer depletion. The MF-FMP modeling results show that the water table in the study area is drawn down, more in eastern areas. The inflow-outflow analysis shows that recharge to the aquifer occurring in response to agricultural supplies. In general, the model provides MF-FMP simulations of natural and anthropogenic components of the hydrologic cycle, the distribution and dynamics of supply and demand in the study area.

Keywords: *Mexico, MODFLOW farm process, Agriculture, Groundwater level, Groundwater recharge*

1. Introduction

The determination of surface-water and groundwater allocations to farms is desirable for legal requirements (e.g. stream volume adjudications), and for agro-economic decision making ahead of the growing season. The need to specify these flow rates applies to historic and future time intervals (Schmid, 2004). In Mexico groundwater already represent 38% of total annual water withdrawal and agriculture represents over three-fourths of the total groundwater withdrawal at national levels (OECD, 2015).

Irrigation unit 16, one of irrigation unit out of the 24 irrigation units of irrigation district 014 in Mexicali valley which is located adjacent to the US-Mexican border , is one of the most productive agricultural areas in the region. However, increases in population and transitions to crops that consume additional water have increased the demand for water within the valley as of other irrigation units.

Although a very few groundwater wells exist in this unit, the effect of groundwater pumping on the adjacent irrigation units which they share the same aquifer brought a negative effect on the groundwater source of the unit. Most of the irrigation water is driven from diverted Colorado River.

The Colorado River is among the most regulated, used, and contaminated waterways in the world. This river is currently used to the extent that it often no longer discharge to its respective termini, whose billions of cubic meters of annual flow no longer reach, the Gulf of California. This situation is largely driven by upstream diversions and economic forces that make the border region one of the most productive geographic regions in México. This is also one of the driest regions in Mexico and its explosive growth has put tremendous strain on the limited water resources.

The water levels throughout most of the Mexicali valley groundwater have not significantly recovered. Mitigation measures are essential to bring the groundwater back into hydrologic balance. To develop a management plan, simulating the supply and demand components can help water managers to assess the effects of the various components on the mitigation of the groundwater system.

The Farm Process (Schmid and others, 2006a) for the U.S. Geological Survey's (USGS) modular groundwater model MODFLOW (Harbaugh, 2005) can simulate the supply and demand components and can help water managers to assess the effects of the

various components for the mitigation of the groundwater system overdraft. A regional hydrologic model on irrigation 16 is developed using MODFLOW Farm process to provide water managers with this capability and to show that using this program can one develop supply and demand components for the whole valley for future water management in the region.

The aim of this particular study is to create a capability for the water managers and regional stakeholders to quantify the potential benefits of various options for bringing the region groundwater back into hydrologic balance. A hydrologic flow model capable of being accurate at scales relevant to water management decisions was developed by using MODFLOW Farm process (MF-FMP).

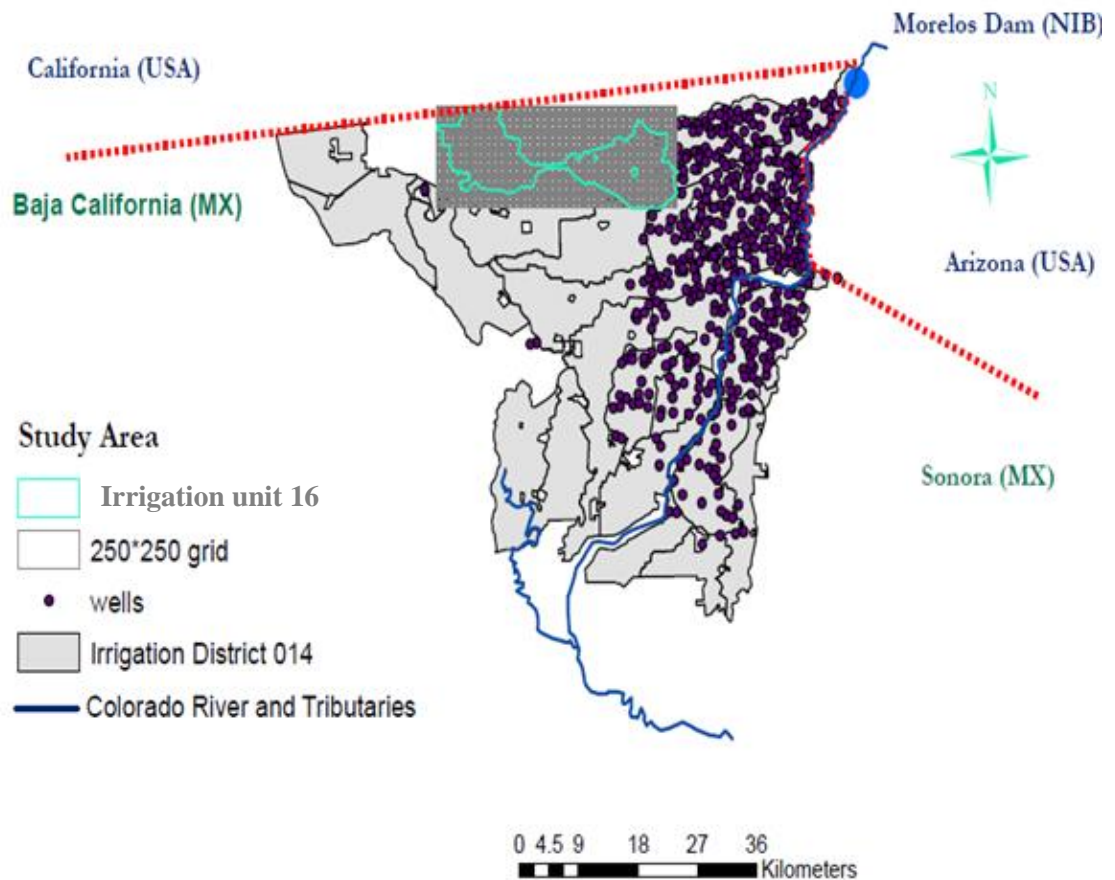


Figure 1 Irrigation District 014 and active cell boundary for irrigation unit 16 for MF-FMP modeling

1.1. Review on MF-FMP

MF-FMP uses MODFLOW-2000 (Harbaugh et al., 2000), MODFLOW-2005 (Harbaugh, 2005), and MODFLOW-OWHM (Hanson et al., 2014) versions. MODFLOW is a widely accepted, open-source, hydrologic model that has been in use since 1988. Over a period of decades, many people from academia, government agencies, and the private sector from all over the world have continuously contributed to its development and bug fixes. It is the most used and trusted groundwater model in the world and recently has been expanded to include more realistic coupling between surface and subsurface processes.

1.1.1. Governing Equations

Conservation equations for groundwater, stream, lake, root zone, and land-surface runoff processes are solved simultaneously to simulate a large portion of the hydrologic cycle, and the agronomic and human effects on the cycle. Among the mass conservation equations, the groundwater-flow equation (1) is the governing equation that is solved for groundwater heads. MF-FMP uses the finite-difference approach. Conservation equations for the other surface water and landscape flow processes are also solved at each iteration until convergence of a groundwater-flow equation solver is reached. The solver is assumed to have converged when a user-specified closure criterion is met for the difference between results of successive iterations using the maximum absolute value of the change in groundwater hydraulic heads and, optionally in MF-FMP, also of residual groundwater flows at all nodes. With the coupled stream-groundwater conservation equations to simulate the stream-aquifer interactions, MF-FMP is a powerful tool to effectively address important issues, such as effects of conjunctive use programs, changes in irrigation methods, and implementation of urban and agricultural water conservation programs, etc. on the hydrologic system modeled.

MF-FMP can simulate the infiltration across unsaturated zones beneath stream beds (Niswonger and Prudic, 2005) and beneath large areas with unsaturated zones (Niswonger et al., 2006). In the horizontal direction, it can simulate stream diversions to agricultural and urban lands, and the surface runoff (i.e., rainfall runoff and irrigation return flow) into streams. The models also simulate the conjunctive use of surface water and groundwater to satisfy the consumptive use requirement of vegetation in excess of the effective precipitation as well as urban water demands.

MF-FMP can be considered a fully coupled surface and groundwater interactive hydrologic model; historically it originates from the groundwater model MODFLOW. While stress periods can be of any length, solution time steps of long-term regional MF-FMP models are commonly on the order of weeks or longer, as is typical for regional hydrologic models used to analyze conjunctive use over decades. At these time steps, and for medium root-zone depths, MF-FMP assumes all inflows into the root zone to be equal to all outflow, on the basis of numerous HYDRUS-2D (Simunek et al., 1999) simulations for various crop and soil types, root zone and capillary-fringe depths, water-table configurations, and levels of potential evapotranspiration (Schmid, 2004; Schmid et al., 2006). In MF-FMP, inflows that meet the crop evapotranspiration requirements are precipitation, irrigation, and root uptake from groundwater. Outflows are transpiration and evaporation, runoff, and deep percolation beneath the root zone.

MF-FMP simulates delayed recharge through a deep vadose zone beneath root zones through a linkage to the Unsaturated Zone Flow package (Niswonger et al., 2006; Schmid and Hanson, 2009b). Through the same linkage, MF-FMP also simulates groundwater discharge to the surface and rejected infiltration from fully saturated conditions under conditions of shallow or above-surface groundwater levels.

MF-FMP also simulates the interaction between streams and groundwater. For streamflow routing and stream-aquifer interaction across the streambed, MF-FMP uses the Streamflow-Routing Package, SFR (SFR1, Prudic et al., 2004; SFR2, Niswonger and Prudic, 2005). MF-FMP can also simulate delayed recharge from infiltration beneath streambeds through a deep vadose zone (Niswonger and Prudic, 2005).

The MF-FMP SFR package uses several options to define the relationship between the stream stage and the flow (e.g., Manning's equation with a rectangular channel or an irregular-shaped cross-section, either a rating table or a power function relating both depth and width to streamflow). The stream-aquifer interaction in MF-FMP expressed using Darcy's equation as,

$$Q_{sg} = \frac{K_{st} W_s L_s}{d} \Delta h_{sg} \quad (1)$$

Where, Q_{sg} : Flow rate between a stream section and the aquifer (L^3T^{-1}),

K_{st} : The hydraulic conductivity of the streambed material (LT^{-1}),

W_s : The width of stream section (L),

L_s : The length of stream section (L),

d : The thickness of streambed material (L),

Δh_{sg} : the vertical head difference between a stream and the aquifer (L).

To comply with Darcy's law in simulating flow through the streambed, the SFR package assumes that the streambed is saturated at all times with zero pressure at the bottom of the streambed. The SFR package represents the stream-aquifer interaction when they are hydraulically disconnected as,

$$Q_{sg} = K_{st}W_sL_s\left(\frac{d+s}{d}\right) = K_{st}W_sL_s\left(1 + \frac{s}{d}\right) \quad (2)$$

Where, s is the stream stage (L).

Equation (2) assumes that the stream bed is saturated at all times. However, following a prolonged drought the stream bed will be dry and it will require some time for re-wetting. If the stream stage compared to the thickness of the stream bed is small, such that s/d in equation (2) is much less than 1, most or all of the stream flow will likely be used in re-wetting the stream bed and no seepage will occur. However, using equation (2), a non-zero seepage rate will be computed that can be as large as the stream flow itself. In MF-FMP, the streambed is assumed to be saturated at all times, which, because of the large time steps used in most groundwater models, is tantamount to assuming that the time for rewetting is short enough to not significantly affect the modeled stream-aquifer water budget terms.

In MF-FMP, the user has the option to simulate delayed recharge from infiltration beneath streambeds through a deep vadose zone (Niswonger and Prudic, 2005). First, using this option imposes a constraint for the Darcy-type stream seepage across the streambed as described above, which cannot exceed the vertical hydraulic conductivity of the underlying unsaturated zone. Second, the infiltration into the unsaturated zone between the streambed and the water table is converted to the water content of leading or trailing waves of wetting or drying fronts by assuming that the vertical flux is driven by gravitational forces only. The propagation of the waves is then simulated by a kinematic wave approximation of vertical seepage through the

unsaturated zone. However, the water content cannot exceed the saturated water content when the infiltration rate exceeds the saturated vertical hydraulic conductivity.

1.1.2. Land Use and Root Zone Processes

MF-FMP considers two types of water budgeting for the control volume horizontally delineated by land surface areas, called “farms”. These water-accounting units can include irrigated and non-irrigated farms, native vegetation, and urban areas. Using the term “farm” in MF-FMP” has become somewhat of an anachronism as MF-FMP has advanced to types of water-accounting units other than just agricultural farms. The water-accounting units in MF-FMP; do not include changes in soil-water storage and, hence, are control interfaces at the land surface. There are two types of budgeting associated with these water-accounting units.

I. Mass balance between all physical inflow and outflow components to and from the control volume;

ii. Economic balance between the irrigation water demand and the water supply from the different surface or groundwater components to meet this demand.

In the real world, the physical water balance is always achieved (i.e. mass is not created or lost), whereas the economic balance may not be maintained. For instance, farmers may apply more water than the true crop irrigation requirements, an unforeseen drought may limit irrigation, non-irrigated lands that depend solely on precipitation may not get enough water in drought seasons and get too much water in wet seasons, or overall source of water may be a limiting factor.

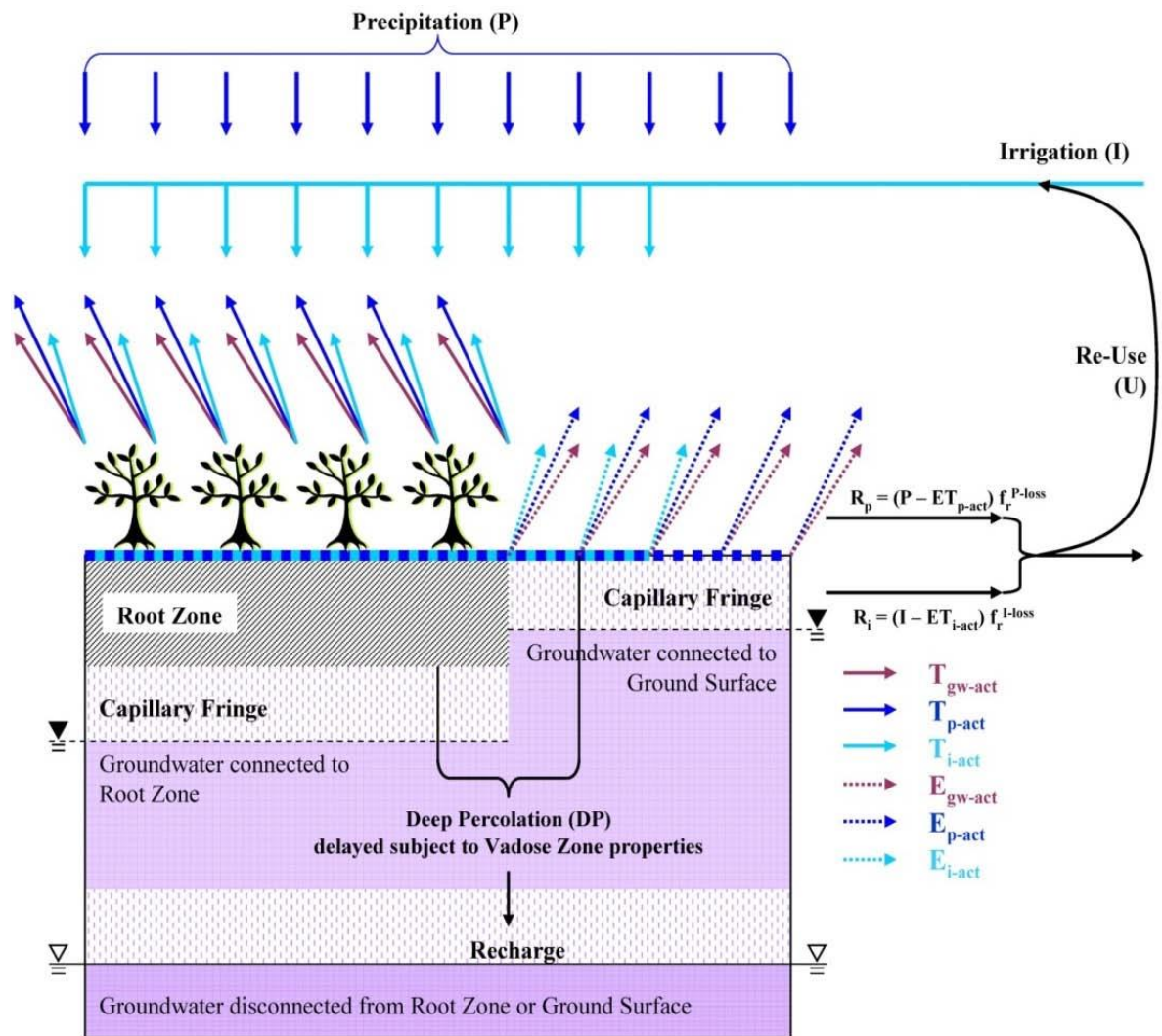


Figure 2 Schematic representation of root zone and land surface flow processes simulated by MF-FMP (Schmid and Hanson, 2009b)

Where,

- | | |
|---|--|
| P - Precipitation | T_{gw-act}, E_{gw-act} - Portion of actual transpiration and evaporation fed by GW |
| I - Irrigation | T_{p-act}, E_{p-act} - Portion of actual transpiration and evaporation fed by P |
| U - Re-use of irrigation water | T_{i-act}, E_{i-act} - Portion of actual transpiration and evaporation fed by I |
| Dp - Deep percolation | ET_{p-act} - Portion of actual evapotranspiration fed by P |
| R_p - Return flow related to precipitation | ET_{i-act} - Portion of actual evapotranspiration fed by I |
| R_i - Return flow related to irrigation | f_r^{p-loss} - fraction of inefficient losses to surface water related to P |
| | f_r^{i-loss} - fraction of inefficient losses to surface water related to I |

For a given computational unit; a particular land use area in a given cell, the general mass-balance equation that MF-FMP is based on for the root zone is the following(refer Figure 2 for mass-balance components):

$$P^{t+1} + I^{t+1} + ET_{gw-act}^{t+1} - ET_{c-act}^{t+1} - R^{t+1} - DP^{t+1} = \frac{\theta^{t+1} - \theta^t}{\Delta t} \quad (3)$$

and

$$R^{t+1} = R_p^{t+1} + R_i^{t+1} \quad (4)$$

where P is precipitation (LT^{-1}), I is irrigation water (LT^{-1}), ET_{gw-act} is root uptake from groundwater (LT^{-1}), ET_{c-act} is the total actual crop evapotranspiration (LT^{-1}), R is the runoff from precipitation and irrigation (LT^{-1}), R_p is the surface runoff from precipitation (LT^{-1}), R_i is the irrigation surface return flow (LT^{-1}), DP is the deep percolation that leaves the root zone as the moisture moves downward (LT^{-1}), θ^{t+1} is the soil moisture at the end of a time step (L), θ^t is the soil moisture at the beginning of a time step (L), Δt is the time step length (T), and t is the time step index (dimensionless).

In MF-FMP, equation (3) is solved for each cell at each iteration (equation 5) because many of the terms depend directly or indirectly on the elevation of the groundwater head, h. ET_{gw-act} and ET_{c-act} vary with groundwater head where the water table is shallow enough to evaporate and(or) be transpired. Since applied irrigation (I) and return flows from excess irrigation (R and DP) depend on $ET(h)$ terms as part of the irrigation requirement calculation, these terms depend indirectly on groundwater head. The following sections (c through f) explain the dependencies of the actual ET components ($ET_{c-act}(h)$ and $ET_{gw-act}(h)$) on the head from the irrigation delivery requirement ($I(h)$) and explain the dependencies of the crop irrigation requirement ($ET_i-act(h)$) on the actual ET, runoff return flow ($R(h)$), deep percolation ($DP(h)$), and irrigation delivery requirement ($I(h)$) for MF-FMP.

MF-FMP does not consider changes in soil-water storage in the root zone (i.e., RHS in equation (6) = 0):

$$P^{t+1} + I^{t+1} + ET_{gw-act}^{t+1} - ET_{c-act}^{t+1} - R^{t+1} - DP^{t+1} = 0 \quad (5)$$

MF-FMP does simulate changes in storage in the deeper vadose zone below the root zone through a linkage to the Unsaturated Zone Flow package (Niswonger et al., 2006) by treating deep percolation out of the root zone as quasi-infiltration into the deeper vadose zone.

A comparison of how each term in equation (3) is computed by MF-FMP is given in the following sections.

MF-FMP does not simulate the rate of change in soil moisture in the root zone. MF-FMP is currently limited to time steps of several days or longer, commonly used in groundwater modeling, and was not designed to simulate root-zone processes in deep root zones (on the order of several meters) with high soil-water storage potential that requires simulation on the order of minutes to days. MF-FMP assumes quasi-steady state conditions in the root zone on the basis of findings from transient HYDRUS-2D soil-column models representing shallow- to medium-depth root zones (Schmid et al., 2006). Simulated inflows into the root zone converged to outflows after time intervals of several days, the minimum time step commonly used in groundwater modeling. Hence, for these conditions in MF-FMP, the rate of change in soil moisture is not tracked.

The potential crop ET, ET_{c-pot} , can be specified for each crop or calculated internally as the product of specified reference ET, ET_r , and crop coefficients, K_c . Using a specified fraction of transpiration, K_t , ET_{c-pot} is separated into potential crop transpiration, $T_{c-pot} = K_t ET_{c-pot}$, and potential crop evaporation, $E_{c-pot} = (1-K_t) ET_{c-pot}$. Separating E and T data input is in line with multi-component ET models (Shuttleworth and Wallace, 1985; Kustas and Norman, 1997; Guan and Wilson, 2009), some variably-saturated-flow models (e.g., HYDRUS, Simunek et al, 1999; or SWAP, Kroes and van Dam, 2003), or with the use of transpiration (K_{cb}) and evaporative (K_e) crop coefficients (Allen et al., 1998). MF-FMP differs from the latter by not composing K_c by separate K_{cb} and K_e coefficients but by optionally making use of literature data K_c and K_{cb} to preprocess fractions of transpiration as ratios of K_c and K_{cb} . However, preprocessing or estimating K_t fractions is required from the user and not part of MF-FMP.

MF-FMP optionally simulates conditions of wilting or anoxia, which is appropriate if ET_{c-pot} input data are derived under ‘unstressed conditions’ as, for instance, stated by Allen et al. (1998) for ET_c listed therein. Using ET_{c-act} as input data for this option would

erroneously double-account for simulated stresses already inherent in the measurement. MF-FMP reduces T_{c-pot} proportionally to the reduction of the active root zone by conditions under which root uptake ceases (Schmid et al., 2006). For a simple ‘Concept 2 (Figure 3),’ a root zone is assumed to be inactive for anoxic conditions caused by saturation through groundwater but not for conditions of wilting. For a more complex ‘Concept 1 (Figure 4),’ a root zone is assumed to be inactive for ranges of pressure heads under variably saturated conditions at which uptake ceases because of stresses of wilting or anoxia. The response of crops to stresses of wilting or anoxia is specified in MF-FMP as crop-specific pressure heads at which uptake is either zero, commonly called wilting or anaerobiosis points (Feddes et al., 1976), or at maximum analogous to reduction functions by Prasad (1988), or Mathur and Rao (1999), or stress response functions by Simunek et al. (1999).

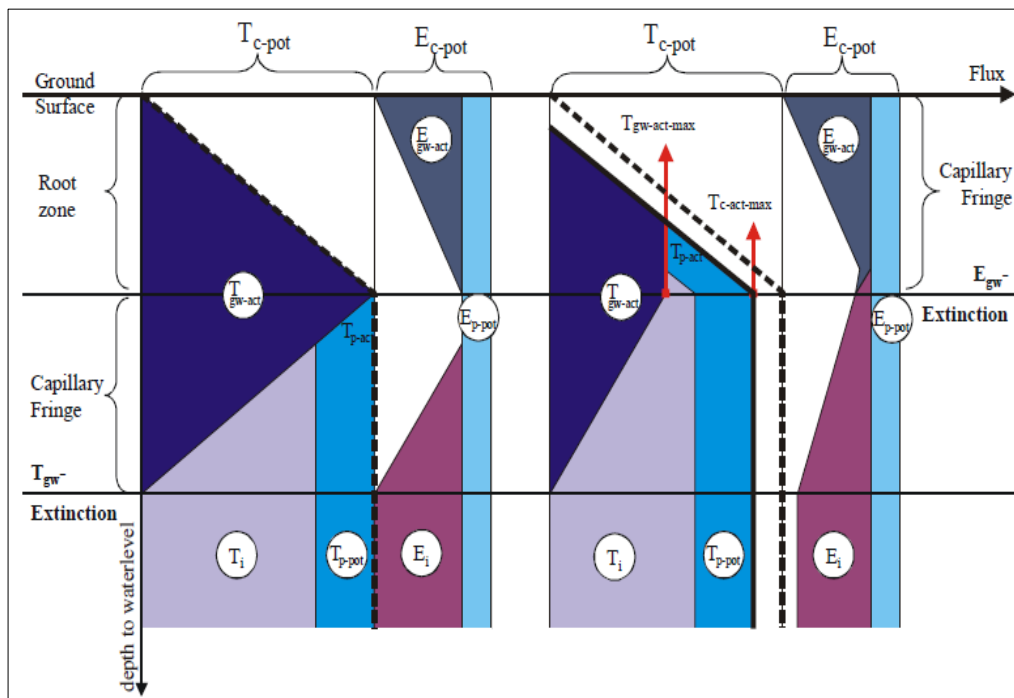


Figure 3 Change of Crop Consumptive Use Components with varying Head (root zone = Capillary Fringe, Concept1, concept2, left to right)

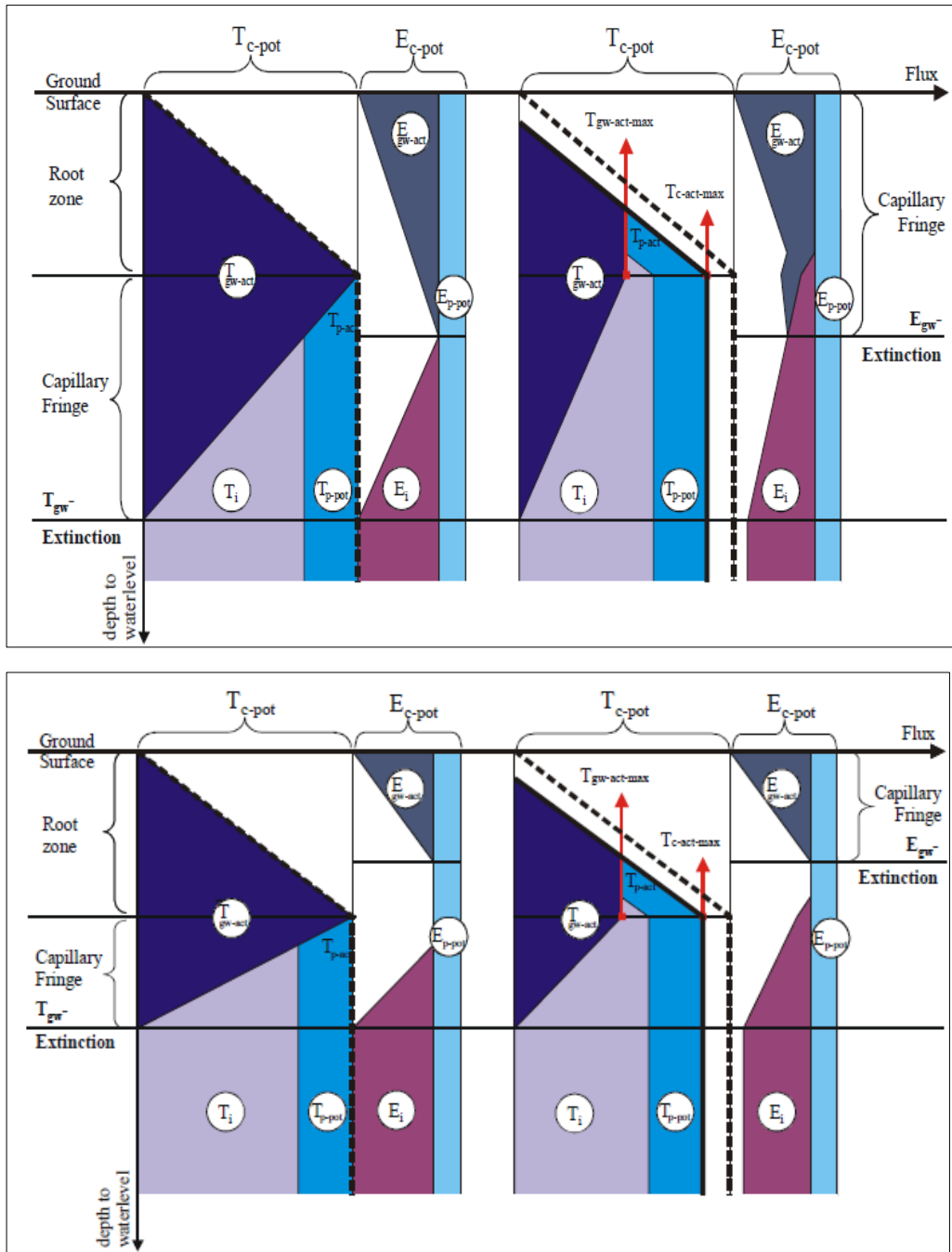


Figure 4 Change of Crop Consumptive Use Components with varying Head (root zone $<$, $>$ Capillary Fringe, Top to Bottom and Concept1, concept2, left to right)

Zones within the root zone where conditions of wilting or anoxia eliminate root uptake (in MF-FMP: wilting or anoxia zones) are found by matching ranges of zero-response

pressure heads with a vertical steady-state pressure-head distribution. One approach would be to solve for vertical transient pressure head distributions using Richard's-equation-based variable-saturation flow models; however, these require soil-water constitutive input parameters and may be computationally expensive when linked to regional groundwater models. Instead, MF-FMP uses analytical solutions of vertical steady-state pressure-head distributions derived from transient, Richard's-equation-based, variably saturated soil-column models upon convergence of atmospheric and moving water-level boundary fluxes after time intervals of several days. Soil-column models were developed using HYDRUS-2D (Simunek et al., 1999) for various soil-specific soil-water constitutive parameters, crop-specific stress-response functions, root-zone depths, depths to groundwater, and rates of potential transpiration with groundwater as the only source for root uptake (Schmid, 2004). For groundwater rising above the root-zone bottom, a wilting zone in the upper part of the root zone decreased linearly, and an anoxia fringe above the water table remained constant until its top reached ground surface. For other HYDRUS-2D simulations, infiltration (e.g., from precipitation or irrigation) was added as an additional source for root uptake. However, the actual transpiration, T_{c-act} , did not reach T_{c-pot} because infiltration wetting-fronts also can contain pressure heads at which the crop's response to anoxia reduces transpiration (Drew, 1997). Hence, even for root zones not influenced by groundwater, T_{c-act} cannot exceed an anoxia-constrained maximum possible $T_{c-act-max}$. Adding infiltration in excess of $T_{c-act-max}$ resulted in transpiration-inefficient losses. $T_{c-act-max}$ might further be diminished if pressure heads of a wetting front are higher than those of an anoxia fringe above a water table or where drainage takes place in lower parts of the root zone that causes wilting.

MF-FMP calculates a maximum actual transpiration (T_{c-act} ; eq. (4)) and portions of transpiration fed by uptake from groundwater (T_{gw-act} ; eq. (5)), precipitation and supplemental irrigation (T_{i-act} ; eq. (9)), assuming no changes in soil-water storage over time steps, and equal spatial distribution of roots and potential transpiration over the root zone. The full development of these features is described by Schmid et al. (2006) and Schmid and Hanson (2009b). In summary, the estimate of actual from potential transpiration in MF-FMP is formulated using the three components of groundwater, precipitation, and irrigation as:

$$T_{c-act} = \begin{cases} 0 & \text{if } h \geq h_{ux} \\ T_{c-pot} \frac{h_{ux}-h}{r} & \text{if } h_{ux} > h > h_{rb}; h_{ux} = g - a \\ T_{c-pot} \left(1 - \frac{a}{r}\right) = T_{c=act-max} & \text{if } h \leq h_{rb} \end{cases} \quad (6)$$

$$T_{gw-act} = \begin{cases} 0 & \text{if } h \geq h_{ux} \\ T_{c-pot} \frac{h_{ux}-h}{r} & \text{if } h_{ux} > h > h_{wx}; h_{ux} = g - a, h_{wx} = g - r + w \\ T_{cpot} \left(1 - \frac{a+w}{r}\right) = T_{gw-act-max} & \text{if } h_{wx} \geq h > h_{rb} \\ T_{gw-ac-max} \left(1 - \frac{h_{rb}+h}{d}\right) = T_{gw-act-max} & \text{if } h_{lx} < h \leq h_{rb}; h_{lx} = g - r - d \\ 0 & \text{if } h \leq h_{lx} \end{cases} \quad (7)$$

$$T_{c-act} = \begin{cases} 0 & \text{if } h \geq h_{wx}; h_{wx} = g - r + w \\ T_{c-act} - T_{gw-act} & \text{if } h < h_{wx}, T_{p-pot} > T_{c-act} - T_{gw-act} \\ T_{c-pot} & \text{if } h < h_{wx}, T_{p-pot} \leq T_{c-act} - T_{gw-act} \end{cases} \quad (8)$$

$$T_{i-act} = T_{c-act} - T_{gw-act} - T_{p-act} \quad (9)$$

Where (Fig. 2):

a = depth of the anoxia fringe (L), w = depth of wilting zone (L).

r = total depth of root zone (L), d = depth of capillary fringe (L),

g = ground-surface elevation (L), h = groundwater head elevation (L),

h_{rb} = groundwater head elevation at the bottom of the root zone (L),

h_{ux} = head elevation where top of anoxia fringe, a , above the water level is at ground surface elevation, g (*elevation of upper transpiration extinction*) (L),

h_{wx} = head elevation at which bottom of the wilting zone, w , is at ground-surface elevation, g (*elevation of wilting zone extinction*) (L),

h_{lx} = head elevation at which top of capillary fringe, d , is at bottom of the root zone, h_{rb} (*elevation of lower transpiration extinction*) (L).

For Concept 1, T_{c-act} varies linearly in eq. (6) between the elevation of upper transpiration extinction, h_{ux} , and the elevation of the root-zone bottom, h_{rb} . For heads below the root-zone bottom, T_{c-act} is constant and reduced by the ratio between the anoxia fringe, a , and

the total root zone, r . In eq. (7), T_{gw-act} varies linearly between the elevation of upper transpiration extinction, h_{ux} , and the elevation of wilting zone extinction, h_{wx} . For heads between h_{wx} and root-zone bottom, T_{gw-act} is constant and reduced from T_{c-pot} to a maximum actual transpiration from groundwater, $T_{gw-act-max}$, by the ratio between the sum of anoxia and wilting zones, $a + w$, and the total root zone, r . T_{gw-act} also varies linearly between the head elevations between the root-zone bottom and lower transpiration extinction, h_{lx} . In eq. (8), T_{p-act} is equal to T_{p-pot} , except when limited to the remainder of T_{c-act} that is not yet satisfied by transpiration fed by T_{gw-act} .

For ‘Concept 2,’ wilting and anoxia above the water level are not simulated ($a = 0$, $w = 0$ in eq. (6) and (7)), but T_{c-pot} is still linearly reduced to T_{c-act} (eq. (6)) or T_{gw-act} (eq. (7)) as the active root zone is reduced by a rising water level. T_{c-act} equals T_{c-pot} for water levels below the root-zone bottom, and T_{gw-act} reaches T_{c-pot} for water levels located at the root-zone bottom.

The actual evaporation from precipitation, E_{p-act} , is equal to the potential evaporation from precipitation, E_{p-pot} , where precipitation in open areas exceeds E_{p-pot} , and equal to precipitation in open areas where E_{p-pot} exceeds this precipitation. The potential evaporation from irrigation, E_{i-pot} , can be reduced in open and exposed areas if not fully wetted. Evaporation fractions of E_{p-pot} related to irrigation, Ke^i , can, therefore, be smaller than $(1-K_t)$. If ET input data reflect local wetting patterns of irrigation methods and a reduction in evaporation is implicitly accounted for, then the user should keep $Ke^i = (1-K_t)$. In eq. (10), the actual evaporation from irrigation, E_{i-act} , accounts for evaporative losses of irrigation and varies proportionally to the transpirative irrigation requirement by a ratio of Ke^i and K_t :

$$E_{i-act} = T_{i-act} (Ke^i/K_t) \quad (10)$$

The remaining saturation water-vapor pressure deficit over the exposed areas that is not yet satisfied by E_{p-act} or E_{i-act} is assumed to be met by evaporative capillary groundwater uptake as long as the groundwater level in a cell allows the capillary fringe to be partially above the extinction depth. The evaporation from groundwater, E_{gw-act} , varies linearly with the groundwater level (eq. (11)) between zero for groundwater heads below the elevation of

evaporation extinction, h_{ex} (= surface elevation, g , minus capillary fringe, c) and a maximum for heads rising to or above the ground surface, g :

$$E_{gw-act} = \begin{cases} E_{c-pot} - E_{p-act} & \text{if } h \geq g \\ (E_{c-pot} - E_{p-act}) \left(1 - \frac{g+h}{c}\right) & \text{if } g < h < h_{ex}, \text{ with } h_{ex} = g - c \\ 0 & \text{if } h < h_{ex} \end{cases} \quad (11)$$

Overland runoff can be composed of several flow components, such as (a) direct runoff, (b) interflow from excess precipitation and irrigation, (c) runoff generated by infiltration in excess of the saturated hydraulic conductivity of the deeper unsaturated zone beneath the root zone, and (d) runoff from groundwater discharge and from rejected infiltration in areas of high groundwater levels. MF-FMP cannot capture all of these components. Historically, MF-FMP was developed to address flood and basin-level irrigation along the Rio Grande of New Mexico, where slopes are small and direct runoff is negligible, but interflow runoff can matter in different intensities for irrigation and precipitation (Schmid et al. 2009c). Hence, MF-FMP simulates runoff component (b). Runoff components (c) and (d) are available in MF-FMP through a linkage to the Unsaturated Zone Flow Package (Schmid and Hanson, 2009b) but are not discussed further here as this linkage is optional for deeper vadose zones that extend below the root zone.

MF-FMP computes R as the portion of crop-inefficient losses from precipitation or irrigation that contribute to runoff:

$$R_p = (P - ET_{p-act}) f_r^{p-loss} \quad (12)$$

$$R_i = (I - ET_{i-act}) f_r^{i-loss} \quad (13)$$

Where, ET_{p-act} and ET_{i-act} are the portions of the ET_{c-act} fed by precipitation or irrigation (LT^{-1}), respectively, and f_r^{p-loss} and f_r^{i-loss} are fractions of the respective crop-inefficient losses from precipitation or irrigation that go to a runoff, given as time series data. Losses from precipitation or irrigation that do not contribute to runoff are assumed to be deep percolation. MF-FMP assumes that all precipitation or irrigation is initially available for crop evapotranspiration before any runoff in the form of crop-inefficient

losses occurs. Instead of specifying f_r^{p-loss} and f_r^{l-loss} manually, MF-FMP also provides an alternative option to calculate these fractions based on the local (cell-by-cell) slope of the surface. In MF-FMP, irrigation return flow is routed to any user-specified stream reach or, alternatively, to let MF-FMP search for a stream reach nearest to the lowest elevation of the farm, where return flow is assumed to gather. The stream network is simulated by a linkage between FMP and the Streamflow Routing Package of MODFLOW. Re-use of irrigation return flow is not explicitly modeled in MF-FMP. However, the user has the option to return the entire runoff from both precipitation and irrigation losses to points of diversion either to the farm, from which the runoff originates, or to a downstream farm. This way, runoff becomes available for diversions and can be re-used.

In MF-FMP, the crop irrigation requirement, CIR, is equal to the actual evapotranspiration from irrigation, ET_{i-act} , and is computed for each model cell and iteration at each transient time step, assuming a quasi-steady state between all flows into and out of the root zone that is reached at the end of time intervals typical in MODFLOW, as follows:

$$CIR = ET_{i-act} = T_{i-act} + E_{i-act} \quad (14)$$

Where, T_{i-act} is the portion of the actual transpiration supplied by irrigation (LT^{-1}), and E_{i-act} is the actual evaporation loss from irrigation (LT^{-1}) proportional to T_{i-act} . The simulation of T_{i-act} and E_{i-act} is discussed in detail in the previous section and expressed in equations (9) and (10).

In MF-FMP, the crop irrigation requirement, CIR, is equal to the actual evapotranspiration from irrigation, ET_{i-act} , and is computed for each model cell and iteration at each transient time step, assuming a quasi-steady state between all flows into and out of the root zone that is reached at the end of time intervals typical in MODFLOW, as follows:

$$CIR = ET_{i-act} = T_{i-act} + E_{i-act} \quad (15)$$

MF-FMP calculates a total irrigation delivery requirement, I , for each cell at each iteration of a particular time step as the evapotranspirative crop irrigation requirement that depends on the groundwater head at the previous iteration divided by the on-farm efficiency of a particular time step:

$$I^{t,k+1} = \frac{ET_{i-act}^{t,k+1}}{e^t} (h^{t,k}) \quad (16)$$

Where e is the on-farm efficiency defined as the fraction of the total irrigation water that is used beneficially in the farm. The total irrigation water demand for each farm is computed as cell delivery requirements accumulated over all cells within the domain of a farm. CIR is computed only for cells that have land use defined as either urban irrigated landscape or an irrigated agricultural crop and is zero for cells with non-irrigated land use.

Comparing (15) to (16), it can be seen that, in MF-FMP, I is calculated for each cell on an iterative level based on a dynamically updated groundwater head-dependent evaporative crop irrigation requirement, ET_{i-act} .

MF-FMP computes deep percolation (DP) as the sum of deep percolation below the root zone from precipitation and irrigation, which can be instantaneous or delayed with linkage to the unsaturated zone infiltration package, UZF (Niswonger et al, 2006). It is the user-specified portion of losses of precipitation and irrigation that are not consumptively used by plants and not lost to surface water runoff:

$$DP = (P - ET_{p-act})(1 - f_r^{p-loss}) + (I - ET_{i-act})(1 - f_r^{i-loss}) \quad (17)$$

1.1.3. Water Demand and Supply

In the real world, computed or estimated water demands and available water supplies don't always balance. For instance, water agencies generally have surface-water rights defined by laws that may or may not equal their actual water demand. In severe drought years, farmers may not receive all the water they need for a target crop yield, creating a supply deficit. Conversely, in wet years, farmers may have more water delivered than is needed for irrigation to sustain surface-water rights, sustain flushing of saline soils, or to enhance deep percolation for later groundwater pumpage. Non-irrigated areas with natural vegetation rely solely on precipitation, which may be more or less than the actual plant evapotranspirative requirement.

MF-FMP is designed to address (i) most of the issues regarding the computation of water demand, (ii) configuration of different sources of water supply to meet this demand, and (iii) computation of the hydrologic effects of unbalanced demand and supply. The next

section discusses features in each model representing total water demand, water supply components, and the balance between supply and demand components.

1.1.3.1. Total water demand

In addition to irrigation water demand, MF-FMP also allows non-irrigation demand, such as urban, municipal, and industrial water demand, to contribute to the total requested demand that needs to be met with surface water and groundwater supply components.

In MF-FMP, other non-crop urban-water demand can be factored into the data input for so-called non-routed deliveries. That is, if non-routed external water transfers are known, then the municipal and industrial water demand needs to be subtracted first. The result is then the input in MF-FMP for non-routed deliveries. This may mean that more urban-water demand is subtracted than water transfers available. A negative non-routed delivery indicates a shortage that needs to be satisfied along with water demand for the urban irrigated landscape by other second and third-level delivery components, that is, routed surface water and pumped groundwater.

Another non-agricultural water demand can be the target percolation rate of a percolation pond or of a set of injection wells of an Aquifer-Storage-and-Recovery System (ASR). This demand can be simulated as a “design” irrigation demand of a “virtual zero-transpiration crop” that is based on the known maximum infiltration rate of the ASR pond or injection wells (Hanson et al., 2008). These and other non-routed deliveries are accounted for separately for each farm.

1.1.3.2. Water-supply components

The initial sources of water to meet the total water demand comes from precipitation, and root uptake from groundwater in MF-FMP. Any unmet demand in the model is satisfied by water imported from outside the model area, stream diversions, and groundwater pumping; referred to as water-supply components.

MF-FMP simulates three types of water deliveries into farms that originate as stream diversions: non-routed deliveries (NRD), semi-routed deliveries (SRD), or fully-routed deliveries (RD). NRDs are deliveries that originate from any source outside the model

domain; i.e., they represent water imported into the modeled area. SRDs and RDs originate from streams within the model domain. Multiple types of NRDs can be specified and are given farm identifiers (IDs) they serve maximum volumes, ranks in which sequence they are used, and information whether to recharge potential excess from NRDs into the stream network or into injection wells. Locations within the stream network from where SRDs are taken are specified by the user at modeled stream reaches. RDs are automatically diverted to a farm from the uppermost stream reach of either segment that are used for diversion only, or from any type of river segment that is located within the domain of the respective farm. The last source of water, groundwater pumping, comes from farm wells located at user-specified cells with specified maximum pumping rates and farm IDs they serve.

MF-FMP first uses NRD types in a sequence of their ranking to meet irrigation water demand. This can indirectly include the pumpage, delivery, and reuse of stored groundwater through ASR operations. Any unmet demand is then served by SRDs and finally by groundwater pumping. The maximum rates specified for each source of water generally represent legal or structural constraints on that source. NRDs are limited by the maximum rates specified for each of them. SRDs (or alternatively RDs) are limited by the available stream flow or by legal constraints such as equal appropriation allotment heights or prior appropriation calls. Diversion rates specified for a diversion from the main stem river into a diversion segment are possible through data input in the SFR Package. These “river-to-canal” diversions can be specified along with a segment near, or further upstream, from which the SDRs or RDs, as “canal-to-farm” diversions, occur. Subject to any canal water losses or gains in between the “river-to-canal” and “canal-to-farm” diversion, this mechanism can be used to construct a demand-driven and supply-constrained surface-water delivery system that is implicitly linked to the potential amount of water that is simulated to be conveyed in the stream to the point of diversion and delivery.

In MF-FMP, water is derived first from natural crop water-supply components such as precipitation and uptake from groundwater and second from delivery requirement-driven supply components (such as NRDs) and surface-water deliveries. All farm wells in MF-FMP are associated with a farm through the Farm-ID and can thus be located inside or outside the farm. The groundwater pumping of each farm equals the residual delivery requirement or the cumulative maximum pumping capacity, whichever is less. The farm

wells in MF-FMP can be single-aquifer wells that pump from the center of the finite-difference cell or multi-node wells which can represent non-uniform wellbore inflow from vertical multi-aquifer wells through a linkage with the multi-node well package (MNW; Halford and Hanson 2002) that is both head-and transmissivity-dependent. MNW allows for wellbore flow between model layers or aquifers typical of large irrigation-supply wells that occur during periods of pumpage and non-pumpage. This feature also allows for additional constraints on farm well pumpage through the head and drawdown features of the MNW package, which also are affected by the radius of each MNW farm well and the entrance losses of water flowing into these wells. The WELLFIELD option of MF-FMP allows for a re-distribution of stored groundwater, by recovery wells or well fields of an Aquifer-Storage-and-Recovery system (ASR), to receiving farms related to the cumulative demand of these farms. This pumpage is, in the case of the recovery wells of an ASR, recovered and reused water that originally was diverted from the stream network and percolated to groundwater by the ASR pond. The pumpage of any well field is distributed as simulated NRDs to receiving farms and given priority over local farm well pumpage. Farms can receive simulated NRDs from any number of well fields in a sequence of user-specified priority ranks designated in the input data (Schmid and Hanson, 2009b). Whenever one well field's pumpage is limited by rate, head, or drawdown constraints, the well field next in priority will contribute to the simulated demand of the NRDs. These ASR and multi-aquifer farm-well features provide a wide range of linkages to the use and reuse of water resources in the supply and demand water balance (Hanson et al., 2008).

1.1.3.3. Balance between water supply and demand

In MF-FMP, the total simulated water supply accounts for inefficient losses and meets crop irrigation requirements. Water supply in excess of the crop-water-demand will be converted into irrigation return flow and deep percolation using equations (16) and (17), respectively. Water supply in excess of the total demand only can occur for excess imported water (NRDs) by user specification to either discharge the excess back into the conveyance network or into injection wells.

MF-FMP does not simulate changes in soil-moisture storage; therefore, no depletion in soil moisture contributes toward satisfying the crop water demand. It is assumed that for most

modeling applications, and based on most irrigation practices; this distinction has minor consequences because most irrigation is performed on a regular basis during the growing season. Hence, an imbalance between irrigation demand and irrigation-supply components is not buffered by a soil-water reservoir. This becomes apparent at the first iteration of an MF-FMP time step. In case of supply deficit, MF-FMP requires that at each time step a solution to a deficit problem must be found according to the user's choice. The user has the choice to assume that (a) the necessary water supply must be guaranteed and that the deficiency will be made up by alternative sources external to the model domain; (b) the available supply will be used, but that after improving the efficiency and minimizing inefficient losses, the actual evapotranspiration will be further reduced, indicating that the crops' yield responds negatively to the deficit irrigation; or (c) profitability of a particular cropping pattern within a farm must be guaranteed by optimizing the profit subject to crop market benefits and water costs associated with a particular water type. The latter option may lead to a reduction of each cropped cell's area. Once MF-FMP detects a deficiency at the first iteration of a time step, the response to the deficit problem is dynamically applied according to the user's choice in the succeeding iterations of the same time step. These features of deficit response are unique to MF-FMP and provide a broad context of response to deficits in the entire supply and demand components of the entire hydrologic budget that spans all the farms within a watershed or groundwater basin.

As with any model, MF-FMP has limitations in the present version (FMP2). Three potential limitations are listed here. First, MF-FMP does not support daily or weekly, local-scale irrigation scheduling: MF-FMP was designed to be used at scales larger than individual fields and for periods of time that can span months to centuries. Second, MF-FMP calculates actual evapotranspiration based on pressure head dependent stress responses and root zone pressure heads. The stress response is calculated using analytical solutions of vertical steady-state, Richard's equation based, pressure head distributions assumed for relatively longer time steps common in groundwater modeling such as weeks. That is, MF-FMP assumes steady-state soil moisture storage within all-time steps that are time periods common in groundwater modeling and currently does not simulate changes in soil-moisture storage. This may result in poor approximations in some settings such as for dry-land farming or some climate change scenarios of natural vegetation that do not include

phreatophytic uptake of groundwater. Third, MF-FMP has simple options for runoff of inefficient losses based on fractions of applied water or local slope calculations. For additional details of other potential limitations that may affect certain hydrologic settings or applications, the reader is referred to Schmid et al. (2006a).

2. Purpose and Scope

Forecasts of irrigation demand and irrigation water supply are important information for the conjunctive management of surface water and groundwater supply to irrigation settings.

Estimates of these waters are needed for periods when irrigation water supply is either sufficient or insufficient to meet the irrigation water demand. Such periods of irrigation water sufficiency or insufficiency may relate both to the past and to the future.

Conveyance losses from surface water deliveries to a farm, groundwater irrigation pumping, and a farm's consumptive use can directly or indirectly impact flows at the boundary of a groundwater flow model.

In heavily inhabited and cultivated basins, the level of urban and agricultural water demands, and the water-resources-management practices implemented to meet these demands affect all processes of the hydrologic cycle. Therefore, to model the conjunctive use of surface and subsurface water effectively, it is necessary to integrate simulation methods for subsurface, surface, and urban and agricultural water demand computations. These models need to simulate conjunctive use in cases where there is not enough water supply to meet the total water demand. (Hanson et al 2010).

Sustainability of water resources is subject to changing demands and supplies that are integrated through conjunctive use and movement of all the water resources within a watershed. Conjunctive use of water is the joint use and management of surface water and groundwater resources to maximize reliable supply and minimize damage to the quantity or quality of the resource. The use and movement of water resources also are constrained by physical properties and other circumstances such as governance, social, or economic constraints as well as urbanization; climate change and ecological requirements; and water and soil chemistry and contamination. Increased agricultural productivity affects the local economy, resulting in prosperity, growth, and further transformation of agri-business to

more dynamic and intensive farming with higher profit crops, multiple cropping's, and multiple annual growing seasons.

The goal to approximate the allocation of surface-water and groundwater flow rates can, therefore, be approached by a mathematical model, which simulates groundwater flow by means of a governing groundwater flow equation, together with equations that describe flows or heads at the boundaries of the model (Anderson and Woessner, 1992).

By knowing or preprocessing a farm's consumptive use and its irrigation demand, and by simulating the surface-water delivery to a farm, a groundwater modeling program can then solve inversely for the flow rate of supplemental groundwater irrigation pumping. For a groundwater model, the determined groundwater pumpage is necessary to complete the mass balance outside the groundwater domain but is dependent on simultaneously keeping the mass balance within the groundwater domain. However, if the irrigation demand cannot be sufficiently supplied by surface- or groundwater, then the computer program must also provide options for how to respond to such a distortion of mass balance.

The ultimate aim of this part is to apply MODFLOW farm process (MF-FMP) at irrigation unit 16 (Figure 5) for calculating historic irrigation demand and irrigation water supply. This work would be an example for future development of integrated model for the whole irrigation District 014 using MF-FMP which helps management strategies for ensuring sustainability.

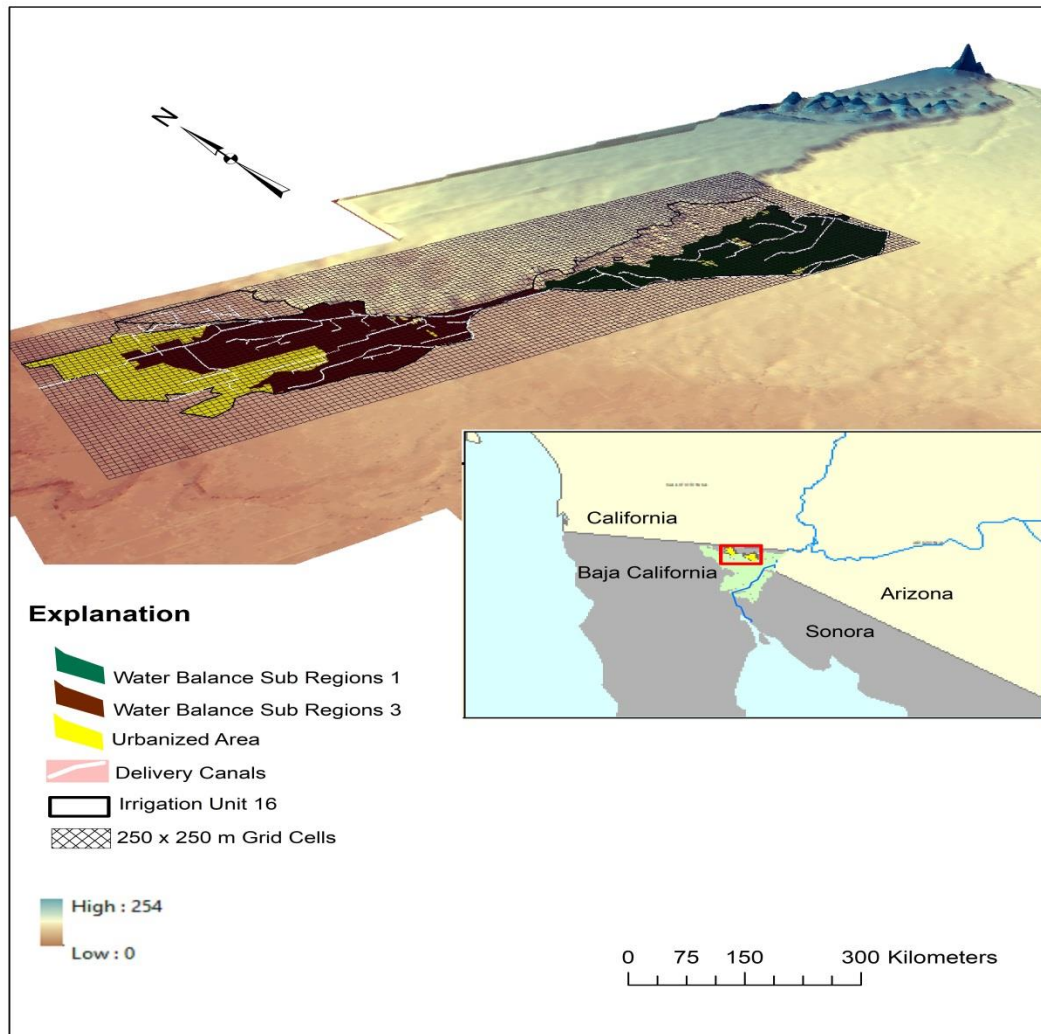


Figure 5. Active cell boundary and grids used for MF-FMP modeling

2.1. Approach

The creation of a new hydrologic model of the irrigation unit 16 in the Valley required the reanalysis of the original parent conceptual model and the hydrogeological framework and the estimation of the components of the hydrologic cycle.

The reanalysis of the hydrogeological framework required the remapping of geologic surfaces and the integration and reconciliation of geologic information from parent model and investigations with available data. The hydrogeological properties for this specific area were digitized and clipped from the calibrated parent model.

The model was constructed on the basis of the new conceptual and hydrogeological models to simulate the flow and use of water in the unit for the period from October 1995

to September 2006. This model employs same aquifer layering, revised values for inflows and outflows, and detailed representation of the hydrogeological properties as of the parent model. The MF-FMP model process and the general description are found in the following subunits.

2.2. Description of the Study Area

Irrigation unit 16 in Mexicali Valley is a 201 km² part of irrigation district 014 which highly depends on diversion of Colorado River and from some groundwater wells to satisfy the irrigation water demand (Figure 1).

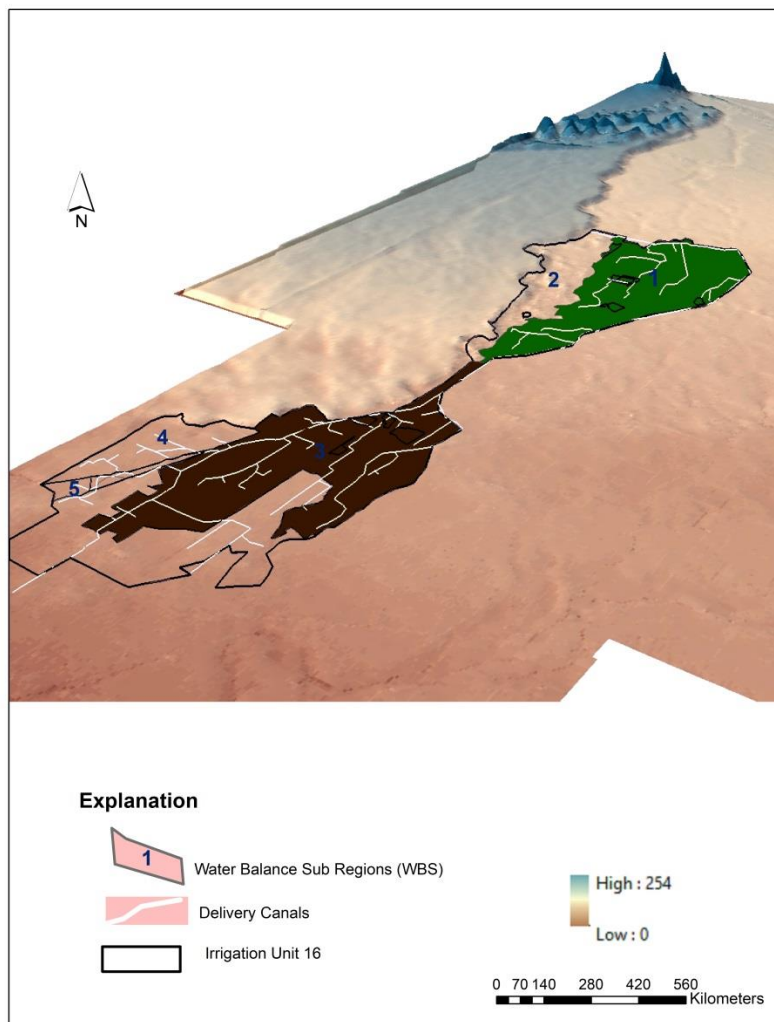


Figure 6. Irrigation unit 16 and distributions of delivery canals. The green color shows WBS1 and the brown color shows WBS 3 boundaries.

The irrigation unit 16 service areas encompass about 10,200 hectares, of which about 85 percent is used for agriculture and, 15 percent is primarily urban land.

2.2.1. Water-Balance Subregions (WBS)

The assessment of sustainable yield and analysis of the supply and demand components relative to the hydrologic cycle requires discretization of the irrigation unit 16 into sub regions that can be used to estimate the water balance of land use, streamflow, and groundwater (Figure. 2). In this study, the WBSs are hydrologic entity delineated farm groups that are used to calculate the overall supply and demand components through time. For further analysis, the irrigation unit 16 was grouped into 6 water-balance regions (Figure 6-7). These subregions represent a combination of virtual farms in the unit that can be used to assess the inflow and outflow components of the hydrologic cycle.

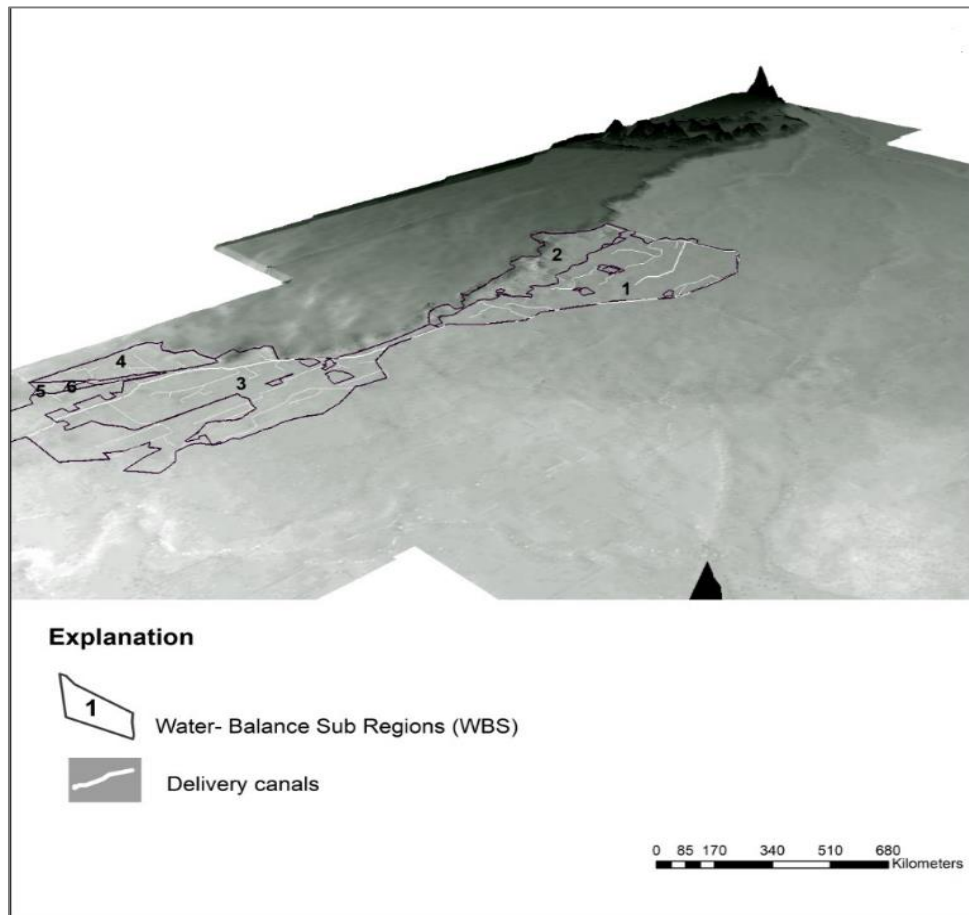


Figure 7. Identified six water balance sub regions (WBS) and delivery canals in irrigation unit 16

The irrigation unit 16 farm delivery requirements is satisfied by 3.5% from groundwater pumping and the remaining 96.5% from the diversion of Colorado river using the delivery canal.

Table 1. Summary of water balance sub-regions in Irrigation unit 16

Water Balance Subregions (WBS)	Area(km ²)	Sources of Farm delivery
1	71	Diversion of Colorado river + groundwater pumping
2	31.6	Diversion of Colorado river + groundwater pumping
3	54	Diversion of Colorado river
4	12.8	Diversion of Colorado river
5	1.30	Diversion of Colorado river
6	0.35	Diversion of Colorado river

3. Irrigation Unit 16 FARM Process Model Development

MODFLOW farm process (MF-FMP) (Schmid et al., 2006a and 2006b; Schmid and Hanson 2009a and 2009b) with ModelMuse Graphical User Interface (GUI) (Winston.2009) was used to detect aquifer depletion and to determine the surface-water and groundwater allocations to farms including components of evaporation and transpiration derived from precipitation, irrigation, and groundwater on a cell-by-cell basis within the selected WBS (Figure 7). The spatial locations and distributions of crop types, soil types and water balance subregions (farms) were pre-prepared as an object shapefile in ArcGIS and exported to ModelMuse, a different crop, soil, and farm id was assigned. The simulated temporal distribution of hydraulic head was used to identify the general potential aquifer drawdown. In addition, cell by cell temporal hydraulic heads distribution at different points including 3 groundwater wells which are located in the eastern edge of the model is analyzed to see the temporal variations of the groundwater table over the decade.

3.1. Temporal and spatial Discretization

Throughout the model, the units of measurements are set to meters for length and days for time. The time frame of the model simulation is 12 hydrologic years from 1st October 1995 to 30th September 2006, each, with a length of one year.

The model (Figure 1) was constructed using uniform grid cells of 250 m by 250 m. The grid network has 50 rows and 147 columns with a total of 7350 grid cells. It was aligned with the coordinate system of WGS-1984-UTM-zone-11-N. The regional stratigraphy was conceptualized in two layers. The first layer has a thickness of 120 m from the ground surface (upper fine-grained zone) and the second layer (combination of wedge zone and coarse gravel zone) has a thickness of 680 m. To hydraulically characterize the hydrogeological units in the model area, data were reviewed on transmissivity, specific storage and storage coefficient from previous studies (Olmsted et al., 1973; Harshbarger 1971; Hill 1993). The degree of permeability in the first layer, in the horizontal directions (K_x , K_y), is spatially differentiated. The hydraulic conductivity values were taken from the calibrated model of part 1.

3.2. Distribution of Landscape Attributes

The landscape attribute for the study area was identified using satellite imagery and the flow direction was delineated using ArcGIS 10.3 for further grouping of water balance subregions (WBS) (“farms) for further farm process analysis. The produced virtual farms were transformed into ModelMuse and assigned farm. The assigned id is found below (Figure 8).

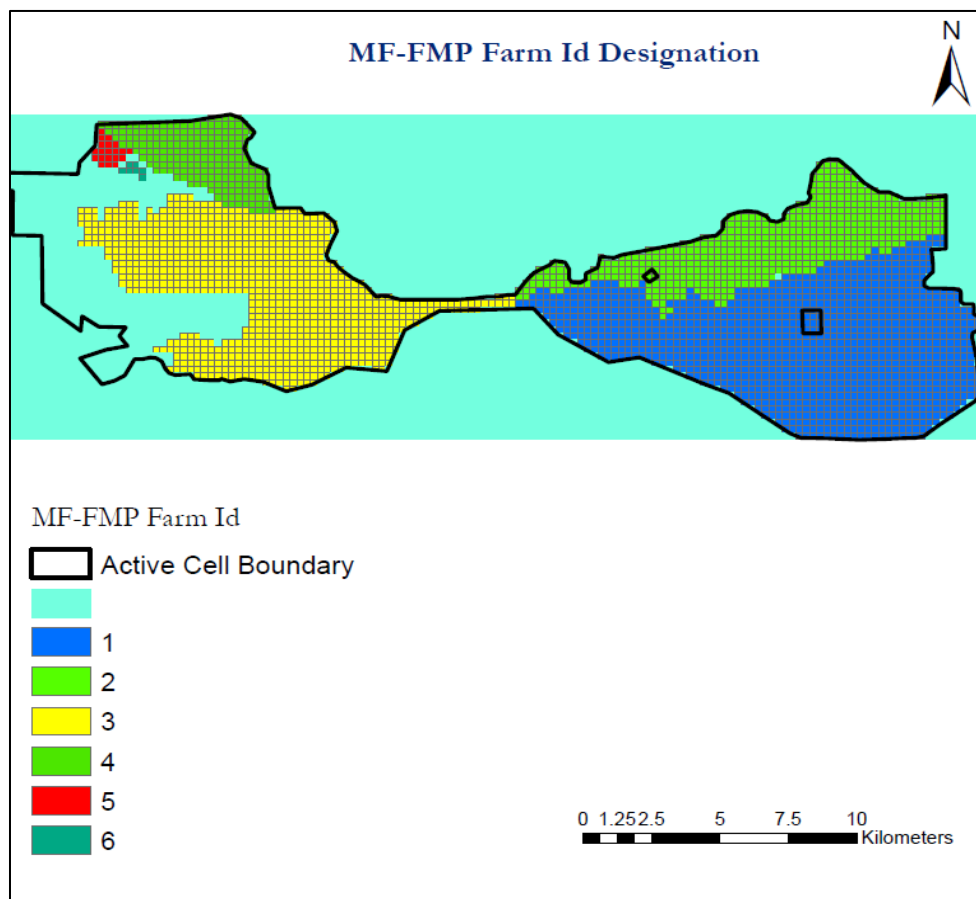


Figure 8: MF-FMP Farm id for Irrigation unit 16

Soils in the valley are generally classified under the principle soil order of Aridisols, according to the soil taxonomy developed by the United States Department of Agriculture (USDA). The defining characteristics of such soils are their lack of sufficient moisture for mesophytic plants and limited soil horizon development. Entisols are also present in the valley given its original formation as the floodplain of the Colorado River (Hillel 2008). While localized variations do exist across the valley, the soil texture is generally a sandy clay loam, with limited areas on the western edge of the valley having a greater concentration of clay as a result of erosion associated with the Sierra Cucapa and Sierra Mayor mountains.

Similarly, the soil distribution was clipped from the whole valley soil distribution AutoCAD map which was originally obtained from CONAGUA. The soil map was further processed until the respective soil was obtained. The original soil distribution obtained used Spanish nomenclature and translated to the correct English name using Soil texture triangle

showing the USDA classification system based on grain size; soil classification system. The soil id (Figure 6) was assigned and transformed into ModelMuse graphical user interface (GUI).

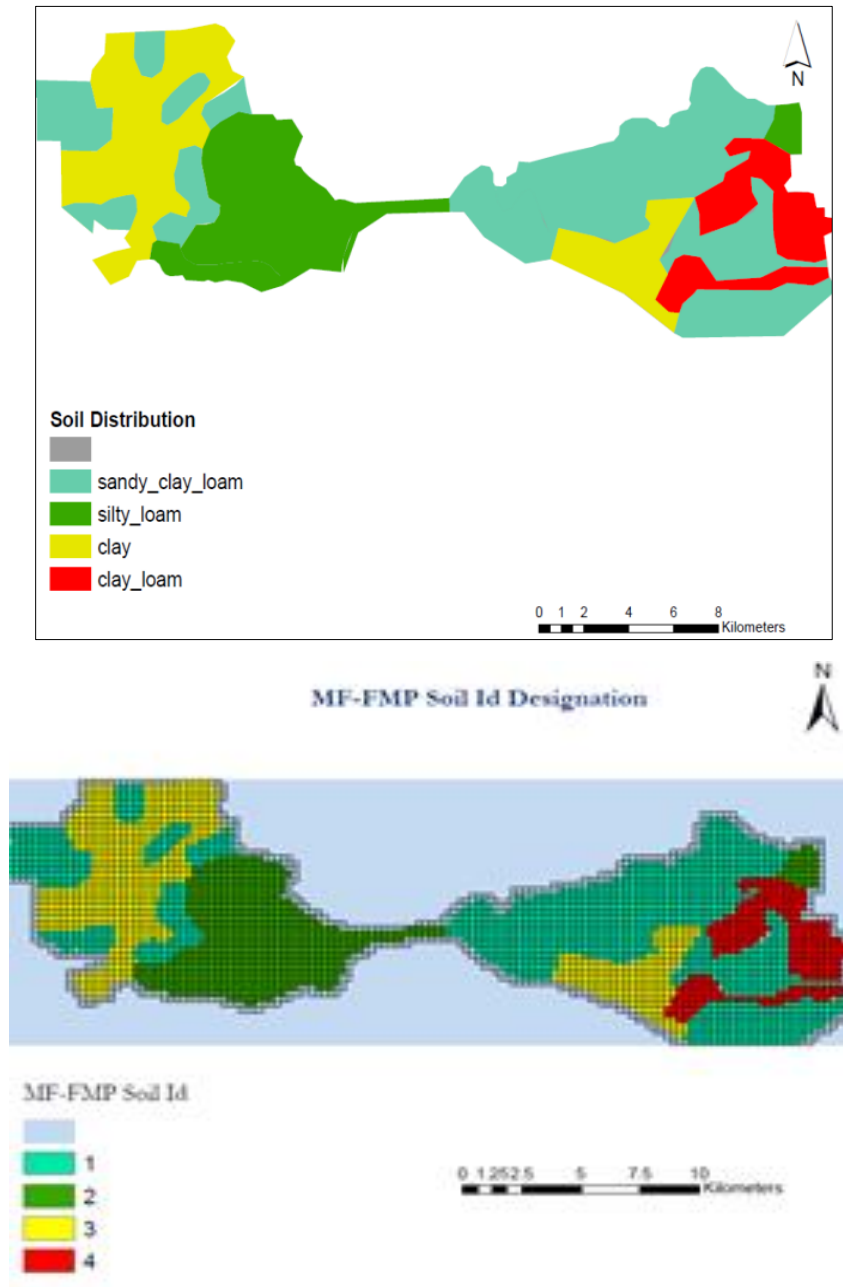


Figure 9. MF-FMP soil id designation for irrigation unit 16

Agriculture within the Mexicali Valley has developed over time to specialize in high value, fall/winter export-oriented produce cultivation. The two principal agricultural seasons include a summer (May to September) season during which field grains, cotton, and oilseed crops dominate and a fall/winter season (October to May) during which a range of very high-value produce crops are cultivated for export markets alongside some field grains.

A total of 521 farmers of irrigation district 014 were interviewed and the main crops grown by the interviewed farmers are wheat (65%), alfalfa (19%), and cotton (8%) (Carrillo-Guerrero, 2009). The main types of crops in irrigation district 014 in terms of water consumption according to 2009-2010 study reported by CONAGUA are wheat, cotton, and alfalfa dominate the area. For this study, wheat and alfalfa were taken as the main crop and this study assumes similar crop distribution throughout the study period. The general computer programs used in this study are summarized below (Table 2 and Table 3).

Table 2. Summary of MODFLOW-OWHM with Farm Process (MF-FMP) packages and processes used with the hydrologic flow model of Irrigation unit 16, Baja-California

Computer program (packages, processes, parameter estimation)	Function	Reference
Processes and solver		
Farm Process	Setup and solve equations simulating use and movement of water on the landscape as irrigated agriculture, urban landscape, and natural vegetation	Schmid and Hanson (2009), Schmid and others (2006a, b)
SIP: Strongly Implicit Procedure Package	Solves groundwater flow equations; requires convergence of heads and(or) flow rates	
Files		
Name File (Name)	Controls the capabilities of MF-FMP utilized during a simulation. Lists most of the files used by the FMP Processes.	Harbaugh (2005)
Output Control Option (OC)	Used in conjunction with flags in other packages to output head, drawdown, and budget information for specified periods into separate files.	Harbaugh (2005)

List File	Output file for allocation information, values used by the GWF process, and calculated results	Harbaugh (2005)
-----------	--	-----------------

Table 3. Summary of MODFLOW-OWHM with Farm Process (MF-FMP) packages and processes used with the hydrologic flow model of Irrigation unit 16, Baja-California, Continued

Computer program (packages, processes, parameter estimation)	Function	Reference
Discretization		
Basic Package (BAS6)	Defines the initial conditions and some of the boundary conditions of the model.	Harbaugh (2005)
Discretization Package (DIS)	Space and time information.	Harbaugh (2005)
Multiplier Package (MULT)	Defines multiplier arrays for calculation of Model-layer characteristics from parameter values.	Harbaugh (2005), Schmid and Hanson (2009)
Zones (ZONE)	Defines arrays of different zones. Parameters may be composed of one or many zones.	Harbaugh (2005)
Aquifer parameters		
Layer Property Flow Package (LPF)	Calculates the hydraulic conductance between cell centers.	Harbaugh (2005)
Boundary conditions		
Drain Package (DRN)	Simulates the head-dependent tile drains of irrigated agriculture within the center of Mexicali Valley	McDonald and Harbaugh (1988), Harbaugh (2005)
Recharge and discharge		
Streamflow Routing (SFR2)	Simulates the routed streamflow, infiltration, exfiltration, runoff, and return flows from FMP	Niswonger and Prudic (2006)
Unsaturated zone flow package(UZF)	The UZF package simulates the vertical flow of water through the unsaturated zone to the saturated zone.	Niswonger et al.,(2006)
Well Package(Well) package	The Well package is used to simulate a specified flux to individual cells and specified in units of length ³ /time.	Harbaugh et al,(2005).
Output and observations		
Head Observation (HOB)	Defines the head observation and weight by layer(s), row, column, and time and generates simulated values for comparison with observed values.	Hill and others (2000) Harbaugh (2005)
USGS-GW chart	for creating specialized graphs used in groundwater studies	Winston., (2000)

3.3. Initial Condition and structural model setting

Initial conditions in the model are the distribution of water levels at every active cell within each of the two model layers. The initial water levels for October 1995 were approximated by starting with water levels from the previous models and replacing these

initial values during calibration with simulated water levels from the end of the first year (October 1995).

The structural model involved input from model layers to resemble physical stratigraphy of the aquifer system. Since the model is made up of two layers as of the parent model, the surfaces of the model top and model bottoms of the aquifers were exactly defined and imported into the Modflow ModelMuse. The model top of the study area is the digital elevation model (DEM) which was obtained from personal communication (Elina Rodriguez) for the whole MCRD area. The DEM for MCRD was further processed and the DEM for the irrigation district 16 was extracted in ArcMap and imported to modelMuse. The DEM (Figure 10) obtained was imported into Modflow ModelMuse as ASCII files.

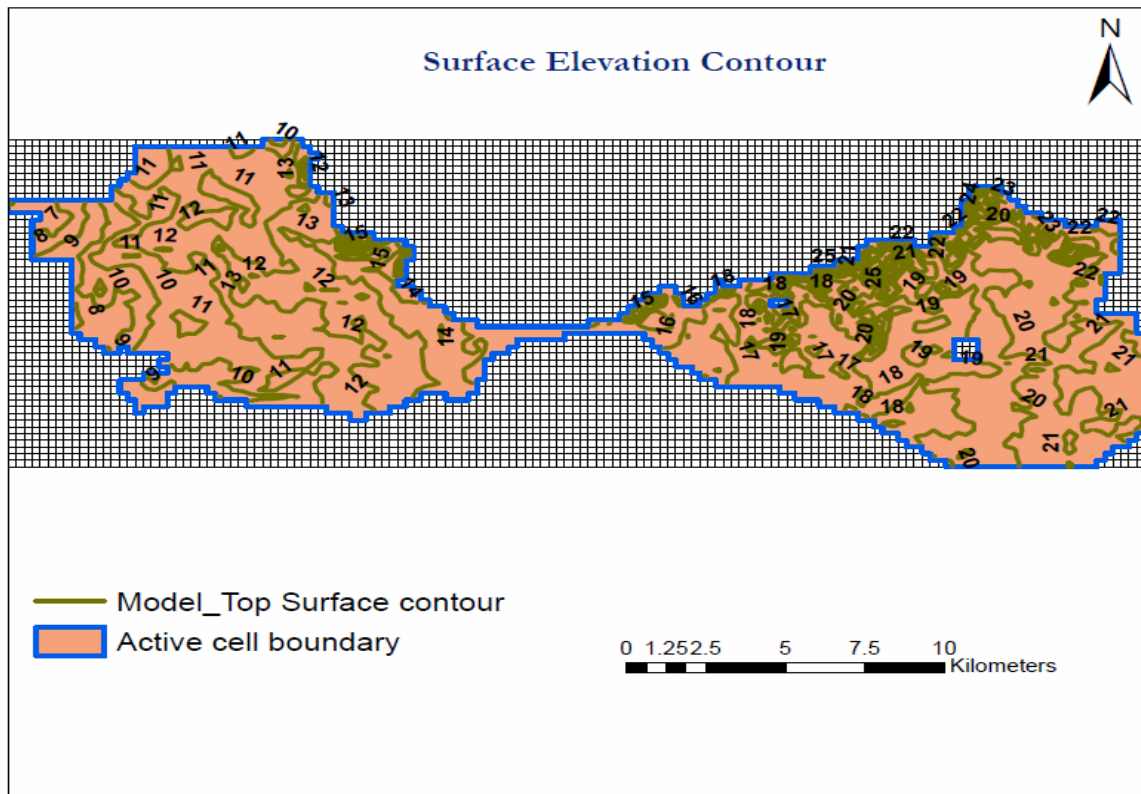


Figure 10:Surface elevation contour of Irrigation Unit 16

The layer groups are defined by two types of layer structures when the UZF and Stream Flow Routing (SFR) Packages are activated. Both structures are the convertible layer in which the heads in the model cells determine the status of the cells. The cells are considered to be in confined or unconfined states when the heads are, respectively, above or

below the cell tops. In the confined layer structure, the heads are always above the cell tops. The vertical dimensions of the aquifers are defined to be similar to the parent model structure.

3.4. Flow Boundary

The drains of the irrigated agriculture were simulated with the drain package in MODFLOW. The drain package and general head boundary was used for the study area as shown in Figure 11. The drains set a specified drain elevation that is about 1.8 m below the land surface of 327 model cells (Figure 11) that are generally coincident with the regions identified as having drains. The regions of drains were delineated and included cells within these regions that were not coincident with stream flow cells with nonzero streambed conductivity. These drains simulate the capture by drains or lowlands of rising groundwater and the deep percolation of excess water from irrigation or precipitation in these regions.

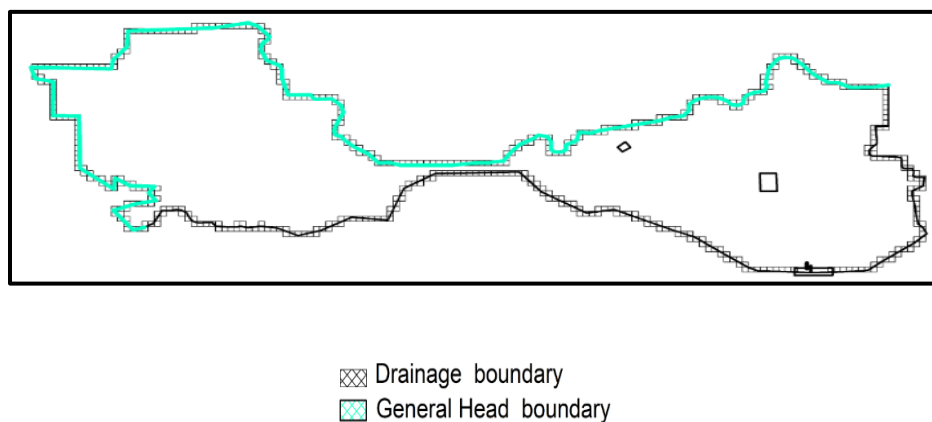


Figure 11. Distribution of model cells used for drainage package (DRN) and general Head Boundary (GHB) package

3.5. Surface Water Inflows and Outflows

Surface-water inflows and outflows were simulated with a streamflow routing network composed of 55 stream segments representing the delivery canal which delivery surface water from Colorado River into the irrigation unit 16. This network was used to simulate the inflows and outflows along the major diversions (Figure 12). These features were simulated using the Streamflow-Routing Package (SFR2; Niswonger and Prudic, 2005;

Prudic and others, 2004); this head-dependent boundary condition allows for streamflow routing and the conveyance of overland runoff and the diversion of water for irrigation.

The data in relation to delivery canals were obtained their distribution of main canal and secondary canal was imported into ModelMuse for further analysis. The information in relation to the tertiary canals is not included in this study.

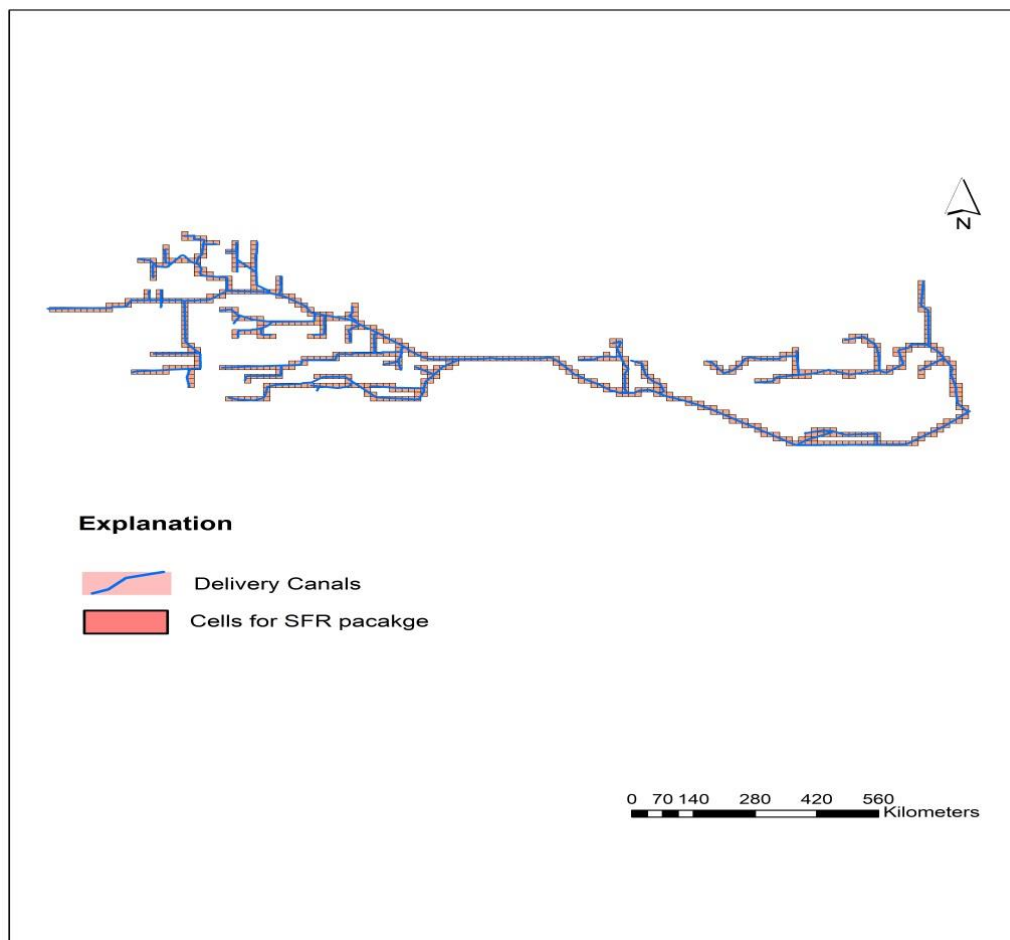


Figure 12. Distribution of model cells used for streams flow routing (SFR) package

3.6. Groundwater Pumpage

Groundwater pumpage is a major component of the hydrologic budget in Mexicali Valley and is used for agricultural water supply. Agricultural pumpage (Table 4), which is estimated using MF-FMP, includes withdrawals from all farm wells used to supply water for irrigation. Farm wells were simulated as single-aquifer wells (Schmid and others, 2006a) that collectively supply water needed for irrigation for each WBS. Farm wells that are single-aquifer wells are simulated using the WEL package (Harbaugh and others, 2000)

and the total pumpage for each WBS (that is, virtual farm) is distributed among each of the farm wells within the WBS based on the fraction of total pumping capacity (Schmid and others, 2006a). A total of six groundwater wells are found in the study area which mostly found on the eastern edge of the modeled area. The groundwater pumpage from three groundwater wells which are found in the WBS1 is distributed for all regions in the virtual farm and similarly for WBS2. For all other water balance subregions, their main water supply is a diversion from Colorado River.

Table 4. Summary of agricultural pumpage in thousand cubic meters per year used for this study

Wells	longitude	latitude	1995	1996	1997	1998	1999	2000	2001	2002	2003	2004	2005	2006
W1	3.08	3.48	3.00	2.43	2.25	2.39	2.57	2.45	2.54	2.50	2.83	2.83	3.08	3.48
W2	5.34	6.04	5.72	4.21	3.90	4.14	4.46	4.26	4.41	4.34	4.92	4.92	5.34	6.04
W3	2.24	2.54	2.40	1.77	1.64	1.74	1.87	1.79	1.85	1.82	2.06	2.06	2.24	2.54
W4	4.72	5.35	5.07	3.73	3.45	3.67	3.94	3.77	3.90	3.84	4.35	4.35	4.72	5.35
W5	3.51	3.98	3.77	2.77	2.56	2.73	2.93	2.80	2.90	2.86	3.23	3.23	3.51	3.98
W6	3.24	3.66	3.47	2.55	2.36	2.51	2.70	2.58	2.67	2.63	2.98	2.98	3.24	3.66

3.7. Crop Data

The virtual crops provide a basis for estimating the consumptive use of water at the land surface, a key component of the total farm delivery requirement (TFDR) (Schmid and others, 2006a). The TFDR is largely determined by the crop irrigation requirement (CIR). The CIR is determined on a cell-by-cell basis from the product of an ET_h and an area-weighted crop coefficient (K_c); these products are summed over all cells within each WBS. Because so many factors affect ET (including weather parameters, soil factors, and plant factors), it is difficult to formulate an equation that can produce estimates of ET under different sets of conditions (California Department of Water Resources, 2007). Therefore, the idea of a reference crop ET was developed (California Department of Water Resources, 2007). The reference ET from a standardized (evenly mowed) grass surface is commonly denoted either as ET_o or ET_h . This study uses ET_h .

Specified root depths, suction pressures for the unsaturated root zone, crop coefficients, and fractions of transpiration and evaporation affect the consumption and movement of water for each crop category. For the study area, the root depths and root

uptake pressures were held constant for the entire simulation and are based on values from the literature (R.T.Hanson et.al, 2014) for a similar type of crop.

Suction pressures in the root zone can range from positive (hydrostatic) for water-saturated settings including the ASR system and riparian vegetation in wetlands, to negative (unsaturated) pressure for agriculture and native vegetation such as grasses, shrubs, and trees. Direct Transpiration (T) and Evaporation (E) from the groundwater occurs for a rising water table when the top of the capillary fringe above the water table reaches the bottom of the root zone of plants and when the top of the capillary fringe above the water table reaches the land surface respectively. For a declining water table, the direct T and E from groundwater are eliminated when the top of the capillary fringe above the water table falls below the bottom of the root zone and when the top of the capillary fringe above the water table falls below the land surface (Schmid and others, 2006a).

The information used in the study area regarding the main types of crop and their properties were identified (Table 5).

Table 5. Summary of irrigation unit 16 virtual crop categories and properties

MF-FMP Crop category	Maximum root depth (m)	Crop Coeff (Kc)	Anoxia	Wilting	Fraction of surface-water runoff from precipitation	Fraction of surface- water runoff from Irrigation
Alfalfa	1.2	0.63	-0.49	-405.8	0.6	0.4
Wheat	1.2	0.63	-0.49	-405.8	0.6	0.4

Other WBS and crop-related properties that were specified include the fraction of total ET that is transpiration (Ftr), a fraction of evaporation from precipitation (Fep), a fraction of evaporation from irrigation (Fei; dimensionless), and the irrigation efficiencies. These fractions vary linearly with the respective area occupied by crops and the area with no crop canopy that is open to soil-evaporation (Schmid and others 2006a). Because of the crop canopy area and the exposed soil area sum to the entire area, Ftr plus Fep equals one. In addition, Fei must be less than or equal to Fep, because transpiration from crop canopy areas inherently reduces the evaporative fraction in canopy areas. The Ftr is assumed to be independent of whether the transpiratory consumptive use is satisfied by irrigation,

precipitation, or groundwater uptake. The fraction of the consumptive use that is transpiratory (F_{tr}) or evaporative (F_{ep} and F_{ei}) depends highly on the type of crop and growth stage. When the vegetation cover reaches nearly 100 percent, then $F_{tr} = 1$ while F_{ep} and $F_{ei} = 0$. In this study, the fractions of transpiration and evaporation assumed similar values for each virtual crop for different years. These values are derived from the literature and from related studies (Schmid and others, 2006a).

Table 6. Summary of fractions of transpiration and evaporation by year for irrigation unit 16 crop categories (virtual crops)

MF-FMP Crop category	Fraction of transpiration (F_{tr})	Fraction of Evaporation from precipitation (F_{ep})	Fraction of Evaporation from irrigation (F_{ei})
Alfalfa	0.05	0.95	0.1
Wheat	0.05	0.95	0.1

The irrigation efficiencies are defined as the fraction of applied water actually consumed by plants (transpiration). Inefficiency in the conveyance and spreading of applied water results in losses to runoff and deep percolation, particularly as a result of excess irrigation and excess precipitation (Schmid and others, 2006a).

The irrigation efficiency for the study area was reviewed from previous studies (Rodríguez-Burgueño, J., 2012 and freistain.2008) and an efficiency value of 0.65 to 0.85 is adopted in this study.

3.8. Potential Evapotranspiration

Detailed data about the crop/vegetation and soil of the area is not available; for this study, the single crop coefficient (K_c) (Table3) method was applied.

$$PET = ET_0 * K_C \dots \dots \dots (18)$$

ET_0 values were obtained from Andrade and Mexicali metrological stations and PET was calculated as per equation 18 and imported into ModelMuse for further analysis.

4. Results and Discussion

4.1. Model calibration

The trial and error basic head calibration was conducted using the available observation points. Resulting values of the horizontal hydraulic conductivities for the first layer after calibration are given in Figure 13. The performance of the calibration is illustrated by comparing simulated versus observed groundwater heads. In view of the available head observation points, the result obtained is fairly acceptable, with an RME (root mean square error) of 0.02 m, a normalized RMS of 2.1% and a correlation coefficient of 0.97.

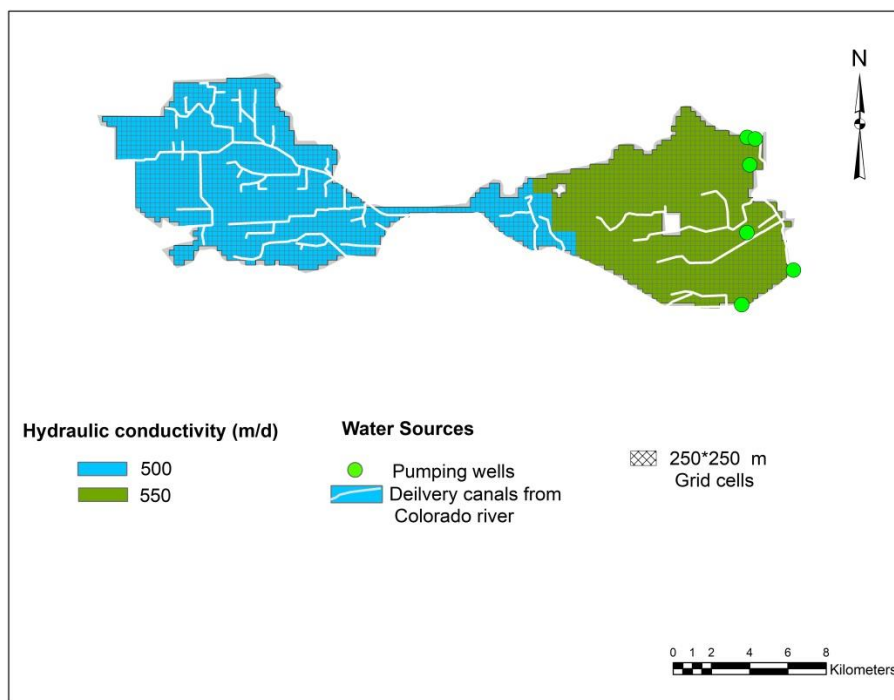


Figure 13. Distributions of calibrated horizontal hydraulic conductivity (Kh) for the 1st layer, water sources and grids used for MF-FMP modeling

Reported (measured) pumpage for the period 1995 through 2006 were available for WBS1 and WBS2. Totals of reported agricultural pumpage were compared with agricultural pumpage estimated through the simulation of water consumption by the Farm Process used in the study area. The reported agricultural pumpage located at WBS1 and WBS2 were used as additional calibration targets.

Simulated and reported total agricultural pumpage are compared for the 2 WBSs (figure 14). The model slightly overestimates agricultural pumpage. The percentages of total reported and simulated agricultural pumpage by WBS are also comparable, within a few percent, for the two subregions. The annual total and total agricultural pumpage (Figure 14) are comparable between reported and simulated values for these 12 years. For WBS1 and WBS2, the average annual differences (reported minus simulated) for total agriculture were $-671 \text{ m}^3/\text{yr.}$ and $-570 \text{ m}^3/\text{yr.}$ for the period 1995–2006, respectively. This represents average differences of about -0.54 and -0.49 percent of the reported agricultural pumpage for WBS1 and WBS2 respectively. These results show that the simulated pumpage is within the range of uncertainty of the reported pumpage.

The resulting average groundwater balance is given in Table 7. The source of water to the groundwater reservoirs in the study area is through agricultural recharge, which amounts in total to $97.84 \times 10^4 \text{ m}^3$, leakage from the stream which amounts $2.10 \times 10^4 \text{ m}^3$ and lateral inflows which amount $1.08 \times 10^4 \text{ m}^3$ are other components of inflows. About $2.52 \times 10^4 \text{ m}^3$ of groundwater drains out of the system. The study area experiences a groundwater evaporation of about $123.16 \times 10^4 \text{ m}^3$. The model balance error is very small, i.e. -0.71% , which shows that the model has converged accurately. The discrepancy is negative; indicating that outgoing groundwater from the study area is higher than incoming groundwater (recharge) which shows aquifer drawdown.

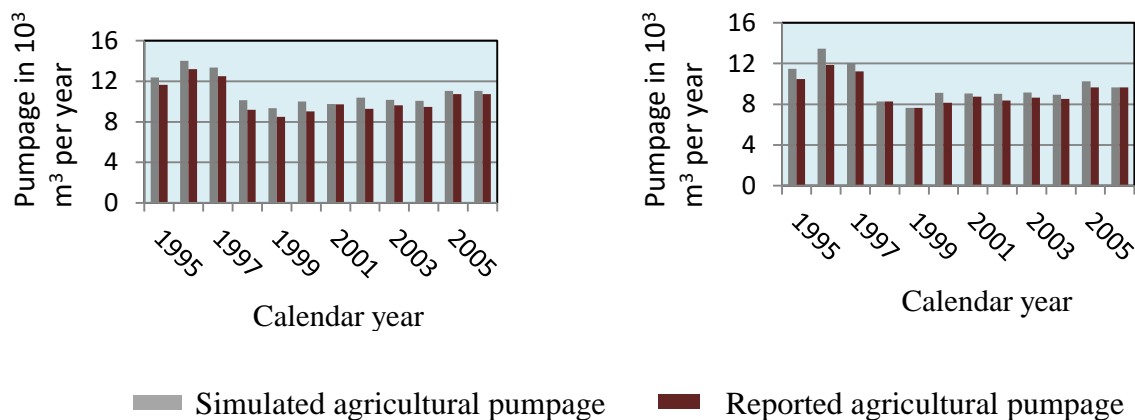


Figure 14 Total annual reported and simulated agricultural pumpage for WBS1 (right) and WBS2 (left) for the period (1995-2006)

4.2. Water Budget

As indicated by the simulated potentiometric level (Figure 15b), groundwater flows laterally from the higher elevation points to the lowlands. Simulated water levels range from 19.6 m in the highland areas to less than 10 m in the lowland. The three-dimensional modeling of groundwater in the study area shows aquifer drawdown for the study period. The drawdown map (Figure 15a) shows a drawdown ranges from 0.3m to 3m. The drawdown is higher in the northeastern modeling area which is expected because most of the groundwater pumping wells existed nearby.

Table 7 Groundwater balance obtained from the MF-FMP model (whole Irrigation unit 16)

Inflow	Amount(10^4 m^3)	Outflow	Amount(10^4 m^3)
Storage	4.15	Storage	123.25
Head dep bounds	1.08	Drains	2.52
Stream leakage	2.10	Head dep bounds	0.14
UZF recharge	178.62	GW ET	123.16
Farm net recharge.	97.84	Surface leakage	36.36
		Farm wells	0.25
Inflow-Outflow		-	-2.02×10^4
Percent discrepancy		-	0.071%

Note: The net recharge is defined as inefficient losses to groundwater recharge after consumption due to excess irrigation and excess precipitation, reduced by losses to surface-water runoff and ET from groundwater (Schmid and others, 2006a).

Figure 16 shows the simulated total farm delivery requirement for irrigation for a WBS1 and WBS3 for the 12- year period from 1995 to 2006 and Figure 17 summarizes the overall 12-year WBS landscape hydrologic budgets for WBS1 and WBS3.

The results show that WBS1, which constitutes the eastern part of the modeling area, receives comparably more runoff and after the year 1999, lesser recharge than WBS3, which constitutes the western part of the modeling area. The simulated total farm delivery requirement (TFDR) shows that TFDR for WBS1 is fulfilled by 73% from the diversion of the Colorado River through delivery canals and 27% from groundwater pumping. In contrast, the TFDR of WBS3 mainly depends on diversion of the Colorado River. There is

a significant component of evapotranspiration (ET) derived from irrigation in both water balance subregions (Figure 16, yellow color).

The simulated component for WBS 1 and WBS 3 (Figure. 16) show that groundwater recharge is derived from agricultural supplies nothing that the precipitation is lost due to evapotranspiration. Figure 16 also demonstrate that the recharge shows a reducing trend.

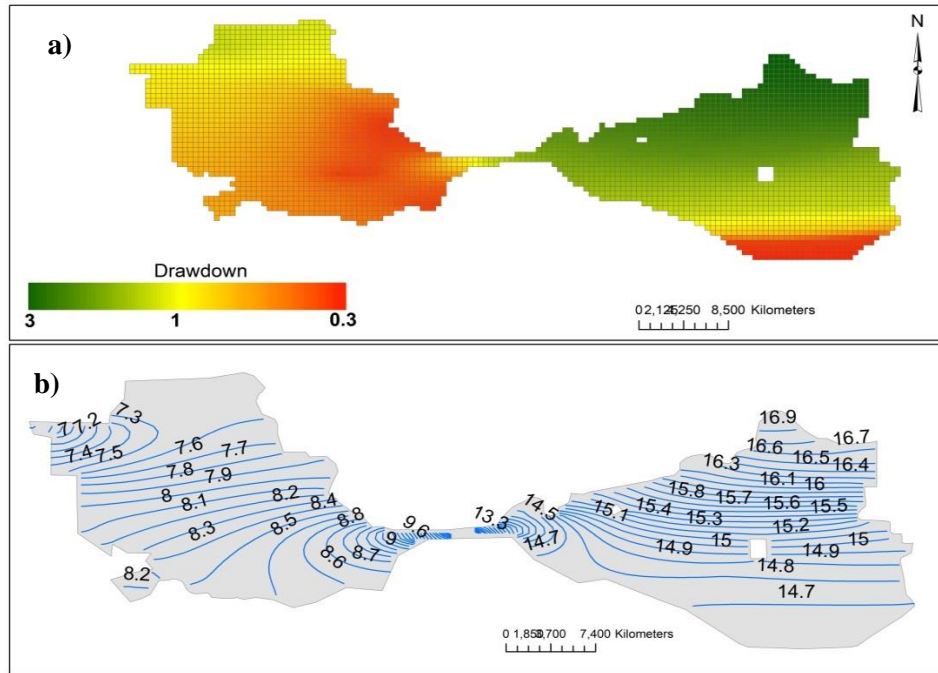


Figure 15 (a) Simulated drawdown (m) and (b) simulated hydraulic heads (m a.s.l.) for Irrigation unit 16

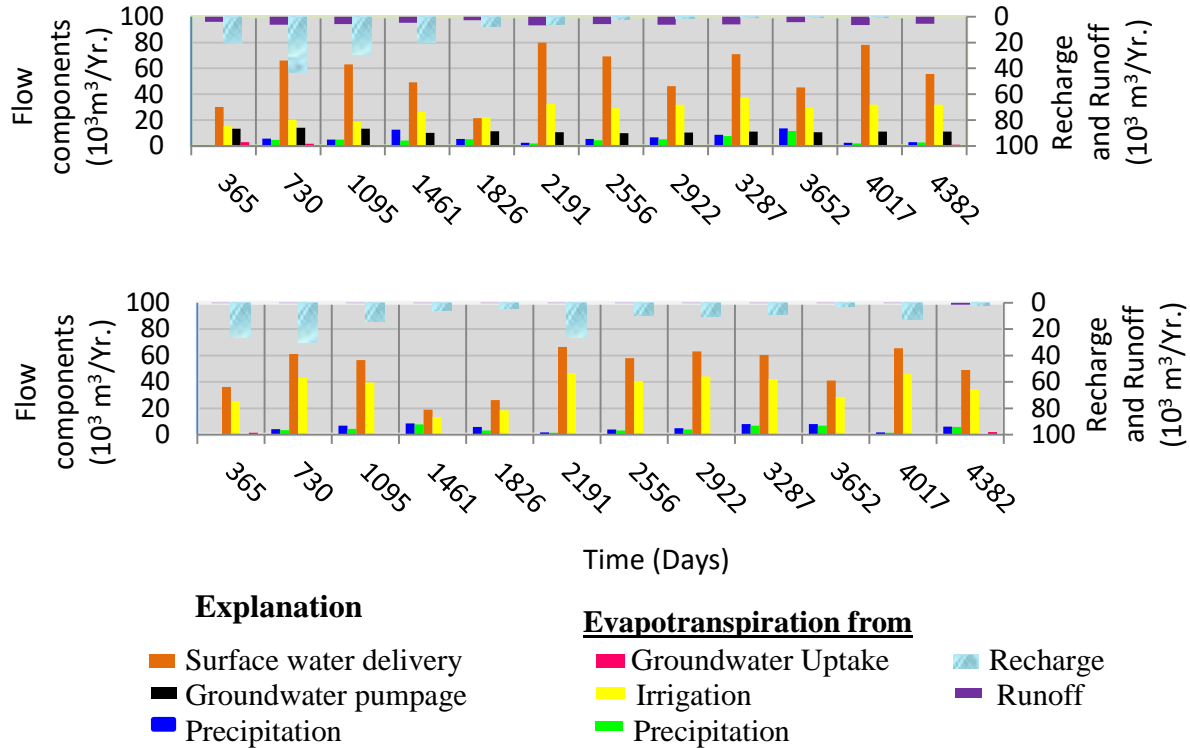


Figure 16 Farm delivery components and the inflows and outflows for two water-balance subregions (WBS1, top, and WBS3, bottom) from 1995 to 2006. Recharge and runoff, refer the second axis

Groundwater-level decline and related storage depletion are occurring in this areas as evapotranspiration (ET) from groundwater uptake are about 3% and 4% (Figure 17, inflow) and recharge to the groundwater is about 19% and 21% on the landscape (Figure 17, outflow) for WBS1 and WBS 3 respectively. Evapotranspiration from groundwater, water from agriculture wells and routed surface water deliveries supplement the crop consumptive use for WBS1 and the crop consumptive use of WBS 3 is supplemented by surface water deliveries and evapotranspiration from groundwater (Figure 17).

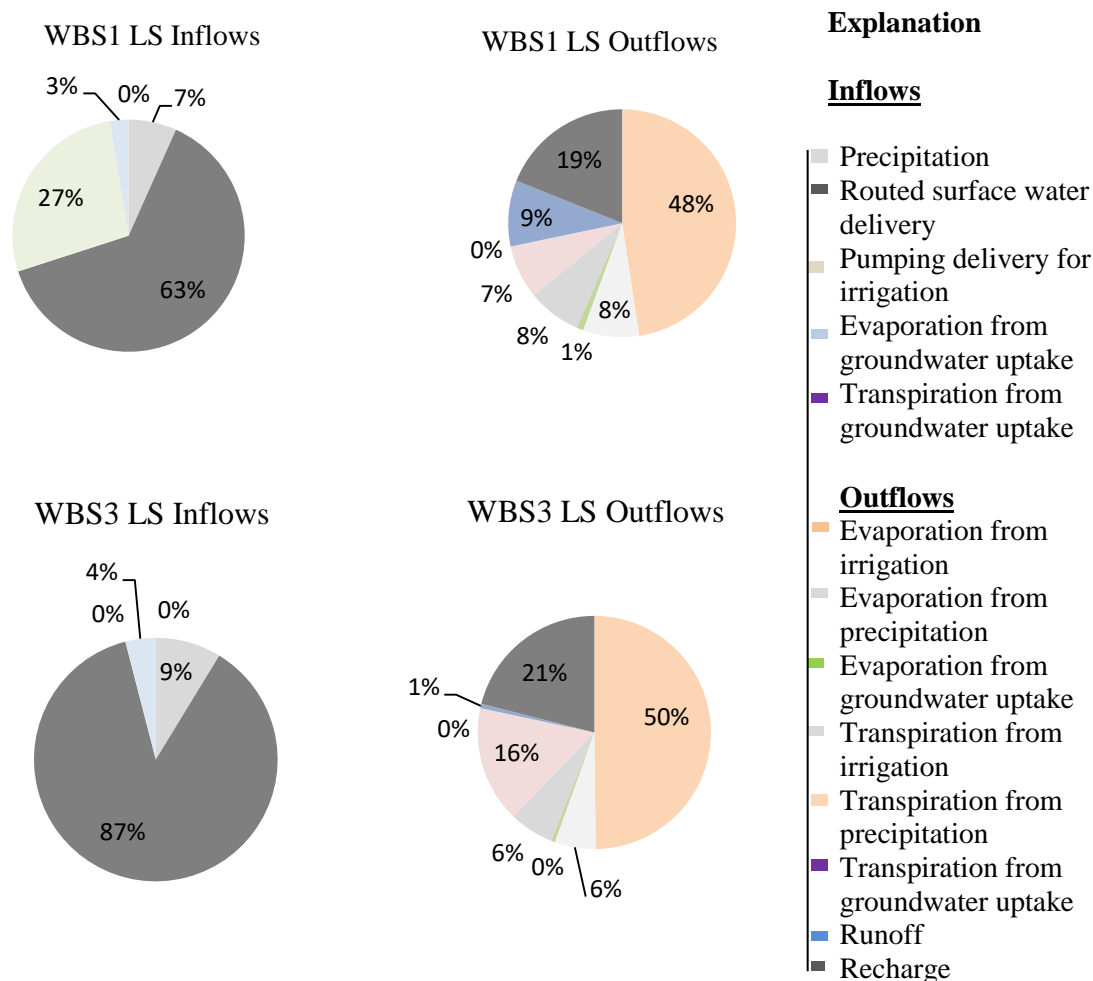


Figure. 17 Graph showing the percentages of total Landscape (LS) inflows and outflows for two water-balance areas from 1995 to 2006 as part of conjunctive use simulated by MF-FMP

Note: water budgets are relative to farm units; direct evaporation and transpiration of groundwater uptake on both the inflow and outflows because those fluxes are passing through the land surface (from groundwater to atmosphere/plants through the land surface). Refer section "MF-FMP Features" in this study or referred to Schmid et al. (2006a) for more detail.

For each WBS represented by many model cells, the results shown in Figures 16 to 17 are the aggregate of the cells involved. Crop types, crop coefficients, potential or specified

evapotranspiration, and other characteristics are defined for each cell, and results such as crop irrigation requirements are simulated for each cell.

4.3. Conclusions and Recommendations

This study shows how WBS can be used to organize input data and simulated results. Farm process (FMP) input files were easily constructed, updated, and maintained using soil, well, and crop data that did not require substantial external estimation of inflows and outflows (pumpage, recharge, evapotranspiration, runoff, surface water deliveries, etc.) prior to simulation. Because these hydrologic components are simulated separately, the flows and movement were easily analyzed.

The sustainability of water resources in part depends on the ability to monitor our aquifers and to simulate and analyze all the components of complex hydrologic systems, including groundwater, surface water, and landscape components. A regional groundwater flow model on irrigation unit 16 was developed and calibrated against available groundwater level observations and measured agricultural pumpage, which converges to a solution with a small water balance error. A conceptual model of the study area with two layers is defined to identify the effects of agricultural activities on groundwater level and groundwater recharges. The main conclusions drawn from the model are:

- The source of water to the groundwater reservoirs in the study area is through net-agricultural recharge, which amounts $97.84 \times 10^4 \text{ m}^3$. The study area experienced high groundwater evaporation of about $123.16 \times 10^4 \text{ m}^3$. The average negative change in storage is indicating that outgoing groundwater from the study area is higher than incoming groundwater (recharge) which shows aquifer depletion.
- Calibration of the model using the available observations of groundwater levels gives a relatively good fit with an RMS of 0.02 m and a normalized RMS of 2.1% with a correlation coefficient of 0.97. The reported agricultural pumpage located at WBS1 and WBS2 were used as an additional calibration target that, the simulated pumpage is within the range of uncertainty of the reported pumpage. The average annual differences (reported minus simulated) for total agriculture were $-671 \text{ m}^3/\text{yr}$. and $-570 \text{ m}^3/\text{yr}$, which represents average differences of about -0.54 and -0.49 percent of the reported agricultural pumpage for WBS1 and WBS2 respectively.

- The simulated potentiometric level shows a hydraulic head range from 19.6 m in some areas to less than 10 m in the lowlands. Groundwater flows toward the Gulf of California.
- The simulated MF-FMP inflow-outflow analysis shows that the WBS1, which constitutes the eastern part of the modeling area, receives comparably more runoff and after the year 1999, lesser recharge than WBS3, which constitutes the western part of the modeling area.
- The simulated component for WBS 1 and WBS 3 confirmed that groundwater recharge is derived from agricultural supplies nothing that most part of precipitation in the area is lost due to evapotranspiration.
- The landscape budget for WBS1 and WBS 3 shows evapotranspiration (ET) from groundwater uptake about 3% and 4% and recharge to the groundwater is about 19% and 21% respectively.
- The modeling effort on irrigation unit 16 shows that the aquifer was drawn down up to 3m in some areas and drawdown was higher in the northeastern region than western regions.

The authors believe that these results are very important for future conjunctive water resources management in the region and that this work is the first and unique example in the region which might serve as a guide for the development of the integrated hydrologic model using MF-FMP on the entire irrigation district 014, which is in needed, and for the integrated modeling of other agricultural regions with similar geological environment. Monitoring of diversion rates from the Colorado River to each farm land on the better scale as a function of time and a detailed database of agricultural crops are recommended for future model development.

5. References

- Barragan, R. M., P. Birkle, E. Portugal M., V. M. Arellano G., and J. Alvarez R. (2001), Geochemical survey of medium temperature geothermal resources from the Baja California peninsula and Sonora, Mexico, *Journal of Volcanology and Geothermal Research*, 110, 101-119, PII: S0377-0273(01)00205-0.
- Bushira.K.M, Ramirez-Hernández. J, Zhuping.S .2017. Surface and groundwater flow modeling for calibrating steady state using MODFLOW in Colorado River Delta, Baja California, Mexico. *Journal of Modeling earth systems and Environment*.no. 3:815–824.
- Chavez, R. E., O. Lazaro-Mancilla, J. O. Campos-Enriquez, and E. L. Flores- Marquez (1999), Basement topography of the Mexicali Valley from spectral and ideal body analysis of gravity data, *Journal of South American Earth Sciences*, 12, 579-587, PII: S0895-9811(99)00041-3.
- Feirstein, E., Zamora-Arroyo, F., Vionnet, L. y Maddock, T. 2008. Simulation of groundwater conditions in the Colorado River Delta, Mexico. Tesis de Maestría. Tucson, AZ.
- Harshbarger, J. W. 1971. Overview report of hydrology and water development, Colorado Delta, United States and Mexico, Preliminary Report PR-235-77-2, Prepared for International Boundary and Water Commission United States Section, Tucson AZ, USA.
- Harbaugh, A.W., Banta, E.R., Hill, M.C., and McDonald, M.G., 2000, MODFLOW-2000, U.S. Geological Survey modular ground-water model—User guide to modularization concepts and the ground-water flow process: U.S. Geological Survey Open-File Report 2000–92, 121 p., <http://pubs.er.usgs.gov/publication/ofr200092>.
- Harbaugh, A.W., 2005. MODFLOW-2005: the U.S. Geological Survey modular ground-water model—the ground-water flow process: U.S. Geological Survey Techniques and Methods 6-A16, variously paginated, <http://pubs.er.usgs.gov/publication/tm6A16>.
- Hillel D (2008) Soil chemical attributes and processes. *Soil in the environment: crucible of terrestrial life*, Chapt 10. Academic Press, San Diego, pp 135–150

- Hill, B. M. 1993. Hydrogeology, numerical model and scenario simulations of the Yuma area groundwater flow model Arizona, California, and Mexico, Modeling Report no. 7, Arizona Department of Water Resources, Phoenix AZ, USA.
- Mock, P. A., E. E. Burnett, and B. A. Hammett (1988), Digital computer model study of Yuma area groundwater problems associated with increased river flows in the lower Colorado River from January 1983 to June 1984, Arizona Department of Water Resources Open-File Report No. 6, Phoenix AZ, USA.
- Niswonger, R.G., D.E. Prudic, and R.S. Regan. 2006. Documentation of the Unsaturated-Zone Flow (UZFI) Package for modeling unsaturated flow between the land surface and the water table with MODFLOW-2005. U.S. Geological Survey Techniques and Methods 6-A19.
- Niswonger, R.G., and Prudic, D.E., 2005, Documentation of the streamflow-routing (SFR2) package to include unsaturated flow beneath streams—A modification to SFR1: U.S. Geological Survey Techniques and Methods 6-A13, 51 p., <http://pubs.er.usgs.gov/publication/tm6A13>.
- Olmsted, F., Loeltz, O. y Irelan, B. 1973. Geohydrology of the Yuma Area, Arizona, and California, Geological Survey Professional Paper 486-H, United States Government Printing Office Washington, DC.
- Pacheco, M., A. Martin-Barajas, W. Elders, J. M. Espinosa-Cardena, J. Helenes, and A. Segura (2006), Stratigraphy and structure of the Altar basin of NW Sonora: implications for the history of the Colorado River Delta and the Salton trough, *Revista Mexicana de Ciencias Geologicas*, 23 (1), 1-22.
- Portugal, E., G. Izquierdo, A. Truesdell, and J. Alvarez (2005), The geochemistry and isotope hydrology of the Southern Mexicali Valley in the area of the Cerro Prieto, Baja California (Mexico) geothermal field, *Journal of Hydrology*, 313,132-148.
- Puente, I. C., and A. De La Pena L. (1979), Geology of the Cerro Prieto geothermal field, *Geothermics*, 8, 155-175.
- Richard B. Winston. 2009. ModelMuse—A Graphical User Interface for MODFLOW—2005 and PHAST
- Roman-Calleros, J., Ramírez-Hernández, J. 2003. Interdependent Border Water Supply Issues: The Imperial and Mexicali Valleys. In: Michel S. (Eds.), *The U.S.-Mexican*

- border environment: Binational water management planning. San Diego State University Press, San Diego, California, Chap: 2, pp. 95-144.
- Rodríguez-Burgueño, J., 2012. Modelación geohidrológica transitoria de la relación acuífero-río de la zona FFCC -vado Carranza del río Colorado con propósito de manejo de la zona riparia., Master Eng., Universidad Autónoma de Baja California, Mexicali, B.C.
- Schmid, W., and R.T. Hanson. 2009a. Appendix 1, Supplemental Information— Modifications to Modflow-2000 Packages and Processes. In Ground-Water Availability of California's Central Valley., ed. C.C. Faunt, 213–225. U.S. Geological Survey Professional Paper 1766.
- Schmid, W., and R.T. Hanson. 2009b. The Farm Process Version 2 (FMP2) for MODFLOW-2005 – Modifications and Upgrades to FMP1. U.S. Geological Survey Techniques in Water Resources Investigations, Book 6, Ch. A32.
- Schmid, W. 2004. A Farm Package for MODFLOW-2000: Simulation of Irrigation Demand and Conjunctively Managed Surface-Water and Ground-Water Supply. Ph.D. Dissertation. Department of Hydrology and Water Resources, the University of Arizona.
- Schmid, W., R.T. Hanson, T.M. Maddock III, and S.A. Leake. 2006a. User's guide for the Farm Package (FMP1) for the U.S. Geological Survey's modular three-dimensional finite-difference groundwater flow model, MODFLOW- 2000. U.S. Geological Survey Techniques and Scientific Methods Report Book 6, Chapter A17.
- Schmid, W., R.T. Hanson, and T.M. Maddock III. 2006b. Overview and Advances in the Farm Process for MODFLOW-2000. MODFLOW and MORE 2006. Managing Groundwater Systems—Conference Proceedings, 23–27.
- Sykes, G. G. (1935), The Colorado Delta, Carnegie Institution of Washington, Washington DC, USA.
- OECD report 2015. Water Resources Allocation, Sharing Risks and Opportunities, (http://www.oecd-ilibrary.org/environment/water-resources-allocation_9789264229631-en).
- Yamilett K.C. G 2009. Water conservation, wetland restoration, and agriculture in Colorado River delta Mexico. Ph.D. dissertation. the University of Arizona.

Annex 1: Data used for developing river package (RIV) in the model

Column	Row	River Bottom (m)	River stage (m)	Conductance (m ² /d)	Conductivity (m/d)
112	2	10	14.5	23.51	0.01
112	3	10	14.5	23.51	0.01
112	4	10	13.5	23.51	0.01
111	5	10	13.5	23.51	0.01
112	5	10	12.5	23.41	0.01
111	6	10	14.5	23.41	0.01
110	7	10	14.5	23.41	0.01
111	7	10	14.5	23.41	0.01
108	8	10	14.5	23.41	0.01
109	8	10	14.5	23.41	0.01
110	8	10	13.5	38.58	0.05
108	9	10	13.5	38.58	0.05
108	10	10	15.5	38.58	0.05
109	10	10	15.5	38.58	0.01
109	11	10	15	46.33	0.01
108	12	10	14.5	46.33	0.01
109	12	10	14.5	46.33	0.01
108	13	10	14.5	46.33	0.13
109	13	10	15.5	39.98	0.13
109	14	10	15.5	39.98	0.13
108	15	10	15.5	18.86	0.13
109	15	10	15.5	18.86	0.13
108	16	10	15.5	18.86	0.13
108	17	10	14.5	18.86	0.13
108	18	10	14.5	23.27	0.13
108	19	10	15	23.27	0.05
108	20	10	15.5	23.27	0.05
109	20	10	15.5	23.27	0.05
109	21	10	5.5	106.31	0.05
109	22	10	5.5	106.31	0.05
109	23	10	5.5	121.16	0.05
103	24	10	5.5	121.49	0.05
108	24	10	6	121.49	0.05
109	24	10	12.5	54.56	0.03
103	25	10	13.83	54.56	0.03
104	25	10	14.5	55.36	0.03

108	25	10	14.5	55.36	0.03
103	26	10	5.5	166.59	0.03
104	26	10	5.5	166.59	0.03
105	26	10	5.5	158.75	0.03
107	26	10	5.5	127.21	0.03
108	26	10	5.5	85.28	0.03
103	27	10	5.5	182.48	0.03
104	27	10	5.5	350.31	0.03
105	27	10	6	69.01	0.03
107	27	10	6.5	69.01	0.03
103	28	10	12.5	440.16	0.03
104	28	10	5.5	440.16	0.03
105	28	10	5.5	542.84	0.03
106	28	10	5.5	82.51	0.03
107	28	10	6.5	201.71	0.03
103	29	10	6.5	109.38	0.03
106	29	10	12.5	112.90	0.03
107	29	10	12.5	1521.98	0.03
103	30	10	4.5	924.3	0.03
106	30	10	5	420.77	0.03
103	31	10	6.5	420.77	0.03
106	31	10	6.5	420.77	0.03
103	32	10	6.5	1784.83	0.03
103	33	10	6.5	696.49	0.03
102	34	10	7	2058.84	0.03
103	34	10	7.5	613.62	0.03
102	35	10	7.5	216.71	0.03
102	36	10	7.5	216.71	0.03
102	37	10	7.5	216.71	0.03
102	38	10	7.5	395.01	0.03
102	39	10	7.5	539.28	0.03
103	39	10	7.5	532.75	0.03
103	40	10	7.5	57.38	0.03
102	41	10	7.83	289.44	0.03
103	41	10	12.5	512.13	0.03
102	42	10	12.5	253.34	0.03
102	43	10	4.5	17.55	0.03
102	44	10	6.5	170.97	0.03
102	45	10	6.5	37.125	0.03
102	46	10	6.5	152.21	0.03

102	47	10	7	13.25	0.03
102	48	10	7.5	98.95	0.06
101	49	10	8.5	126.9	0.06
102	49	10	8.5	54.99	0.06
101	50	10	8.5	143.55	0.06
101	51	10	8.5	64.18	0.06
101	52	10	8.5	64.18	0.06
101	53	10	12	43.88	0.06
102	53	10	12.5	43.88	0.06
102	54	10	4.5	45.15	0.06
101	55	10	8.5	45.15	0.06
102	55	10	9	67.16	0.06
101	56	10	9.5	67.16	0.06
101	57	10	11.5	112.90	0.06
101	58	10	11.83	116.03	0.06
102	58	10	4.5	24.717	0.06
101	59	10	4.5	82.56	0.06
102	59	10	9.5	87.07	0.06
100	60	10	10	137.00	0.06
101	60	10	11	113.20	0.06
100	61	10	7.8	60.30	0.01
96	62	10	8	58.78	0.01
97	62	10	7.8	120.70	0.01
98	62	10	7.8	95.88	0.01
99	62	10	7.9	101.52	0.01
100	62	10	7.9	167.83	0.01
93	63	10	7.9	81.58	0.01
94	63	10	7.85	42.64	0.01
95	63	10	9.9	143.63	0.01
96	63	10	9.9	150.02	0.01
97	63	10	5	96.61	0.05
92	64	10	7.7	103.41	0.05
93	64	10	7.6	125.24	0.05
94	64	10	7.9	139.83	0.01
90	65	10	7.65	57.89	0.01
91	65	10	7.7	69.55	0.01
92	65	10	8.23	289.87	0.01
83	66	10	8.2	204.75	0.13
84	66	10	8.5	163.94	0.13
86	66	10	8.5	141.26	0.13

87	66	10	8.4	116.06	0.13
88	66	10	9.5	435.67	0.13
89	66	10	9.8	319.14	0.13
90	66	10	5	174.91	0.13
91	66	10	8.5	113.28	0.13
72	67	10	8.6	112.78	0.05
73	67	10	8.7	105.21	0.05
74	67	10	9.5	166.98	0.05
75	67	10	9.5	98.01	0.05
76	67	10	5	98.01	0.05
77	67	10	5	98.01	0.05
78	67	10	8.8	98.01	0.05
79	67	10	9.3	98.01	0.05
80	67	10	9.4	98.01	0.03
81	67	10	5	98.01	0.03
82	67	10	5	98.01	0.03
83	67	10	5	98.01	0.03
84	67	10	5	98.01	0.03
85	67	10	5	435.7	0.13
86	67	10	5	319.14	0.13
88	67	10	5	174.91	0.13
59	68	10	5	113.28	0.13
60	68	10	4	112.78	0.05
61	68	10	4	105.21	0.05
62	68	10	4	166.98	0.05
63	68	10	4	98.01	0.05
64	68	10	3.5	98.01	0.05
65	68	10	3.5	98.01	0.05
66	68	10	3.5	98.01	0.05
67	68	10	3	98.01	0.05
68	68	10	1	98.010	0.03
69	68	10	1	98.010	0.03
70	68	10	5	98.010	0.03
71	68	10	5	98.010	0.03
72	68	10	8.8	98.010	0.03
73	68	10	9.3	319.140	0.03
55	69	10	9.4	174.912	0.03
56	69	10	5	113.280	0.03
57	69	10	5	112.776	0.03
58	69	10	5	105.210	0.03

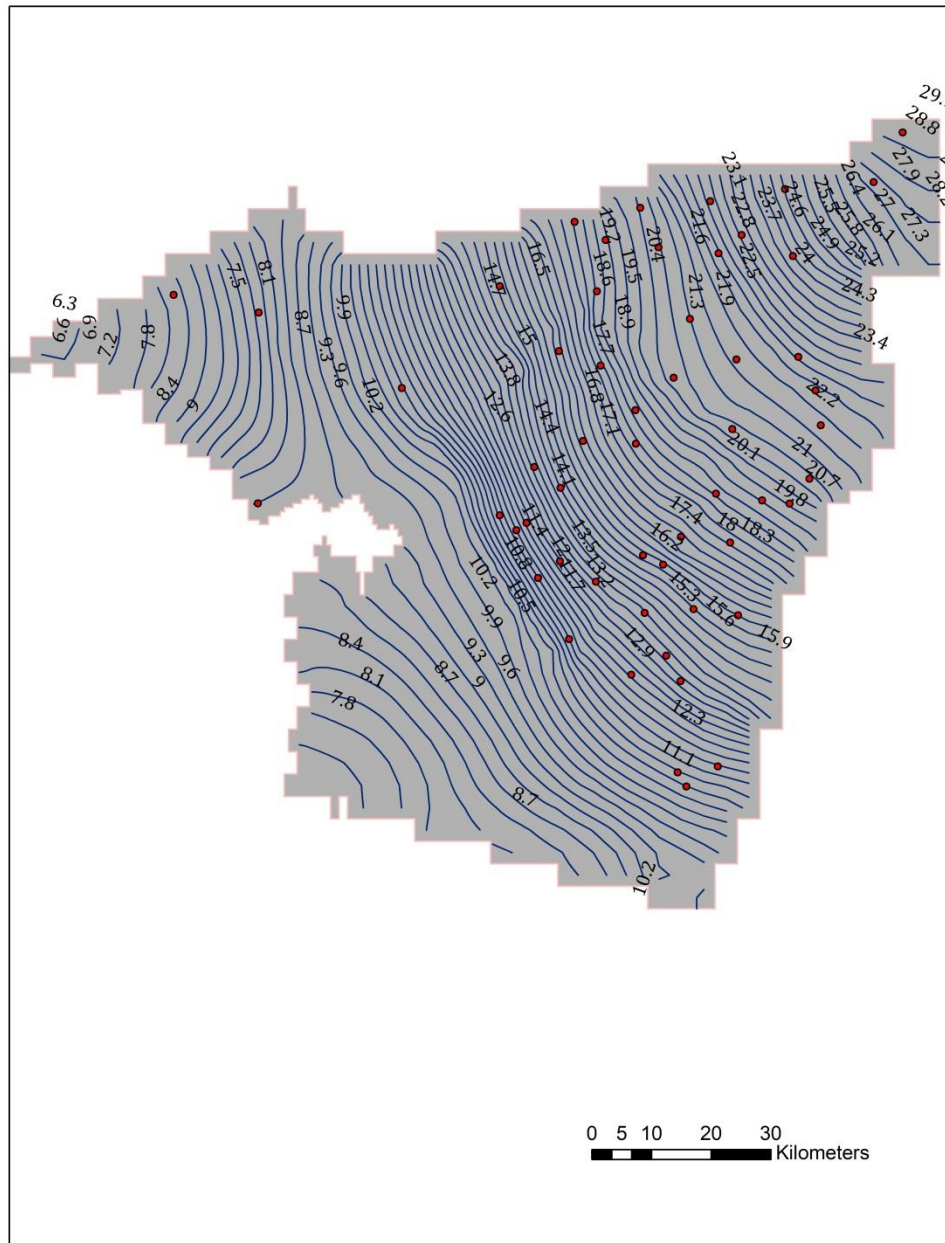
59	69	10	5	97.644	0.03
----	----	----	---	--------	------

Annex 2: Data used for developing drain package (DRN) in the model

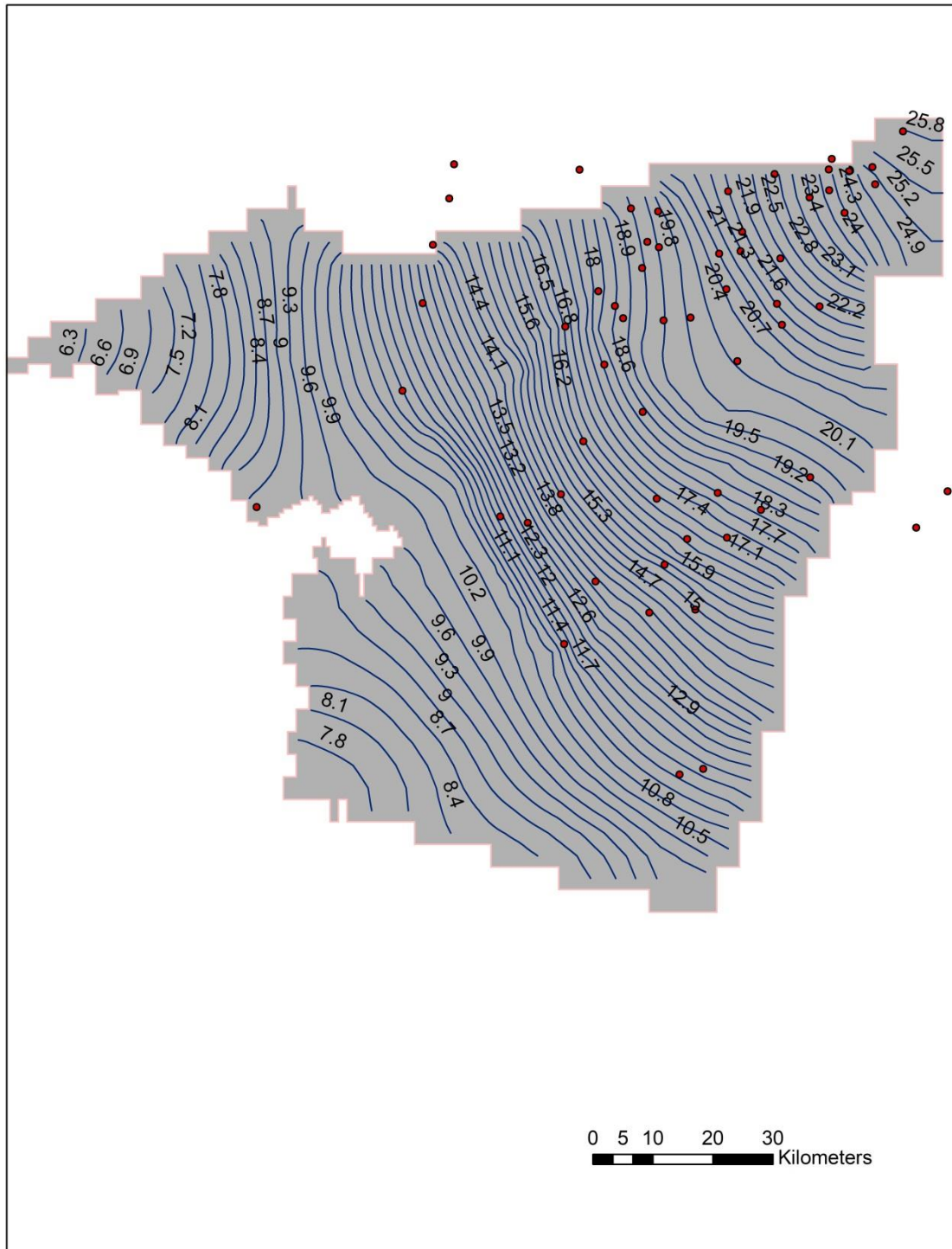
Column	Row	elevation (m)	conductivity (m/d)	conductance (m ² /d)
27	59	5	0.0006	0.5378
28	59	5	0.0006	0.7657
29	59	5	0.0006	0.9256
30	59	5	0.0006	2.9347
25	60	5	0.0006	3.2202
26	60	5	0.0006	4.4664
27	60	5	0.0006	10.5043
24	61	5	0.0006	18.8965
25	61	5	0.0006	11.6522
26	61	5	0.0006	17.4816
24	62	5	0.0006	10.965
25	62	5	0.0006	19.0714
26	62	5	0.0006	19.0714
27	62	5	0.0006	18.1796
25	63	5	0.0006	18.1796
26	63	5	0.0006	14.5278
27	63	5	0.0006	14.5278
27	64	5	0.0006	14.5278
28	64	5	0.0006	14.5278
28	65	5	0.0006	11.4265
29	65	5	0.0006	11.4265
30	65	5	0.0006	11.4265
27	66	5	0.0006	14.9602
28	66	5	0.0006	14.9602
29	66	5	0.0006	14.9602
30	66	5	0.0006	14.9602
31	66	5	0.0006	14.9602
32	66	5	0.0006	14.9602
33	66	5	0.0006	14.9602
34	66	5	0.0006	14.9602
35	66	5	0.0006	14.9602
36	66	5	0.0006	14.9602
37	66	5	0.0006	14.9602
38	66	5	0.0006	14.9602
35	67	5	0.0006	14.9602

36	67	5	0.0006	14.9602
37	67	5	0.0006	14.9602
38	67	5	0.0006	14.9602
39	67	5	0.0006	14.9602
40	67	5	0.0006	14.9602
41	67	5	0.0006	14.9602
31	68	5	0.0006	14.9602
32	68	5	0.0006	14.9602
33	68	5	0.0006	14.9602
34	68	5	0.0006	14.9602
35	68	5	0.0006	14.9602
36	68	5	0.0006	14.9602
37	68	5	0.0006	14.9602
38	68	5	0.0006	14.9602
39	68	5	0.0006	14.9602
40	68	5	0.0006	14.9602
31	69	5	0.0006	14.9602
32	69	5	0.0006	14.9602
33	69	5	0.0006	14.9602
34	69	5	0.0006	14.9602
35	69	5	0.0006	14.9602
36	69	5	0.0006	14.9602

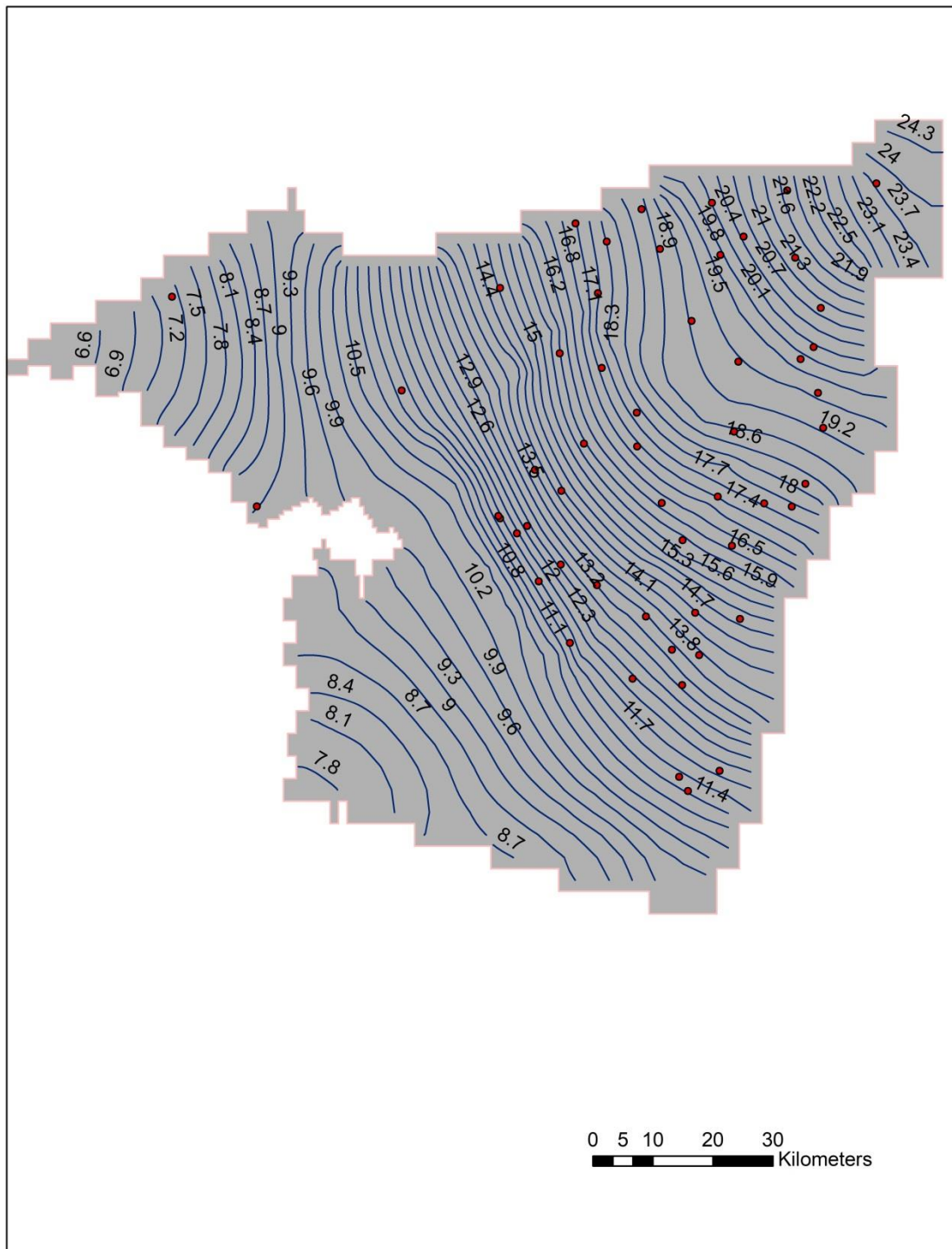
Annex 3: Distribution of simulated head (m.asl) at the year 2003-2004



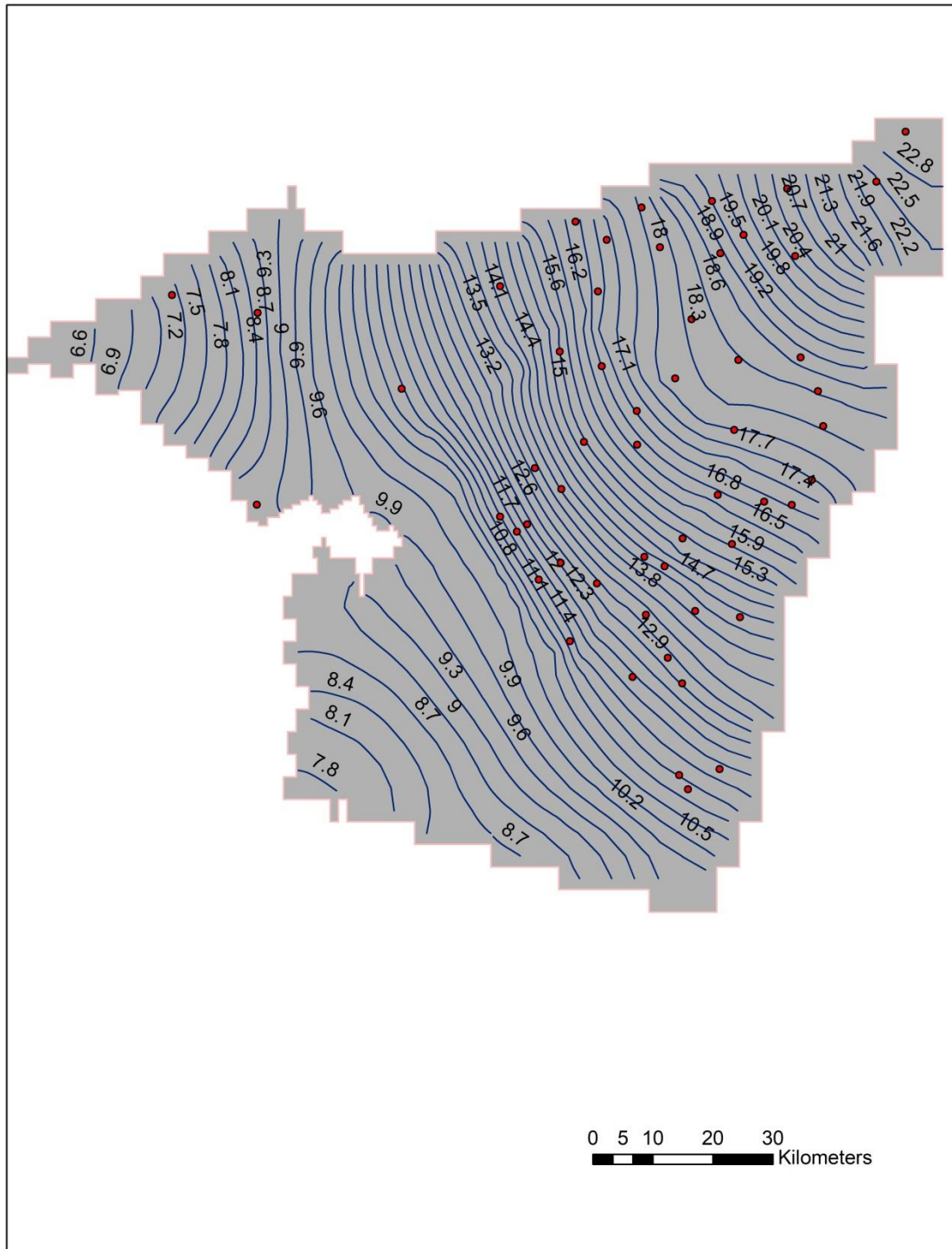
Annex 5: Distribution of simulated head (m.asl) at the year 2005-2006



Annex 6: Distribution of simulated head (m.asl) at the year 2006-2007



Annex 7: Distribution of simulated head (m.asl) at the year 2007-2008



Annex 8: Calculated agricultural Related Recharge for each irrigation units in irrigation district 014

	Agricultural units Area (m ²)	Assigned agricultural water(m ³)	Assigned agricultural water(m/d)	Recharge (m/d)								
				2002	2003	2004	2005	2006	2007	2008	2009	2010
1	131,712,610.55	114,859,000.00	2.39E-03	5.61E-04	5.97E-04	5.73E-04	6.69E-04	6.69E-04	3.58E-04	5.97E-04	7.17E-04	2.09E-03
2	121,952,936.64	73,235,000.00	1.65E-03	3.87E-04	4.11E-04	3.95E-04	4.61E-04	4.61E-04	2.47E-04	4.11E-04	4.94E-04	1.31E-03
3	85,932,901.70	113,180,000.00	3.61E-03	8.48E-04	9.02E-04	8.66E-04	1.01E-03	1.01E-03	5.41E-04	9.02E-04	1.08E-03	3.05E-03
4	179,955,084.46	137,366,000.00	2.09E-03	4.91E-04	5.23E-04	5.02E-04	5.86E-04	5.86E-04	3.14E-04	5.23E-04	6.27E-04	1.54E-03
5	112,476,216.82	101,580,000.00	2.47E-03	5.81E-04	6.19E-04	5.94E-04	6.93E-04	6.93E-04	3.71E-04	6.19E-04	7.42E-04	2.37E-03
6	86,838,652.43	69,244,000.00	2.18E-03	5.13E-04	5.46E-04	5.24E-04	6.12E-04	6.12E-04	3.28E-04	5.46E-04	6.55E-04	2.10E-03
7	122,980,488.80	126,275,000.00	2.81E-03	6.61E-04	7.03E-04	6.75E-04	7.88E-04	7.88E-04	4.22E-04	7.03E-04	8.44E-04	1.65E-03
8	114,270,359.48	116,715,000.00	2.80E-03	6.58E-04	7.00E-04	6.72E-04	7.84E-04	7.84E-04	4.20E-04	7.00E-04	8.39E-04	2.43E-03
9A	92,816,831.69	102,479,000.00	3.02E-03	7.11E-04	7.56E-04	7.26E-04	8.47E-04	8.47E-04	4.54E-04	7.56E-04	9.07E-04	2.42E-03
9B	121,975,642.61	104,917,000.00	2.36E-03	5.54E-04	5.89E-04	5.66E-04	6.60E-04	6.60E-04	3.53E-04	5.89E-04	7.07E-04	1.79E-03
10	158,617,585.15	152,322,000.00	2.63E-03	6.18E-04	6.58E-04	6.31E-04	7.37E-04	7.37E-04	3.95E-04	6.58E-04	7.89E-04	2.65E-03
11	106,577,933.93	105,983,000.00	2.72E-03	6.40E-04	6.81E-04	6.54E-04	7.63E-04	7.63E-04	4.09E-04	6.81E-04	8.17E-04	2.74E-03
12	128,672,227.76	110,197,000.00	2.35E-03	5.51E-04	5.87E-04	5.63E-04	6.57E-04	6.57E-04	3.52E-04	5.87E-04	7.04E-04	2.36E-03
14	125,216,146.32	104,675,000.00	2.29E-03	5.38E-04	5.73E-04	5.50E-04	6.41E-04	6.41E-04	3.44E-04	5.73E-04	6.87E-04	2.29E-03
15	180,318,679.25	149,231,000.00	2.27E-03	5.33E-04	5.67E-04	5.44E-04	6.35E-04	6.35E-04	3.40E-04	5.67E-04	6.80E-04	2.31E-03
16	181,965,111.33	122,921,000.00	1.85E-03	4.35E-04	4.63E-04	4.44E-04	5.18E-04	5.18E-04	2.78E-04	4.63E-04	5.55E-04	1.92E-03
17	127,852,464.01	105,289,000.00	2.26E-03	5.30E-04	5.64E-04	5.41E-04	6.32E-04	6.32E-04	3.38E-04	5.64E-04	6.77E-04	2.27E-03
18	129,289,049.86	93,046,000.00	1.97E-03	4.63E-04	4.93E-04	4.73E-04	5.52E-04	5.52E-04	2.96E-04	4.93E-04	5.92E-04	2.02E-03
19	66,591,684.99	90,549,000.00	3.73E-03	8.75E-04	9.31E-04	8.94E-04	1.04E-03	1.04E-03	5.59E-04	9.31E-04	1.12E-03	3.76E-03
21	62,066,788.03	56,963,000.00	2.51E-03	5.91E-04	6.29E-04	6.03E-04	7.04E-04	7.04E-04	3.77E-04	6.29E-04	7.54E-04	2.52E-03
22	65,947,702.59	50,716,000.00	2.11E-03	0.000495	0.000527	0.000506	0.00059	0.00059	3.16E-04	5.27E-04	6.32E-04	2.11E-03

Part two

Annex 9. Farm Budget for Farm 2 for a specific stress period and time step in m³/year

Time (Days)	Q-p-in: Farm 2	Q-egw-in: Farm 2	Q-ei-out: Farm 2	Q-ep-out: Farm 2	Q-run-out: Farm 2	Rech-Farm 2	Surface Water Del.	Pumpa
365	205.4348	1546.178	80576.2	164.3	483.72	178145.9	82504.2	11785.5
730	2476.848	522.9496	146696.	1981.4	788.66	84327.0	138082.1	12201.5
1095	6973.155	78.0407	149657.	5578.5	782.68	35762.5	138082.1	13917.9
1461	5512.5	1240.087	126879.	4410	649.86	16141.9	126667.9	13917.9
1826	14153.42	967.867	99963.8	11322.	506.24	6035.33	98833.39	22359.6
2191	1070.136	152.5161	162279.	856.10	821.30	2276.51	138082.1	22359.6
2556	2347.395	99.9146	145515.	1877.9	735.71	506.073	138082.1	5639.17
2922	2856.574	96.7929	158577.	2285.2	801.30	67.9634	137704.9	18829.4
3287	12461.02	967.867	177559.	9968.8	896.97	6035.33	138082.1	37140.2
3652	14153.42	152.5161	135494.	11322.	683.91	506.073	133601.9	37140.2
4017	1070.1369	118.7842	159961.	856.10	809.14	12141.9	138082.1	19983.3
4382	12461.02	11975.83	645481.	9968.8	5628.8	10240.9	138082.1	10219.7

Annex10. Farm Budget for Farm 4 for a specific stress period and time step in m³/year

Time (Days)	Q-p-in: Farm 4	Q-egw-in: Farm 4	Q-ei-out: Farm 4	Q-ep-out: Farm 4	Q-run-out: Farm 4	Rech-Farm 4	Surface Water Del.
365	472.010	2961.721	15252.837	377.6087	3968.434	20824.875	30208.755
730	5690.85	1631.157	18428.695	4552.6828	6237.492	42822.143	66087.085
1095	5021.65	267.5864	26772.244	4817.323	5699.852	29153.731	63121.34
1461	12665.6	149.0667	22506.105	4132.5	4762.78	19949.050	49165.397
1826	5519.17	267.5860	12500.121	5160.4638	2639.523	7443.3997	21377.327
2191	2458.76	264.5839	31662.080	1967.0135	6659.590	5777.4472	79915.948
2556	5393.42	162.2162	27673.524	4314.7369	5814.748	2359.683	69304.678
2922	6563.31	147.8735	29993.174	5250.6557	6300.569	1096.6880	46157.139
3287	8630.68	198.3853	28785.110	7687.1671	6046.794	400.42159	71078.668
3652	13519.1	433.026	19542.737	11649.260	4105.283	54.792408	45166.927
4017	2458.76	198.3853	31224.54	1967.0135	6559.237	54.792408	78163.706
4382	2963.68	833.026	23372.965	2704.5452	5484.513	540.79240	55730.636

